# CHARACTERIZATION OF S-PALMITOYLATION OF JUNCTIONAL ADHESION MOLECULE C AND INVESTIGATION OF THE LYSINE DEFATTY-ACYLASE ACTIVITY OF HDAC8

A Dissertation

Presented to the Faculty of the Graduate School

of Cornell University

In Partial Fulfillment of the Requirements for the Degree of

Doctor of Philosophy

by

Pornpun Aramsangtienchai

August 2016

# CHARACTERIZATION OF S-PALMITOYLATION OF JUNCTIONAL ADHESION MOLECULE C AND INVESTIGATION OF THE LYSINE DEFATTY-ACYLASE ACTIVITY OF HDAC8

Pornpun Aramsangtienchai, Ph. D.

Cornell University 2016

S-palmitoylation has been implicated in numerous biological processes. Due to advances in proteomic technologies, the number of S-palmitoylated proteins has markedly increased. However, not all of the identified S-palmitoylated proteins have been well characterized. Here, I investigated the S-palmitoylation on Junctional adhesion molecule C (JAM-C), an immunoglobulin superfamily protein expressed in epithelial cells, endothelial cells, and leukocytes. I demonstrated that JAM-C undergoes S-palmitoylation on two juxtamembrane cysteine residues, Cys264 and Cys265 and identified DHHC7 as a JAM-C palmitoyltransferase. Ectopic expression of DHHC7, but not a DHHC7 catalytic mutant, enhanced JAM-C S-palmitoylation, and DHHC7 knockdown decreased the S-palmitoylation level of JAM-C. Palmitoylation of JAM-C promoted its localization to cell tight junction and inhibited transwell migration of A549 lung cancer cells. These results suggest that S-palmitoylation of JAM-C by DHHC7 can potentially be targeted to control cancer metastasis.

Different from S-acylation, protein lysine fatty acylation is not well-known. Our lab previously demonstrated that certain $NAD^+$-dependent deacetylases, or sirtuins (SIRT1, SIRT2, SIRT3 and SIRT6), can catalyze lysine defatty-acylation. SIRT6 can remove lysine fatty acylation on TNFα, and this defatty-acylation can regulate TNFα secretion. This suggests that lysine fatty acylation is physiologically relevant. I investigated if the zinc-dependent deacetylases, or HDACs, also possess

defatty-acylation activity similar to the activity observed with some sirtuins. Considering the low deacetylase activity, compared to other class I HDACs, I chose HDAC8 for defatty-acylase activity screening. I found that HDAC8 can catalyze the removal of acyl groups with 2-16 carbons from lysine 9 of the histone H3 peptide (H3K9). Interestingly, the catalytic efficiencies ($k_{cat}/K_m$) of HDAC8 on octanoyl, dodecanoyl, and myristoyl lysine are several folds better than that on acetyl lysine. T-cell leukemia Jurkat cells treated with a HDAC8 specific inhibitor, PCI-34051, exhibited an increase in global fatty acylation compared to control treatment. Thus, the defatty-acylation activity of HDAC8 is likely physiologically relevant. This is the first report of a zinc-dependent HDAC with defatty-acylation activity, and further investigation of HDAC8 defatty acylation targets will provide more insight into the physiological roles of HDAC8.

## BIOGRAPHICAL SKETCH

Pornpun (Polly) Aramsangtienchai was born in Bangkok, Thailand. Polly earned a B.S. and M.S. degree in Biochemistry from Chulalongkorn University in Thailand. During her Master's study, she joined Dr. Piamsook Pongsawasdi's lab and worked on characterizing cyclodextrin glycosyltransferase (CGTase) for synthesizing epicatechin glycosides. After graduating, she worked as a project analyst where she evaluated and monitored the overall of genomic medicine project at the National Science and Technology Development Agency. After one year, she received a scholarship from the Royal Thai government to pursue her PhD. She will join the faculty at Burapha University in Thailand after obtaining her doctorate degree.

To my parents and all my teachers

## ACKNOWLEDGMENTS

I would like to express my gratitude to my advisor, Dr. Hening Lin for his support, insightful guidance and encouragement throughout my PhD study. I always believe I am a lucky person to join his lab. I express my appreciation to my committee members, Dr. Richard Cerione and Dr. Marcus Smolka for their invaluable suggestions and guidance. In addition, I would like to thank Bin He, Xiaoyang Xu and Ji Cao for their technical training and assistance. I am also grateful the Graduate Field of Biochemistry, Molecular, and Cell Biology (BMCB), Department of Molecular Biology and Genetics for providing me an opportunity to study at Cornell University.

I am thankful to my classmate/roommate, Jie (Gia) Wang, for her sharing and caring throughout my PhD study. She is the sunshine on my rainy days. In addition, I really appreciate all of the support from Nicole Alexis Spiegelman. Every moment we spent together is amazing and I cherish the friendship with her. Moreover, I would like to thank everyone in the Lin lab for creating a friendly working environment. It really has been a pleasure working with everyone. I am also grateful to the Linder, Crane, Cerione, and Smolka labs for generously sharing plasmids and reagents with us.

I greatly appreciate the scholarship from the Royal Thai Government which allowed me to pursue my PhD at Cornell University.

Last but not least, I deeply appreciate my parents and my brothers for their endless love and support throughout my life.

## TABLE OF CONTENTS

## LIST OF FIGURES

## LIST OF TABLE

# CHAPTER 1

# INTRODUCTION

Protein lipidation is one of the most prevalent classes of protein post-translational modifications (PTMs). This class of PTMs has been found to play crucial roles in a variety of biological processes, including subcellular localization, protein activity, protein-protein interaction, and protein stability (Resh et al, 2006). Aberrant lipid modification has been implicated in different diseases. Protein lipidation occurs on different side chains of various amino acid residues via different linkages as shown in Table 1.1. My dissertation research concerns acylation of cysteine and lysine side chains. Thus, in this chapter, I will summarize the structures, catalytic enzymes, protein targets, and physiological functions of cysteine and lysine fatty acylation.

## 1.1 S-PALMITOYLATION

S-palmitoylation is the addition of a 16-carbon, or palmitate group, to cysteine residues of proteins via a labile thioester linkage. S-palmitoylation was first discovered several decades ago by Schmidt and colleagues (Schlesinger et al, 1980). Shortly after that, various S-palmitoylation substrates were identified including: G protein coupled receptor, bovine rhodopsin (O'Brien and Zatz et al, 1984) and p21 Ras proteins (Chen et al, 1985). S-palmitoylation has been extensively studied and many other proteins have been reported to have this post translational modification.

**Table 1.1 Structures and linkages of different protein lipidations**

| Modification | chemical structure | Linkage | Enzyme |
|---|---|---|---|
| N-terminal Gly myristoylation | 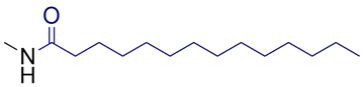 | Amide to N-terminal Gly α-amino group | NMT1, NMT2 |
| S-palmitoylation | 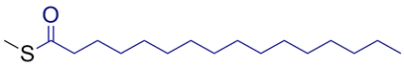 | Thioester to Cys | DHHCs |
| Lys-myristoylation | 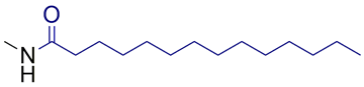 | Amide to Lys side chain | unknown |
| Wnt O-acylation | 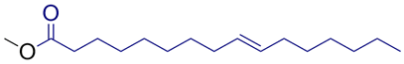 | Ester to Ser | Porcupine |
| S-farnesylation (C15) | 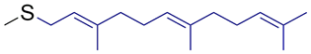 | Thioether to Cys | FTase |
| S-geranylgeranylation (C20) | 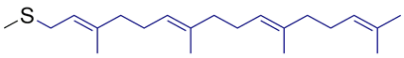 | Thioether to Cys | GGTase |
| Hedgehog N-terminal Cys palmitoylation |  | Amide to N-terminal Cys α-amino group | Hedgehog acyltransferase (Hhat) |
| Hedgehog O-cholesterylation | 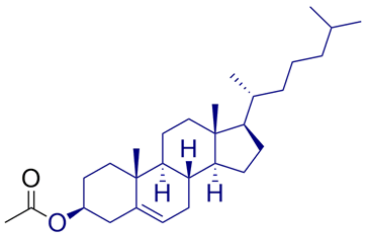 | Ester to C-terminus of Hh | autocatalytic |

S-palmitoylation is a reversible PTM. Palmitoylation of cysteine residues is catalyzed by protein acyltransferases (PATs or DHHCs), while the removal of S-palmitoyl groups is regulated by acyl protein thioesterases (APTs) (Figure 1.1) (Smotrys et al, 2004). Setting it apart from other lipidation PTMs, there is no consensus sequence that can be used to predict if a protein has S-palmitoylation. Nevertheless, S-acylated proteins have some common characteristics. First, these proteins often have cysteine residue(s) within transmembrane domains, or in membrane proximal regions. Second, they have S-palmitoylation next to another lipid modification, such as cysteine prenylation (S-prenylation) or N-terminal glycine myristoylation. For some proteins, glycine myristoylation is required for membrane localization prior to S-palmitoylation by membrane-bound PATs (e.g. the Src family proteins). Similarly, S-palmitoylation on the C-terminal domain of some proteins is dependent on S-prenylation on a CAAX motif (e.g. the Ras family proteins) (Korycka et al, 2012; Resh 2006; Varner et al, 2003).

For certain cytosolic proteins, some structural properties are critical for determining palmitoylated substrates (Bijlmakers et al, 2003). For example, glutamate receptor interacting protein 1 (GRIP1) has two isoforms, GRIP1a and GRIP1b which are different only in their N-terminal regions. While both containing N-terminal cysteine residues, only GRIP1b is found to be palmitoylated (Yamazaki et al, 2001). Similarly, only one isoform of glutamic acid decarboxylase (GAD), GAD65, undergoes s-palmitoylation, while the other isoform, GAD67, does not. This was surprising as both isoforms contain cysteine residues around the central region of the protein (Solimena et al, 1994).

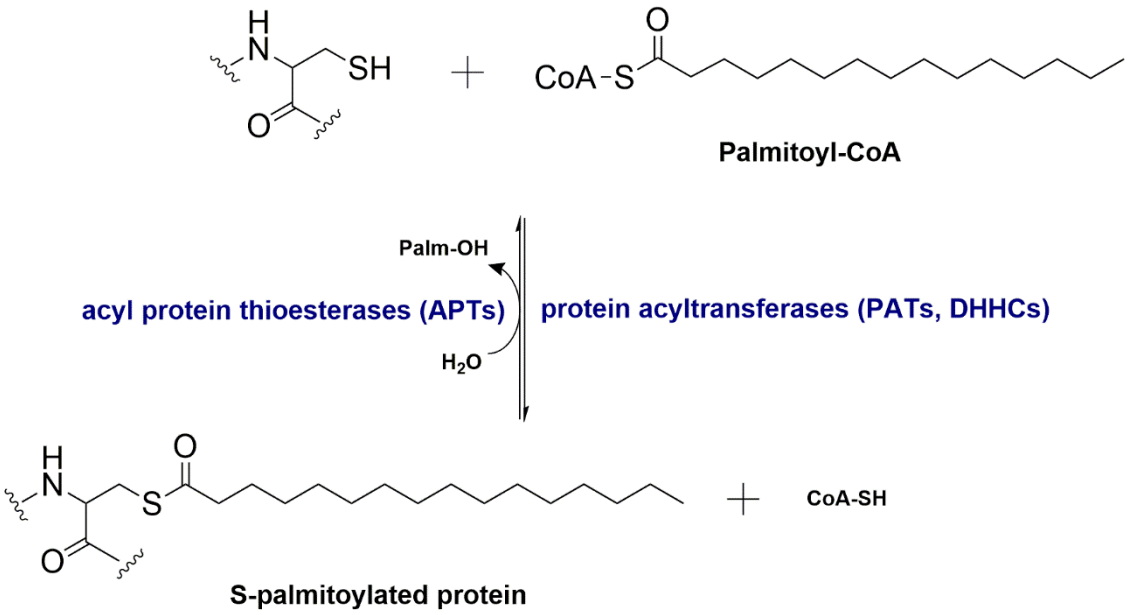


**Figure 1.1. Reversible protein S-palmitoylation.** The palmitate attachment using palmitoyl-CoA as a co-substrate is catalyzed by protein acyltransferases (PATs), also known as DHHC family proteins. The removal of the palmitoyl is mediated by acyl protein thioesterase (APTs).

### 1.1.1 Structure, mechanism and intracellular localization of DHHCs

The enzymes that catalyze the S-palmitoylation modification were first discovered in 2002. Through genetic studies, Erf2p (effect on Ras function 2 protein) and Erf4p were identified as a protein complex required for the S-palmitoylation of Ras (Lobo et al, 2002). Erf2p, localized at the ER-membrane in yeast, contains a conserved Asp-His-His-Cys (DHHC)-Cys rich domain (CRD) and mutation of any conserved DHHC residues eliminates the acyltransferase activity. At the same time, Davis and co-workers identified the ankyrin repeat-containing protein Akr1p as a palmitoyl transferase for Yck2p (yeast casein kinase 2) (Roth et al, 2002). Akr1p was essential for Yck2 S-palmitoylation and plasma membrane localization. Similar to Erf2p, Akr1p also contains the conserved DHHC-CRD motif that is required for the catalytic activity.

The first mammalian DHHC was reported by Lüscher and co-workers when they identified a Golgi-specific DHHC zinc finger protein (GODZ), also known as DHHC3. They found GODZ mediated the S-palmitoylation of the gamma2 subunit of GABA(A) receptors (Keller et al, 2004). Bredt and co-workers were subsequently able to isolate 23 mammalian DHHC proteins encoded by *ZDHHC* genes. These proteins all contain a DHHC-CRD motif and mutations in this motif abolished the enzyme activity (Fukata et al, 2004; Roth et al, 2002).

Based on the membrane topology prediction, DHHC proteins are integral membrane proteins with four to six transmembrane domains (Figure 1.2). The N-and C-terminal regions are in the cytosol and the conserved DHHC domain is located between the second and the third transmembrane domains in the cytosolic loop. The DHHC-

CRD consensus sequence based on an alignment of the yeast and human DHHC proteins is as follow (Linder and Jennings, 2003);

$$CX_2CX_3(R/K)PXRX_2HCX_2CX_2CX_4DHHCXW(V/I)XNC(I/V)GX_2NX_3F$$

An ankyrin repeat (AR) domain is found in the cytosolic N-terminal region of DHHC13 and DHHC17, and is implicated in interacting or recruiting DHHC substrates (Mitchell et al, 2006). Through the AR domain, DHHC13 and DHHC17 can recognize a consensus sequences of [V/I/A/P][V/I/T]$X_2$QP in different target proteins e.g. SNAP23, SNAP25, and Huntingtin (Lemonidis et al, 2015).

Most mammalian DHHCs are predominately localized at the membranes of the Golgi apparatus and endoplasmic reticulum (ER), while a few of them are found in the plasma membrane (Ohno et al, 2006). A Ping-Pong catalytic mechanism for the DHHCs enzymatic activity was proposed by Mitchell and colleagues (Mitchell et al 2006). First**,** an acyl group is transferred from palmitoyl-CoA to the Cys residue on DHHC motif to form the acyl-enzyme intermediate. This step is known as “autoacylation step”. Second, the acyl group is transferred from the DHHC to the protein substrate. The first step occurs faster than the second step, allowing the autoacylated DHHC proteins to accumulate (Mitchell et al 2006; Linder and Jennings, 2013).

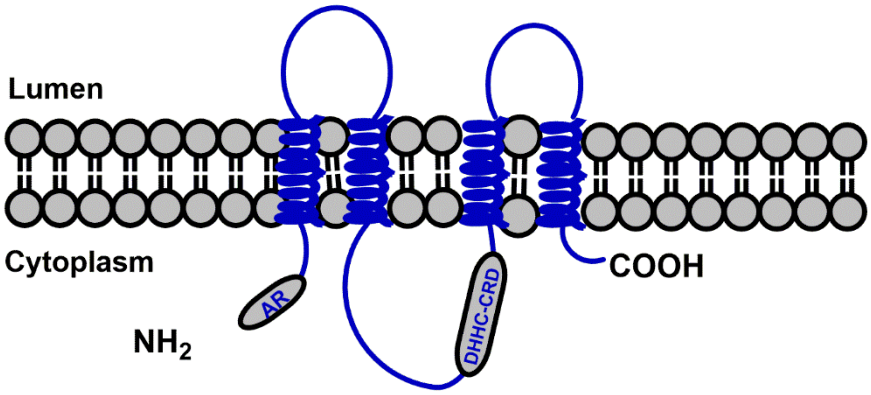


**AR = Ankyrin repeat**
**DHHC-CRD consensus sequence**
**$CX_2CX_3(R/K)PXRX_2HCX_2CX_2CX_4DHHCXW(V/I)XNC(I/V)GX_2NX_3F$**

**Figure 1.2. The predicted DHHC proteins topology.** In general, DHHCs membrane topology is composed of four to six transmembrane domains with N- and C-terminal regions in the cytoplasm. All of the enzymes contain a conserved DHHC sequence located between the second and the third transmembrane domain. Based on a Clustal X alignment of the yeast and human DHHC proteins, the consensus sequence was proposed (Mitchell et al, 2006).

DHHCs also contain S-palmitoylation on other Cys residues, and this may affect their specificity and activity. For example, DHHC5, 6 and 8 have been reported to be S-palmitoylated on three cysteine residues in a motif downstream of the DHHC domain. The modification presumably can block the interaction between DHHCs and their substrates, thereby inhibiting S-palmitoylation of the protein substrates (Yang et al, 2010).

Even though S-palmitoylation is known to be catalyzed by DHHCs, *in vitro* non-enzymatic acylation has also been reported (Bijlmakers and Marsh, 2003; Dietrich et al, 2004). A strong nucleophillic SH group of a cysteine residue can attack the thioester bond of palmitoyl CoA. This autoacylation has been found to occur on several proteins including SNAP25 (Veit, 2000), Gα subunits (Duncan and Gilman, 1996), rhodopsin, Src kinase Yes, and β2-adrenergic receptor (Bijlmakers et al, 2003).

### 1.1.2 Substrates of DHHCs

Through overexpression and knockdown studies, substrates of the 23 mammalian DHHCs have been identified. These DHHC target proteins together with the S-palmitoylation-related functions are summarized in Table 1.2.

**Table 1.2 Mammalian (human) DHHCs and putative substrates**

| DHHC[a] (protein) | *ZDHHC*[a] (gene) | Localization | Tissue specificity[b] | Putative substrates | S-Palm Function | Ref. |
|---|---|---|---|---|---|---|
| DHHC1 | ZDHHC1 | ER | lung, liver and gallbladder, pancreas, kidney, skin | Ncdn | early endosome localization | Oku et al, 2013 |
| DHHC2 | ZDHHC2 | Golgi, ER, recycling endosome, plasma membrane in neuro-endocrine cells (Greaves et al, 2010) | bone marrow, pancreas, GI tract, kidney | AKAP79/150 | recycling endosomes targeting | Woolfrey et al, 2015 |
| | | | | CKAP4/p63 | ER to plasma membrane targeting and nuclear localization | Zhang et al, 2008 |
| | | | | ENaC | channel activity modulation | Mukherjee et al, 2014 |
| | | | | PSD-95 | plasma membrane targeting | Fukata et al, 2013 |
| | | | | Lck | plasma membrane targeting | Zeidman et al, 2011 |
| | | | | R7BP | plasma membrane localization | Jia et al, 2011 |
| | | | | tetraspanins CD9 and CD151 | protein-protein interaction and protein stability | Sharma et al, 2008 |
| | | | | Gp78 | peripheral ER targeting | Fairbank et al, 2012 |
| DHHC3 | ZDHHC3 | Golgi | brain, endocrine tissues, bone marrow, lung, liver, GI tract, kidney | PPT1 | protein activity | Segal-Salto et al, 2016 |
| | | | | PI4KIIα | Golgi targeting | Lu et al, 2012 |
| | | | | RGS4 | protein stability | Wang et al, 2010 |
| | | | | SNAP25/23 | plasma membrane association | Greaves et al, 2010 |

| DHHC[a] (protein) | *ZDHHC*[a] (gene) | Localization | Tissue specificity[b] | Putative substrates | S-Palm Function | Ref. |
|---|---|---|---|---|---|---|
| | | | | Galpha(q), Galpha(s), Galpha(i2) | plasma membrane localization | Tsutsumi et al, 2009 |
| | | | | CSP | plasma membrane association | Greaves et al, 2008 |
| | | | | TARP γ-8, CaMKIIα, and Syd-1 | n/a | Oku et al, 2013 |
| | | | | Ncdn | early endosome localization | Oku et al, 2013 |
| | | | | Integrin α6β4 | protein stability | Sharma et al, 2012 |
| | | | | STREX | plasma membrane association | Tian et al, 2008 |
| | | | | GluR1, GluR2 | perinuclear targeting | Huang et al, 2009 |
| DHHC4 | ZDHHC4 | Golgi, ER | pancreas, kidney | n/a | n/a | n/a |
| DHHC5 | ZDHHC5 | Plasma membrane | endocrine tissues, lung, liver, GI tract | δ-catenin | synapse efficacy/ protein interaction | Brigidi et al 2014 |
| | | | | Grip1b | dendritic endosomes targeting | Thomaset al, 2012 |
| | | | | Flotillin-2 | protein oligomerization | Li et al, 2012 |
| | | | | Somatostatin receptor 5 | n/a | Kokkola et al, 2011 |
| | | | | Ankyrin-G | lateral membrane localization | He et al, 2014 |
| | | | | PLM | $Na^+$ pump regulation | Howie et al, 2014 |
| | | | | STREX | plasma | Tian et al, |

| DHHC[a] (protein) | *ZDHHC*[a] (gene) | Localization | Tissue specificity[b] | Putative substrates | S-Palm Function | Ref. |
|---|---|---|---|---|---|---|
| | | | | | membrane association | 2008 |
| DHHC6 | ZDHHC6 | ER | brain, bone marrow, endocrine tissue, lung, kidney, skin, testis, ovary | IP3R | plasma membrane localization | Fredericks et al, 2014 |
| | | | | Calnexin | perinuclear rough ER localization | Lakkaraju et al, 2012 |
| | | | | Gp78 | peripheral ER targeting | Fairbank et al, 2012 |
| DHHC7 | ZDHHC7 | Golgi | bone marrow, GI tract, kidney, ovary | PPT1 | protein activity | Segal-Salto et al, 2016 |
| | | | | Fas | protein stability | Rossin et al, 2015 |
| | | | | PI4KIIα | Goligi targeting | Lu et al, 2012 |
| | | | | RGS4 | protein stability | Wang et al, 2010 |
| | | | | SNAP25/23 | plasma membrane localization | Greaves et al, 2010 |
| | | | | Galpha(q), Galpha(s), and Galpha(i2) | plasma membrane localization | Tsutsumi et al, 2009 |
| | | | | CSP | plasma membrane association | Greaves et al, 2008 |
| | | | | TARP γ-8, CaMKIIα, and Syd-1 | n/a | Oku et al, 2013 |
| | | | | Ncdn | early endosome localization | Oku et al, 2013 |
| | | | | STREX | plasma membrane association | Tian et al, 2008 |
| DHHC8 | ZDHHC8 | Golgi | brain, kidney | Grip1b | dendritic endosomes targeting | Thomas 2012 |

| DHHC[a] (protein) | *ZDHHC*[a] (gene) | Localization | Tissue specificity[b] | Putative substrates | S-Palm Function | Ref. |
|---|---|---|---|---|---|---|
| | | | | Ankyrin-G | lateral membrane localization | He et al, 2014 |
| | | | | PICK1 | synaptic plasticity | Thomas et al, 2013 |
| | | | | ABCA1 | plasma membrane association | Singaraja et al 2009 |
| DHHC9 | ZDHHC9 | Golgi, ER | brain, bone marrow, muscle, liver | H-Ras, N-Ras | membrane trafficking | Swarthout et al, 2005 |
| | | | | STREX | plasma membrane association | Tian et al, 2008 |
| DHHC10 | ZDHHC11 | ER | brain, muscle, kidney | Ncdn | early endosome localization | Oku et al, 2013 |
| DHHC11 | ZDHHC23 | ER, Plasma membrane | brain, bone marrow, endocrine tissue, lung, liver, muscle, pancreas, kidney, skin, testis, placenta | BK | plasma membrane association | Tain et al, 2012 |
| | | | | Gp78 | peripheral ER targeting | Fairbank et al, 2012 |
| DHHC12 | ZDHHC12 | Golgi, ER | brain, endocrine tissues, bone marrow, liver, GI tract, kidney, testis | n/a | n/a | n/a |
| DHHC13 | ZDHHC24 | ER, Plasma membrane | liver, pancreas, GI tract, kidney, testis, placenta | Gp78 | peripheral ER targeting | Fairbank et al, 2012 |
| | | | | HTT | n/a | Huang et al, 2011 |
| DHHC14 | ZDHHC14 | ER | bone marrow, liver, pancreas, kidney | n/a | n/a | n/a |
| DHHC15 | ZDHHC15 | Golgi | endocrine tissues, | CSP | plasma membrane | Greaves et al, 2008 |

| DHHC[a] (protein) | *ZDHHC*[a] (gene) | Localization | Tissue specificity[b] | Putative substrates | S-Palm Function | Ref. |
|---|---|---|---|---|---|---|
| | | | pancreas, testis | | association | |
| | | | | SNAP25b | plasma membrane association | Greaves et al, 2010 |
| DHHC16 | ZDHHC16 | ER | muscle, breast | PLN | protein partner interaction | Zhou et al, 2015 |
| DHHC17 | ZDHHC17 | Golgi | brain, kidney, placenta | NMNAT2 | golgi targeting | Milde et al, 2014 |
| | | | | ClipR-59 | plasma membrane association | Ren etal, 2013 |
| | | | | MPP1 | membrane lateral organization | Łach et al, 2012 |
| | | | | SNAP25/23 | plasma membrane association | Greaves et al, 2010 |
| | | | | CSP | plasma membrane association | Greaves et al, 2008 |
| | | | | STREX | plasma membrane association | Tian et al, 2008 |
| | | | | PSD-95 | perinuclear accumulation | Huang et al, 2004 |
| | | | | HTT | Golgi targeting | Huang et al, 2004; Yanai et al 2006 |
| | | | | GAD65 | perinuclear accumulation | Huang et al, 2004 |
| | | | | Synapto tagmin I | perinuclear accumulation | Huang et al, 2004 |
| | | | | GluR1, GluR2 | perinuclear targeting | Huang et al, 2009 |
| | | | | Lck | n/a | Fukata et al, 2004 |
| DHHC18 | ZDHHC18 | Golgi | brain, liver, | H-Ras | n/a | Fukata et al, 2004 |

| DHHC[a] (protein) | *ZDHHC*[a] (gene) | Localization | Tissue specificity[b] | Putative substrates | S-Palm Function | Ref. |
|---|---|---|---|---|---|---|
| | | | lung, GI tract, kidney, testis, placenta | Lck | n/a | Fukata et al, 2005 |
| DHHC19 | ZDHHC19 | TGN, perinuclear regions | brain, testis, placenta | R-Ras | plasma membrane association | Baumgart et al, 2010 |
| DHHC20 | ZDHHC20 | Plasma membrane | GI tract | δ-catenin | synapse efficacy/ protein interaction | Brigidi et al 2014 |
| DHHC21 | ZDHHC21 | golgi, | brain, liver, testis | Lck | plasma membrane assocation | Tsutsumi et al, 2009 |
| | | plasma membrane | | eNOS | perinuclear targeting | Fernández-Hernando et al, 2006 |
| | | | | sex steroid receptors (estrogen, progesterone, and androgen receptors) | plasma membrane assocation | Pedram et al, 2012 |
| | | | | PECAM-1 | membrane microdomain association | Sardjono et al 2006; Marin et al, 2012 |
| | | | | Fyn | Golgi targeting | Mill et al, 2009 |
| DHHC22 | ZDHHC13 | Golgi, ER | lung, GI tract, testis | MT1-MMP | cell migration | Song et al, 2014; Anilkumar et al 2005 |
| DHHC24 | ZDHHC22 | Golgi, ER | brain, eye, lung | BK | plasma membrane association | Tain et al, 2012 |
| | | | | Gp78 | peripheral ER targeting | Fairbank et al, 2012 |

[a] - The nomenclature of human DHHCs follows Ohno et al, 2012

[b] - www.proteinatlas.org & Korycka et al. 2012

### 1.1.3 DHHC substrate specificity

Through co-expression and knockdown studies, it has been revealed that some DHHCs show distinct substrate specificity while others exhibit promiscuity. How the substrate specificity is determined is unknown. Certain domains on a target protein can contribute to DHHC specificity. For example, Vac8 is S-palmitoylated specifically by the yeast DHHC, Pfa3, on cysteine residues in the SH4 domain of its N-terminal region. When the SH4 region of Vac8 is fused to GFP, the protein can still be palmitoylated by Pfa3. However, it loses the Pfa3 specificity since other PATs can also palmitoylate this fusion protein. This suggests that the region far from the S-palmitoylated cysteine residues is essential for determining substrate specificity (Nadolski and Linder, 2009). The localization of DHHCs may also determine the substrate specificity through DHHC-substrate interaction (Greaves et al, 2011).

### 1.1.4 Functions of S-Palmitoylation

S-palmitoylation has been reported to be involved in diverse physiological functions. These functions are summarized as follows.

**Membrane association.** For some cytosolic proteins, the function of S-acylation is coupled with other lipid modifications such as N-terminal Gly myristoylation or S-prenylation. The single lipid modification typically only leads to transient membrane interactions while dual fatty acylation can enhance stable membrane interactions (Shahinian and Silvius et al 1995). Moreover, some polybasic and hydrophobic amino acids can promote membrane association. The Ras and Gα subunit proteins are

examples of proteins that require dual lipid modifications for stable membrane interactions (Bijlmaker et al, 2003).

The function of S-palmitoylation of transmembrane proteins is less likely for stable membrane association. Rather, the S-palmitoylation on cysteine residues in the cytoplasmic region can modulate overall topology of the modified proteins relative to membrane (Chamberlain and Shipston, 2015).

**Protein targeting**. S-palmitoylation can regulate protein sorting or trafficking to distinct intracellular localizations. S-palmitoylation of several neuronal proteins plays an important role for sorting to dendrites or axons. Postsynaptic density-95 (PSD-95), typically localized in dendrites, undergoes S-palmitoylation which is critical for the dendritic targeting while the palmitoylated growth-associated protein-43 (GAP-43) mainly localized to axonal membranes. Replacing the N-terminal of PSD-95 with those of GAP-43 can redirect the targeting the GAP-43 to the axons (El-Husseini et al, 2001).

Targeting some proteins to the lipid rafts requires S-palmitoylation. The lipid raft microdomains are enriched with cholesterol and sphingolipids, and are resistant to detergent. The Src-family kinases, including LAT, Lck and Fyn, show S-palmitoylation-dependent raft association (Levental et al, 2010). Prevention of S-palmitoylation by using the DHHC pan-inhibitor, 2-bromopamitate, or replacing S-palmitoylation with unsaturated fatty acids led to the loss of detergent resistance, and a decrease in raft localization (Levental et al, 2010; Liang et al, 2001). Similarly, guanine-nucleotide-binding protein-α (Gα) subunits and the Ras family of GTPases, primarily H-Ras, N-Ras, and K-Ras, have been shown to be associated with detergent-resistant membrane

fractions only when they are palmitoylated (Levental et al, 2010). Therefore, S-palmitoylation is important for lipid raft partitioning.

S-palmitoylation has been recently related to cell migration of highly invasive breast cancer cells (MCF-10a and MDA-MB-231) (Babina et al, 2014). An adhesion protein, CD44, is an integral protein enriched in the lipid raft of highly metastatic cancer cells. Interestingly, it was demonstrated that S-palmitoylation of CD44 in the cytoplasmic tail regulates the cancer cell migration through its lipid raft localization. The non-palmitoylable CD44 mutant showed a decrease in lipid raft association, but increased the interaction with ezrin, and ultimately led to an enhanced cell migration. Since ezrin is an actin-binding linker, this S-palmitoylation effect might be mediated through the actin rearrangement. This study thus supports that the s-palmitoylation of CD44 regulates the breast cancer cell migration, and might be a future potential target for breast cancer therapeutics (Babina et al, 2014).

**Protein trafficking**. S-palmitoylation was found to mediate the trafficking of certain integral membrane proteins from the ER (Chamberlain and Shipston, 2015). For example, lipoprotein receptor-related proteins 6 (LRP6) undergoes S-palmitoylation on membrane proximity cysteine residue. Abrami and colleagues showed that the non-palmitoylable LRP6 mutant was retained in the ER, and failed to transport to the plasma membrane (Abrami et al, 2008). Interestingly, this study also demonstrated that S-palmitoylation of the cytosolic region of an integral protein can modulate the topology of the transmembrane domain (TMD). The TMD of LRP6 is predicted to be 23 amino acids long. With the perpendicular orientation, the LRP6 TMD is longer than the thickness of

ER membrane. This potentially leads to the hydrophobic mismatch and subsequently ER retention of a non-palmitoylable LRP6 mutant. However, the ER retention effect of non-palmitoylable mutant was rescued by the truncation of the LRP6 transmembrane domain (TMD). These results suggest that S-palmitoylation can tilt the LPR6 TMD and decrease the imbalance of the length between the TMD and the ER membrane (Abrami et al, 2008).

**Protein stability**. S-palmitoylation has been shown to prevent certain proteins from degradation, thereby increasing protein stability. Anthrax toxin receptor (ATR, also known as TEM8) is an integral membrane containing S-palmitoylation on a juxtamembrane cysteine residue. The non-palmitoylable TEM8 mutant showed lower expression than the wild type TEM8. Based on pulse-chase experiments using [$^{35}$S] cysteine/methionine labeling, the non-palmitoylable TEM8 mutant had a shorter half-life than the TEM8 wild type. When the cells were treated with the lysosomal enzyme inhibitor, leupeptin, there was an increase in expression of the TEM8 mutant, while less effect was observed on the TEM8 wild type. This suggests that S-palmitoylation of TEM8 can regulate the proteins lifetime by preventing premature targeting to lysosomes (Abrami et al, 2006). Similar roles of S-palmitoylation in preventing protein from lysosomal degradation was also observed in the death receptor, Fas (CD95, TNFRSF6), and the chemokine and HIV receptor, CCR5 (Rossin et al, 2014; Percherancier et al, 2001). S-palmitoylation thus can protect certain proteins from lysosomal degradation and therefore enhance the protein stability.

The S-palmitoylation of the yeast SNARE, called “T-SNARE affecting a late Golgi compartment protein1” or Tlg1, can prevent its ubiquitination and degradation (Taubas and Pelham, 2005). Tlg1 is palmitoylated by SWF1, an ER-localized DHHC protein. Typically, Tlg1 is localized in the TGN/endosomal membrane. However, the deletion of the *swf1* gene results in the mis-localization of Tlg1 to the vacuole and a reduced half-life of Tlg1. It was found that the non-palmitoylated Tlg1 can be recognized and ubiquitinated by the ubiquitin ligase Tul1, which promotes targeting of Tlg1 to the multivesicular bodies (MVBs) and ultimately the vacuole for degradation. Therefore, S-palmitoylation of Tlg1 can prevent recognition by Tul1 and thus protein degradation (Taubas and Pelham, 2005).

### 1.1.5 Depalmitoylation

The removal of S-palmitoylation, or depalmitoylation, is mediated by thioesterases. Three types of these enzymes have been identified so far, including acyl protein thioesterase-1 (APT1, also known as lysophospholipase 1 (LYPLA1)), acyl protein thioesterase-2 (APT2, also known as lysophospholipase 2 (LYPLA2)) and palmitoyl-protein thioesterase 1 (PPT1) (Koycka et al, 2012).

APT1 is mainly localized in the cytosol, and is thought to play a role in regulating the intracellular dynamics of S-palmitoylated proteins. APT1 has been reported to remove palmitoyl groups from $G_{\alpha}$, H-Ras, eNOS, SNAP-23 (Koycka et al, 2012; Salaun et al, 2010) and NMNAT2 (Milde et al, 2014). It remains elusive how APT1 get access to these membrane associated targets. One possibility is that the S-palmitoylation of

APT1 mediates the tethering of enzyme to the membrane, thereby making its targets accessible (Koycka et al, 2012).

APT2, with the 65% sequence similarity to APT1, is mostly localized in the cytosol. It has been reported that APT2 can catalyze the depalmitoylation of GAP-43. APT2 is endogenously expressed in both HeLa and CHO-K1 cells. Its overexpression can enhance the depalmitoylation rate of GAP-43 while APT1 did not (Tomatis et al, 2010). However, overexpression of APT1 or APT2 can decrease the palmitoylation of NMNAT2 suggesting that these enzymes do have some redundant functions (Mlide et al, 2014; Davda et al, 2014).

PPT1 is predominantly localized in the lysosomal lumen, where protein degradation occurs (Hellsten et al, 1996), but it is potentially also localized in the cytosol (Kim et al, 2008). PPT1 showed thioesterase activity on different $G_{\alpha}$ subunits and H-Ras (Salaun et al, 2010). A mutation in the *PPT1* gene has been linked to the common progressive encephalopathy called neuronal ceroid lipofuscinoses (NCL) in young children (Vesa et al, 1995). Recently, PPT1 was found to be palmitoylated by DHHC3 and DHHC7, and the non-palmitoylable PPT1 showed an increase in depalmitoylation activity (Segal-Salto et al, 2016).

So far, it remains unclear whether these depalmitoylation enzymes recognize any consensus sequence on the substrates.

### 1.1.6 Inhibition of S-palmitoylation/depalmitoylation

The most commonly used inhibitor for S-palmitoylation, for both *in vitro* and *in vivo* studies, is the palmitate analog 2-bromopalmitate (2-BP) (Pedro et al. 2014). Resh and colleagues discovered that 2-BP can inhibit S-palmitoylation on Src-kinases, Fyn, Lck, and LAT, thereby decreasing the localization of these proteins to lipid rafts (Webb et al, 2000). It has been used to study the effect of palmitoylation on several proteins including Rho, H-Ras, and Src kinases (Draper and Smith, 2009). However, 2-BP does not selectively inhibit DHHCs. It has been reported to inhibit several other enzymes, including those in the lipid metabolism pathway (fatty acid CoA ligase and glycerol-3-phosphate acyltransferase), NADPH cytochrome-c reductase, and glucose-6-phosphatase (Coleman et al, 1992). Moreover, 2-BP was recently found to inhibit the activity of both APT1 and APT2 *in vitro* (Pedro et al. 2014). Therefore, the effect of 2-BP on S-palmitoylation should be interpreted with caution. Other lipid-based palmitoylation inhibitors have been developed, such as tunicamycin and cerulenin analogs (Draper and Smith, 2009). However, none of these inhibitors are highly potent and selective for DHHCs (Tate et al, 2015).

Several small molecules have been developed for inhibiting thioesterase (APT1, APT2) activities. Palmostatin B, an APT1 inhibitor, was developed by Waldmann and co-workers. It can inhibit the depalmitoylation of Ras *in vivo*, leading to the disruption of the Golgi-targeting and downregulation of oncogenic signaling (Dekker et al, 2010). However, it seems likely that Palmostatin B does not only inhibit APT1, but also APT2. Several other APT1 and APT2 inhibitors have been reported with different levels of potency and selectivity (Davda et al, 2014). The Cravatt group reported selective APT1

and APT2 inhibitors. These inhibitors (compound 1 and 21) are piperazine amides that were shown to selectively inhibit APT2 and APT1, respectively, in both *in vitro* and *in vivo* studies (Adibekian et al, 2012). These inhibitors, therefore, could be useful for studying the physiological functions of APTs in the living systems.

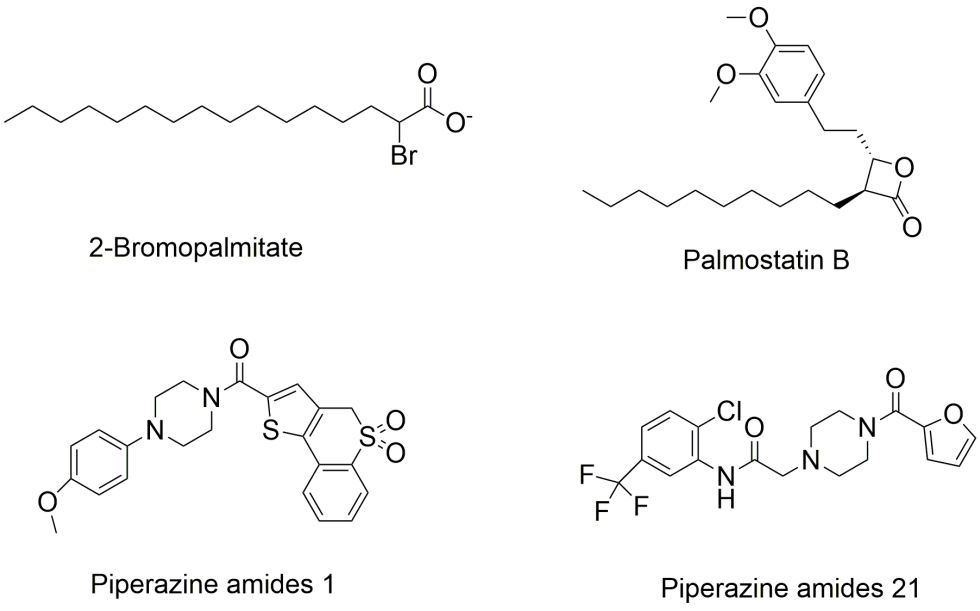


**Figure 1.3. The chemical structures of different inhibitors of DHHCs and APTs.** Pan-DHHC inhibitor (2-Bromopalmitate), APT inhibitors (Palmostatin B), APT2 selective inhibitor (piperazine amide 1), and APT1 selective inhibitor (piperazine amide 21).

### 1.1.7 Methods to detect S-acylation

The study of S-palmitoylation has previously relied on growing cells in radioactive ([$^{3}$H]-palmitate or [$^{125}$I]-palmitate) containing media, and then detecting S-palmitoylation on proteins with autoradiography. However, the sensitivity of this method is quite low and long exposure time is required.

A more sensitive technique to detect the S-palmitoylation, developed by Drisdel and Green, is the acyl-biotin exchange (ABE) method (Drisdel and Green, 2004). In this method, cell lysates are first treated with N-ethylmaleimide (NEM), which forms a stable covalent linkage to the free thiol groups, thereby blocking the free cysteine residues. The palmitate groups on cysteine residues are then removed by hydroxylamine treatment, and the thiol-reactive biotin analogues (BMCC, 1-biotinamido-4-(4′-(maleimidoethyl-cyclohexane) carboxamido) butane) are added to cross link with the free thiol cysteine residues. The biotinylated proteins are then purified by using the streptavidin beads and eluted for resolving on SDS-PAGE gel and western blot or analyzing by mass spectrometry (Linder and Deschenes, 2007). Nevertheless, the disadvantages of this technique are a high false positive rate due to the incomplete blocking of reduced cysteines, and the loss of S-palmitoyl group during analysis (Martin et al, 2009; Tate et al, 2015).

Another method for studying of S-palmitoylation is the direct metabolic incorporation of palmitic acids analogues into the proteins with S-palmitoylation. These analogues are Alkyne14 (Alk14) and 17-octadecynoic acid (17-ODYA), which are commercially available. The modified proteins are then conjugated with either a fluorescence tag (e.g. Bodipy-azide and Rhodamine azide) or affinity tag (e.g. biotin

azide) using copper-catalyzed click chemistry. The S-palmitoylated proteins are subsequently resolved by SDS-PAGE for fluorescence imaging or characterized by LC-MS (Yount et al, 2011; Martin et al, 2009; Martin et al, 2011).

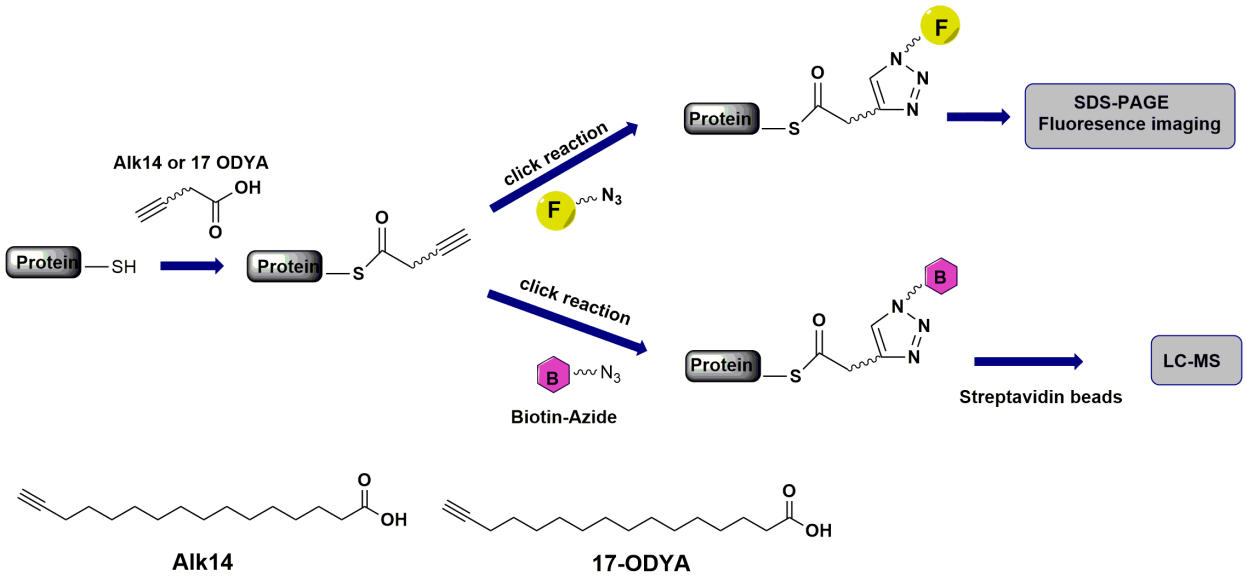


**Figure 1.4. Metabolic labeling of S-palmitoylated proteins.** Cells are cultured with the fatty acid probe (Alk14 or 17-ODYA). A fluorescent reporter or an affinity handle is then conjugated to the acylated proteins via click chemistry. The S-palmitoylated proteins are subsequently detected by fluorescence imaging or characterized by LC-MS.

## 1.2 LYSINE SIDE-CHAIN FATTY ACYLATION

Lysine side-chain fatty acylation was first discovered over two decades ago in both prokaryotic and eukaryotic cells. Revealed through [$^3$H] myristic acid labeling, the cytochrome C oxidase 1 subunit 1 of Neurospora crassa, a filamentous fungus, is myristoylated on a lysine residue in the predicted transmembrane domain of the protein. The function of this modification is likely for interacting with other subunit of Cytochrome C oxidase complex (Vassilev et al, 1995).

*E coli* hemolysin (HlyA) is a toxin that forms a pore on the host cells and modulates the membrane permeability, leading to the cell lysis and death. It was found that the N-lysine myristoylation on K564 and K690 residues of HlyA is required for pore formation and its hemolytic activity. This lysine modification was found to be regulated by a specific acyl transferase, HlyC that utilizes a myristoyl group-tethering acyl carrier protein (acyl-ACP) as a myristoyl donor (Stanley et al, 1998).

Reported N-lysine myristoylated proteins from mammalian cells are all inflammatory cytokines, including tumor necrosis factor (TNF-α), interleukin-1 alpha (IL-1α) and interleukin-1 beta (IL-1β). The N-lysine myristoylation was found on K19 and K20 residues of the TNF-α, and on K82 and K83 residues of IL-1α. IL-1β, sharing amino acid sequence similarity with IL-α, was also N-lysine myristoylated but with lower efficiency than IL-1α. This modification on TNF-α is involved in regulating its secretion since demyristoylation of TNF-α by SIRT6 promotes its secretion (Jiang et al, 2013). It was shown later that the N-lysine myristoylation of TNF-α can mediate the lysosome targeting and this explains why demyristoylation can increase the protein secretion (Jiang et al, 2016). The function of the lysine-myristoylation on both IL-1α and IL-1β,

however, remains unclear, but it is possible it plays a role in facilitating the membrane association of these proteins (Stevenson et al, 1992 and Stevenson et al, 1993).

## 1.3 LYSINE SIDE-CHAIN DEFATTY-ACYLATION

### 1.3.1 Sirtuins

Recently, it has been discovered that several of the nicotinamide adenine dinucleotide ($NAD^+$)-dependent deacetylases, known as “sirtuins”, can catalyze lysine defatty-acylation (Jiang et al, 2013; Feldman et al, 2013; Teng, 2015). Mammalian sirtuins consist of SIRT1-7 and they are classified into four classes on the basis of sequence similarity. These sirtuins are localized at different organelles as shown in Table 1.3 (Houtkooper et al, 2012; Breda et al, 2016).

**Table 1.3 Sirtuin classification, localization and enzymatic activities**

| Class | sirtuins | intracellular localization | catalytic activity |
|---|---|---|---|
| I | SIRT1 | Nucleus, cytosol | deacetylation, defatty-acylation |
| | SIRT2 | Cytosol | deacetylation, defatty-acylation |
| | SIRT3 | Mitochondria | deacetylation, defatty-acylation |
| II | SIRT4 | Mitochondria | weak deacetylation, ADP-ribosylation |
| III | SIRT5 | Mitochondria | weak deacetylation, demalonylation, desuccinylation |
| IV | SIRT6 | Nucleus | weak deacetylation, ADP-ribosylation, defatty-acylation |
| | SIRT7 | Nucleolus | weak deacetylation |

Several crystal structures of sirtuin in complex with different ligands have been reported. In general, the conserved catalytic core of sirtuins is composed of a $Zn^{2+}$-binding domain which is a small domain derived from two insertions of the large domain called a Rossman fold domain as shown in Figure 1.5. The acylated substrate and $NAD^+$ bind to the cleft between these two domains (Breda et al, 2016).

The $NAD^+$-dependent catalytic mechanism of sirtuins begins with a nucleophillic attack of a carbonyl oxygen of acyl-lysine to the C1' position of the ribose in $NAD^+$. The nicotinamide is released and the alkylamidate intermediate (intermediate I) is formed. Then, a conserved histidine residue in the catalytic domain acts as a general base to deprotonate the 2'-OH of the ribose, and the 2′-O subsequently attacks the alkylamidate intermediate to generate a 1′, 2′-cyclic intermediate (intermediate II). The cyclic intermediate is then hydrolyzed to lysine-deacylated product and 2′-*O*-acyl-ADP-ribose which can be automatically isomerized to 3′-*O*-acyl-ADP-ribose (Figure 1.6) (Breda et al, 2016).

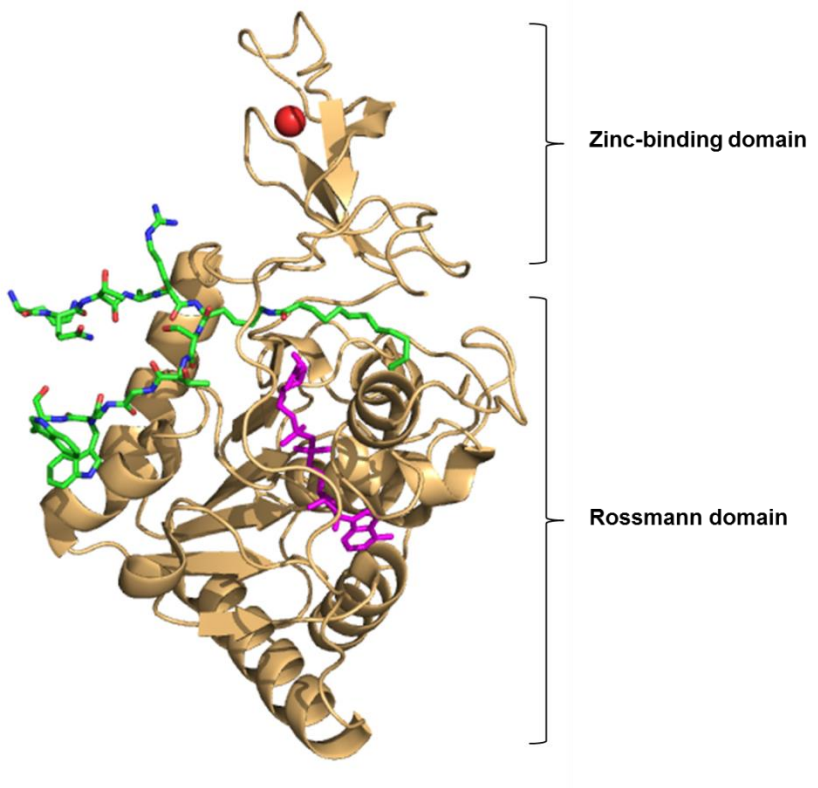


**Figure 1.5.** Overall structure of sirtuin (SIRT6) in complex with a H3K9 myristoyl peptide (green), ADP-ribose (pink) and zinc (red) bound. The protein picture is generated using Pymol (PDB ID: 3ZG6)

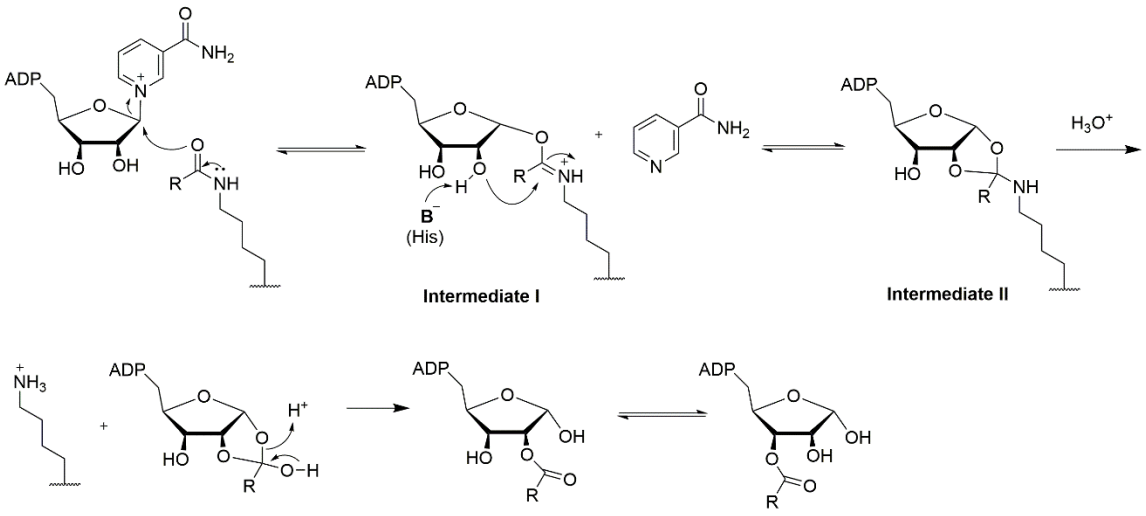


**Figure 1.6. Catalytic mechanism of sirtuins is dependent on $NAD^+$**

Different from other sirtuins, SIRT4, SIRT5, SIRT6 and SIRT7, have a very weak deacetylase activity. SIRT5 has been shown to possess demalonylase and desuccinase activities. SIRT6 can hydrolyze the long chain fatty acyl groups and TNFα as a lysine defatty-acylation target of SIRT6. Interestingly, SIRT6 promotes the TNFα secretion through its lysine defatty-acylase activity (Jiang et al, 2013). Similarly, other sirtuins, including SIRT1, SIRT2 and SIRT3 also show defatty-acylation activity. Interestingly, the defatty-acylation efficiency is comparable to the to the deacetylation catalytic efficiency (Feldman et al, 2013; Teng et al, 2015).

Besides mammalian sirtuins, Zhu et al demonstrated that the *Plasmodium falciparum* sirtuin, or PfSir2A, can remove long chin fatty acyl group. From a detailed kinetic study, the demyristoylation catalytic efficiency is hundreds-fold better than that of the deacetylation. The increased $k_{cat}$, and the lower $K_m$ for the demyristoylation activity resulted in the increased catalytic efficiency. Moreover, the crystal structure of PfSir2A in complex with a myristoyl H3K9 peptide shows that PfSir2A can accommodate the long chain fatty acyl group in the enzyme active site. These results suggest that the demyristoylation of PfSir2A might be physiological relevant (Zhu et al, 2012).

### 1.3.2 HDACs

The metal ion-dependent histone deacetylases (HDACs) are a family of enzymes that play essential roles in diverse biological processes through the deacetylation of lysine residues on both histone and non-histone proteins. Histone acetylation by histone acetyltransferases (HATs) can neutralize the positive charges on lysine residues at histone tails. Histone acetylation leads to the relaxing of the chromatin structure and the histones are then accessible to transcription factors, thereby activating the transcription. In contrast, the deacetylation of histone residues by HDACs serves as a repressor of transcription as shown in Figure 1.7. This dynamic process has been implicated in developmental processes and the aberrant regulation results in several diseases (West et al, 2014).

#### 1.3.2.1 HDAC classification

Based on sequence homology and phylogenetic analysis, mammalian HDACs are classified into four classes. Class I, homologous to yeast Rpd3, consists of HDAC 1, 2, 3 and 8. They are ubiquitously expressed, and predominantly localized in the nucleus except for HDAC3 and HDAC8 which are found in both the nucleus and the cytosol (Yao et al, 2011, Waltregny et al, 2005; Yamauchi et al, 2011). HDAC1 and HDAC2, have very similar sequences, and are found to associate with each other, as well as with other protein complexes, including CoRest, NuRD, Sin3, and PML. HDAC3 is associated with other distinct protein complexes, including HDAC4, HDAC5, HDAC7, and NCoR/SMRT. In contrast, HDAC8 has not been found associated to any proteins (Yang et al, 2008).

The class II HDACs, homologous to yeast Hda1, are divided into two subclasses: IIa (HDAC 4, 5, 7, 9) and IIb (HDAC 6, 10). The Class IIa HDACs can shuttle between the nucleus and cytoplasm, and the expression pattern is tissue-restricted as shown in Table 1.4. The N-terminus of the class IIa HDACs contains a conserved binding sites for the myocyte enhancer factor2 (MEF2) transcription factor, and a chaperone protein, called 14-3-3. It has been shown that the class IIa HDACs specifically interact with, and suppress the MEF2 transcription factor. Once the class IIa HDACs are dissociated from MEF-2, the protein acetyltransferases, p300 is able to associate with MEF2 and convert it to a transcriptional activator (Lu et al, 2000). The class IIa HDACs distinctively contain a conserved histidine residue in the active site, while it is a tyrosine residue in other HDACs. This tyrosine residue, in the other HDAC classes, serves as a transition state stabilizer in the catalytic reaction. The replacement of the tyrosine residue with a histidine residue in the active site of the class IIa HDACs leads to low deacetylation activity, which can be restored by mutating the histidine to a tyrosine residue (Jones et al, 2008). The class IIb HDACs are mainly localized in the cytosol. HDAC6 is unique as it contains two catalytic domains with a zinc finger in the C-terminal region. The functions and targets of HDAC10 are unclear.

The nicotinamide adenine dinucleotide ($NAD^+$)-dependent deacylases or sirtuins (described in 1.3.1) are annotated as Class III HDACs, although their catalytic mechanism is totally different from the metal ion-dependent HDACs. HDAC11 is the only member in Class IV HDACs. HDAC11 contains a deacetylase domain homologous to both class I and class II HDACs. HDAC11 is localized in the cytosol, but also can

shuttle between the nucleus and cytosol, and is highly expressed in muscle, brain, and kidney tissues. The function of HDAC11 still remains elusive (Haberland et al, 2009).

Based on gene deletion study, HDACs have been implicated in development. Various physiological functions have been associated with each HDAC through HDAC knockout in mice. While each HDAC may have its own physiological effect, some have redundant functions as summarized in Table 1.3 (Haberland et al, 2009).

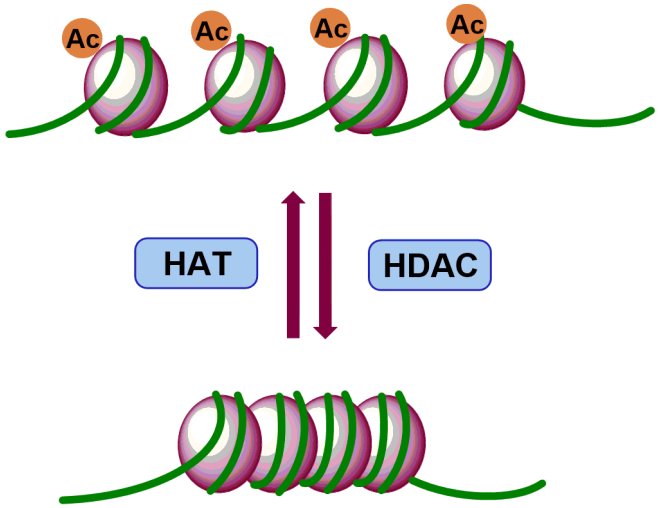


**Figure 1.7. The Histone acetyltransferase (HAT) and Histone deacetylase (HDAC) families.** Dynamics of global histone acetylation and deacetylation modulates the chromatin structure leading to either transcription activation or repression

**Table 1.4 Summary of HDAC families with associated proteins, role in development and related inhibitors**

| Class | HDAC | associated proteins[a] | tissue specificity[b] | phenotypes from HDAC knockout mice[c] | selective inhibitors[d] |
|---|---|---|---|---|---|
| I | 1 | HDAC2, Sin3, NuRD, CoREST, PRC2, PML, BCL6, PLZF, AR, ER, Rb/E2F1, AML-ETO, p53 | Ubiquitously expressed | - die before embryonic day 10.5 with preliferation defect and growth retardation<br>- increased level of p21 and p27 | MRLB-223, compound 60 |
| | 2 | HDAC1, Sin3, NuRD, CoREST, PRC2, PML, BCL6, PLZF, AML1-ETO | | -die within 24 hrs with severe cardiac malfunction | MRLB-223, compound 60 |
| | 3 | HDAC4, HDAC5, HDAC7 NCoR-SMRT, STAT1, STAT3, GATA1, GATA2, NF-αB, BCL6, PML, PLZF | | -die before embryonic day 9.5 with gastrulation defect | RG2833, RGFP966, BG45 |

| Class | HDAC | associated proteins[a] | tissue specificity[b] | phenotypes from HDAC knockout mice[c] | selective inhibitors[d] |
|---|---|---|---|---|---|
| | 8 | | | -die after birth with skull instability | PCI-34051, C149, Jδ, BRD73954 |
| IIa | 4 | HDAC3-NCoR,HP1, CTBP1, GATA1 | brain, growth plates of the skeleton | -die within 14 days with ectopic ossification (the transformation of the cartilage into bone) | |
| | 5 | HDAC3-NCoR, GATA1, GATA2 | brain, heart, muscle | -viable<br>-die with myocyte differentiation and proliferation defects if knocked out with HDAC9 | |
| | 7 | HDAC3-NCoR, Erα | thymocytes, endothelial cells | -die with endothelial cell differentiation defect | |
| | 9 | | brain, heart, muscle | -viable but very sensitive to denervation-induced changes in gene expression<br>-die with myocyte differentiation and proliferation defects if knocked out with | |

| Class | HDAC | associated proteins[a] | tissue specificity[b] | phenotypes from HDAC knockout mice[c] | selective inhibitors[d] |
|---|---|---|---|---|---|
| | | | | HDAC5 | |
| IIb | 6 | alpha-tubulin, HSP90, HDAC11 | kidney, testis | -viable with tubulin hyperacetylation | Rocilinostat (ACY-1215), ACY-738, ACY-775, Tubacin, Tubastatin A, C1A, HPOB, Quinazolin-4-one derivatives, BRD73954 |
| | 10 | | brain, lung, kidney | n/a | |
| IV | 11 | HDAC6 | n/a | n/a | |

[a], West et al, 2014

[b], Haberland et al, 2009 and http://www.proteinatlas.org

[c], Haberland et al, 2009

[d], Falkenberg and Johnstone, 2014

#### 1.3.2.2 HDAC structure

The crystal structure of human HDAC in complex with different inhibitors revealed a single α/β-domain with a core eight-stranded parallel β-sheet and 11 α-helices as shown in Figure 1.8 (Somoza et al, 2004; Vannini et al, 2004; Vannini et al, 2007). The HDAC active site contains a long and narrow tunnel, and the wall is formed by hydrophobic amino acids (F152, F208, H180, G151, M274, and Y306 in HDAC8) (Somoza et al, 2004).

Interestingly, structural comparisons between class I HDACs and histone deacetylase-like protein (HDLP) demonstrated that HDAC8 has two unique features. First, HDAC8 has a shorter C-terminal domain, thereby lacking the region extended from the catalytic domain. This region in other HDACs is typically responsible for recruiting other proteins to form a complex. Therefore, large complexes are generally formed by HDAC1, 2 and 3, but not by HDAC8 (Haberland et al, 2009). Second, the L1 loop (amino acids residue S30-K36) at the N-terminus of HDAC8 is distinct in both size and sequence from other class I HDACs.

The unique L1 loop causes HDAC8 to have a wider active pocket and larger surface opening. Interestingly, structural complexes between HDAC8 and inhibitors showed the structural variation at the protein surface around the active site mediated by L1 loop suggesting that this region was conformational flexible and may accommodate different substrates. These distinguished HDAC8 features imply the different physiological functions of the enzyme from other class I HDACs (Somoza et al, 2004).

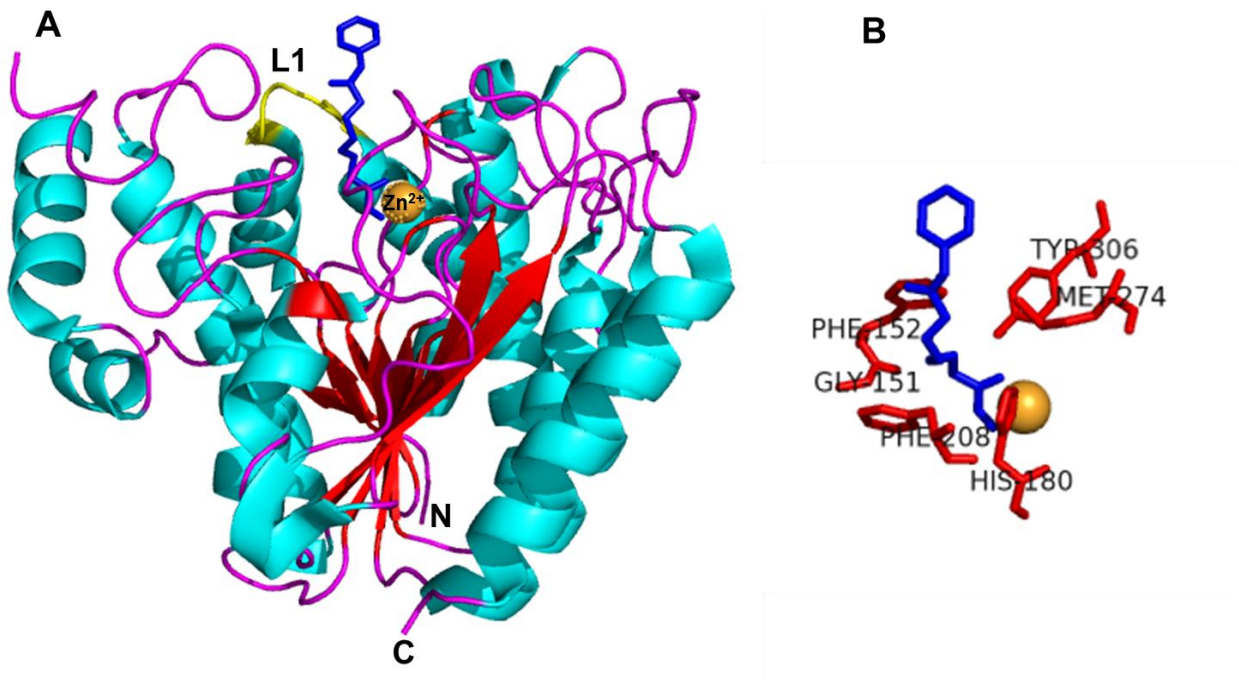


**Figure 1.8. A, Overall structure of HDAC using HDAC8 as a model.** SAHA (blue) and the L1 loop (S30-K36, yellow) of HDAC8 are shown. B, Hydrophobic residues in the HDAC8 active site. The protein structure picture is generated using PyMol, PDB ID: 1T69.

### 1.3.2.3 HDAC Catalytic Mechanism

HDAC1-11 have a homologous catalytic site that requires zinc for catalysis. Based on biochemical and structural studies of HDACs and HDLP (Histone deacetylase-like protein in bacteria), an HDAC catalytic mechanism has been proposed (Figure 1.9A). The reaction begins with the nucleophillic attack of the $Zn^{2+}$ bound-water molecule at the carbonyl group of the acetyl lysine substrate. The $Zn^{2+}$ ion lowers the pKa of the water making it more nucleophillic. His142 (HDAC8 number) also facilitates this step by acting as a general base, and the tetrahedral intermediate is stabilized by

the hydroxyl group of Tyr306. His143 then acts as a general acid, as it is protonated during the formation of the tetrahedral intermediate. As a general acid, His143 is able to facilitate the leaving of the amino group of the lysine residue (Finnin et al, 1999).

An alternative catalytic mechanism based on molecular dynamics simulation was proposed by the Zhang lab, as shown in Figure 1.9B (Chen et al, 2014; Wu et al, 2010). In this mechanism, His143 acts both as the general base to receive a proton from water to form tetrahedral intermediate, and as the general acid to cleave the intermediate. His142, however, is not directly involved in the reaction. Instead, it promotes the reaction by hydrogen bonding with the water molecule at the initial step of the reaction.

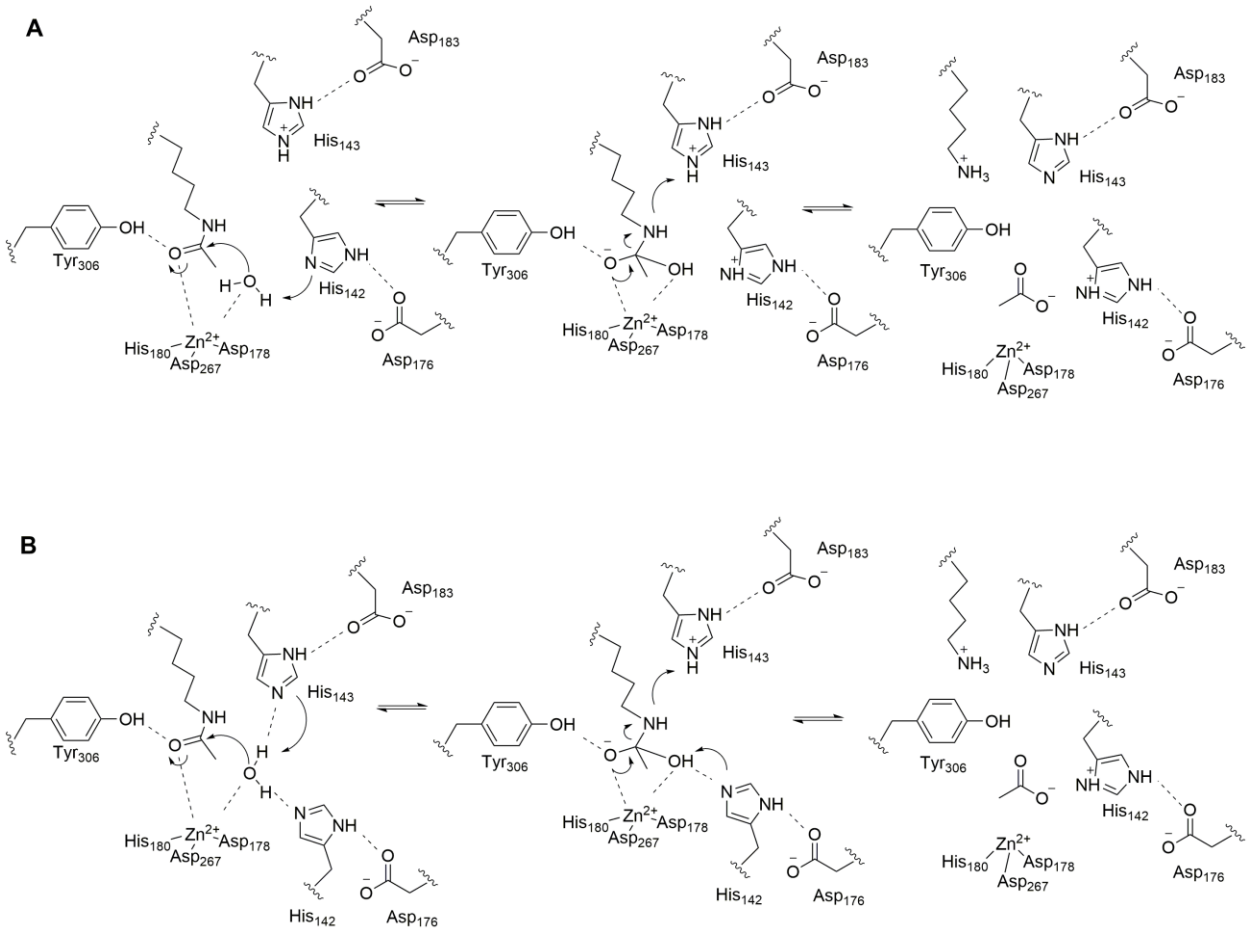


**Figure 1.9. The catalytic mechanisms of HDAC.** A. The catalytic mechanism proposed based on biochemical and structural studies. His143 and His142 in HDAC8 act as a general base and a general acid, respectively (Finnin et al, 1999). B. The catalytic mechanism proposed based on molecular dynamics simulation. H143 in HDAC8 acts both the general base and acid (Wu et al, 2010).

## 1.4 RELEVANCE OF MY DISSERTATION RESEARCH TO S-ACYLATION AND LYS-ACYLATION

S-palmitoylation has been implicated in numerous biological processes. Due to advances in proteomic technologies, the number of S-palmitoylated proteins has markedly increased. Nevertheless, only several S-palmitoylated proteins have been extensively studied suggesting that most of these S-palmitoylated proteins identified through recent proteomics studies have not been well characterized. In the second chapter of this dissertation, I investigated the S-palmitoylation on Junctional adhesion molecule C (JAM-C), a type I transmembrane protein containing two conserved cysteine residues, and characterized both the biochemical and biological functions of this modification.

Different from S-acylation, lysine side-chain fatty acylation is not well-known. Our lab previously demonstrated that certain $NAD^+$-dependent deacetylases or sirtuins (SIRT1, SIRT2, SIRT3 and SIRT6) can catalyze lysine defatty-acylation. SIRT6 can remove lysine fattyacylation on TNFα and this defatty-acylation can regulate TNFα secretion. This suggests that lysine (de)fattyacylation is physiologically relevant. In the third part of this dissertation, I investigated if the zinc-dependent deacetylases, or HDACs, would also possess defatty-acylation activity, similar to the activity observed with some sirtuins. Considering the low deacetylase activity compared to other class I HDACs, we chose HDAC8 for defatty-acylase activity screening.

The last part of this dissertation is a discussion of the questions that still remain regarding both the S-acylation on JAM-C and lysine defatty-acylation activity of HDAC8. The future directions aim to further elucidate the novel enzymatic activity of HDAC8

through identification of defatty-acylation targets. Understanding the role of this post-translational modification will provide more insight into lysine fatty acylation as well as expand the physiological roles of HDAC8.

## 1.5 REFERENCES

Abrami, L., Kunz, B., Iacovache, I., and van der Goot, F. G. (2008) Palmitoylation and ubiquitination regulate exit of the Wnt signaling protein LRP6 from the endoplasmic reticulum. Proc Natl Acad Sci U S A 105, 5384-5389

Abrami, L., Leppla, S. H., and van der Goot, F. G. (2006) Receptor palmitoylation and ubiquitination regulate anthrax toxin endocytosis. J Cell Biol 172, 309-320

Adibekian, A., Martin, B. R., Chang, J. W., Hsu, K. L., Tsuboi, K., Bachovchin, D. A., Speers, A. E., Brown, S. J., Spicer, T., Fernandez-Vega, V., Ferguson, J., Hodder, P. S., Rosen, H., and Cravatt, B. F. (2012) Confirming target engagement for reversible inhibitors in vivo by kinetically tuned activity-based probes. J Am Chem Soc 134, 10345-10348

Anilkumar, N., Uekita, T., Couchman, J. R., Nagase, H., Seiki, M., and Itoh, Y. (2005) Palmitoylation at Cys574 is essential for MT1-MMP to promote cell migration. FASEB J 19, 1326-1328

Babina, I. S., McSherry, E. A., Donatello, S., Hill, A. D., and Hopkins, A. M. (2014) A novel mechanism of regulating breast cancer cell migration via palmitoylation-dependent alterations in the lipid raft affiliation of CD44. Breast Cancer Res 16, R19

Baumgart, F., Corral-Escariz, M., Perez-Gil, J., and Rodriguez-Crespo, I. (2010) Palmitoylation of R-Ras by human DHHC19, a palmitoyl transferase with a CaaX box. Biochim Biophys Acta 1798, 592-604

Bijlmakers, M. J., and Marsh, M. (2003) The on-off story of protein palmitoylation. Trends Cell Biol 13, 32-42

Brigidi, G. S., Sun, Y., Beccano-Kelly, D., Pitman, K., Mobasser, M., Borgland, S. L., Milnerwood, A. J., and Bamji, S. X. (2014) Palmitoylation of delta-catenin by DHHC5 mediates activity-induced synapse plasticity. Nat Neurosci 17, 522-532

Chamberlain, L. H., and Shipston, M. J. (2015) The physiology of protein S-acylation. Physiol Rev 95, 341-376

Charollais, J., and Van Der Goot, F. G. (2009) Palmitoylation of membrane proteins (Review). Mol Membr Biol 26, 55-66

Chen, K., Zhang, X., Wu, Y. D., and Wiest, O. (2014) Inhibition and mechanism of HDAC8 revisited. J Am Chem Soc 136, 11636-11643

Chen, Z. Q., Ulsh, L. S., DuBois, G., and Shih, T. Y. (1985) Posttranslational processing of p21 ras proteins involves palmitylation of the C-terminal tetrapeptide containing cysteine-186. J Virol 56, 607-612

Coleman, R. A., Rao, P., Fogelsong, R. J., and Bardes, E. S. (1992) 2-Bromopalmitoyl-CoA and 2-bromopalmitate: promiscuous inhibitors of membrane-bound enzymes. Biochim Biophys Acta 1125, 203-209

Davda, D., and Martin, B. R. (2014) Acyl protein thioesterase inhibitors as probes of dynamic S-palmitoylation. Medchemcomm 5, 268-276

Dekker, F. J., Rocks, O., Vartak, N., Menninger, S., Hedberg, C., Balamurugan, R., Wetzel, S., Renner, S., Gerauer, M., Scholermann, B., Rusch, M., Kramer, J. W., Rauh, D., Coates, G. W., Brunsveld, L., Bastiaens, P. I., and Waldmann, H. (2010) Small-molecule inhibition of APT1 affects Ras localization and signaling. Nat Chem Biol 6, 449-456

Draper, J. M., and Smith, C. D. (2009) Palmitoyl acyltransferase assays and inhibitors (Review). Mol Membr Biol 26, 5-13

Drisdel, R. C., and Green, W. N. (2004) Labeling and quantifying sites of protein palmitoylation. Biotechniques 36, 276-285

Duncan, J. A., and Gilman, A. G. (1996) Autoacylation of G protein alpha subunits. J Biol Chem 271, 23594-23600

El-Husseini Ael, D., Craven, S. E., Brock, S. C., and Bredt, D. S. (2001) Polarized targeting of peripheral membrane proteins in neurons. J Biol Chem 276, 44984-44992

Fairbank, M., Huang, K., El-Husseini, A., and Nabi, I. R. (2012) RING finger palmitoylation of the endoplasmic reticulum Gp78 E3 ubiquitin ligase. FEBS Lett 586, 2488-2493

Falkenberg, K. J., and Johnstone, R. W. (2014) Histone deacetylases and their inhibitors in cancer, neurological diseases and immune disorders. Nat Rev Drug Discov 13, 673-691

Feldman, J. L., Baeza, J., and Denu, J. M. (2013) Activation of the protein deacetylase SIRT6 by long-chain fatty acids and widespread deacylation by mammalian sirtuins. J Biol Chem 288, 31350-31356

Fernandez-Hernando, C., Fukata, M., Bernatchez, P. N., Fukata, Y., Lin, M. I., Bredt, D. S., and Sessa, W. C. (2006) Identification of Golgi-localized acyl transferases that palmitoylate and regulate endothelial nitric oxide synthase. J Cell Biol 174, 369-377

Finnin, M. S., Donigian, J. R., Cohen, A., Richon, V. M., Rifkind, R. A., Marks, P. A., Breslow, R., and Pavletich, N. P. (1999) Structures of a histone deacetylase homologue bound to the TSA and SAHA inhibitors. Nature 401, 188-193

Fredericks, G. J., Hoffmann, F. W., Rose, A. H., Osterheld, H. J., Hess, F. M., Mercier, F., and Hoffmann, P. R. (2014) Stable expression and function of the inositol 1,4,5-triphosphate receptor requires palmitoylation by a DHHC6/selenoprotein K complex. Proc Natl Acad Sci U S A 111, 16478-16483

Fukata, M., Fukata, Y., Adesnik, H., Nicoll, R. A., and Bredt, D. S. (2004) Identification of PSD-95 palmitoylating enzymes. Neuron 44, 987-996

Fukata, Y., Dimitrov, A., Boncompain, G., Vielemeyer, O., Perez, F., and Fukata, M. (2013) Local palmitoylation cycles define activity-regulated postsynaptic subdomains. J Cell Biol 202, 145-161

Gorleku, O. A., Barns, A. M., Prescott, G. R., Greaves, J., and Chamberlain, L. H. (2011) Endoplasmic reticulum localization of DHHC palmitoyltransferases mediated by lysine-based sorting signals. J Biol Chem 286, 39573-39584

Greaves, J., and Chamberlain, L. H. (2011) DHHC palmitoyl transferases: substrate interactions and (patho)physiology. Trends Biochem Sci 36, 245-253

Greaves, J., Gorleku, O. A., Salaun, C., and Chamberlain, L. H. (2010) Palmitoylation of the SNAP25 protein family: specificity and regulation by DHHC palmitoyl transferases. J Biol Chem 285, 24629-24638

Haberland, M., Mokalled, M. H., Montgomery, R. L., and Olson, E. N. (2009) Epigenetic control of skull morphogenesis by histone deacetylase 8. Genes Dev 23, 1625-1630

Haberland, M., Montgomery, R. L., and Olson, E. N. (2009) The many roles of histone deacetylases in development and physiology: implications for disease and therapy. Nat Rev Genet 10, 32-42

He, M., Abdi, K. M., and Bennett, V. (2014) Ankyrin-G palmitoylation and betaII-spectrin binding to phosphoinositide lipids drive lateral membrane assembly. J Cell Biol 206, 273-288

Hellsten, E., Vesa, J., Olkkonen, V. M., Jalanko, A., and Peltonen, L. (1996) Human palmitoyl protein thioesterase: evidence for lysosomal targeting of the enzyme and disturbed cellular routing in infantile neuronal ceroid lipofuscinosis. EMBO J 15, 5240-5245

Howie, J., Reilly, L., Fraser, N. J., Vlachaki Walker, J. M., Wypijewski, K. J., Ashford, M. L., Calaghan, S. C., McClafferty, H., Tian, L., Shipston, M. J., Boguslavskyi, A., Shattock, M. J., and Fuller, W. (2014) Substrate recognition by the cell surface palmitoyl transferase DHHC5. Proc Natl Acad Sci U S A 111, 17534-17539

Huang, K., Sanders, S., Singaraja, R., Orban, P., Cijsouw, T., Arstikaitis, P., Yanai, A., Hayden, M. R., and El-Husseini, A. (2009) Neuronal palmitoyl acyl transferases exhibit distinct substrate specificity. FASEB J 23, 2605-2615

Huang, K., Sanders, S. S., Kang, R., Carroll, J. B., Sutton, L., Wan, J., Singaraja, R., Young, F. B., Liu, L., El-Husseini, A., Davis, N. G., and Hayden, M. R. (2011) Wild-type HTT modulates the enzymatic activity of the neuronal palmitoyl transferase HIP14. Hum Mol Genet 20, 3356-3365

Huang, K., Yanai, A., Kang, R., Arstikaitis, P., Singaraja, R. R., Metzler, M., Mullard, A., Haigh, B., Gauthier-Campbell, C., Gutekunst, C. A., Hayden, M. R., and El-Husseini, A. (2004) Huntingtin-interacting protein HIP14 is a palmitoyl transferase involved in palmitoylation and trafficking of multiple neuronal proteins. Neuron 44, 977-986

Jia, L., Linder, M. E., and Blumer, K. J. (2011) Gi/o signaling and the palmitoyltransferase DHHC2 regulate palmitate cycling and shuttling of RGS7 family-binding protein. J Biol Chem 286, 13695-13703

Jiang, H., Khan, S., Wang, Y., Charron, G., He, B., Sebastian, C., Du, J., Kim, R., Ge, E., Mostoslavsky, R., Hang, H. C., Hao, Q., and Lin, H. (2013) SIRT6 regulates TNF-alpha secretion through hydrolysis of long-chain fatty acyl lysine. Nature 496, 110-113

Jiang, H., Zhang, X., and Lin, H. (2016) Lysine fatty acylation promotes lysosomal targeting of TNF-alpha. Sci Rep 6, 24371

Jones, P., Altamura, S., De Francesco, R., Gallinari, P., Lahm, A., Neddermann, P., Rowley, M., Serafini, S., and Steinkuhler, C. (2008) Probing the elusive catalytic activity of vertebrate class IIa histone deacetylases. Bioorg Med Chem Lett 18, 1814-1819

Keller, C. A., Yuan, X., Panzanelli, P., Martin, M. L., Alldred, M., Sassoe-Pognetto, M., and Luscher, B. (2004) The gamma2 subunit of GABA(A) receptors is a substrate for palmitoylation by GODZ. J Neurosci 24, 5881-5891

Kim, S. J., Zhang, Z., Sarkar, C., Tsai, P. C., Lee, Y. C., Dye, L., and Mukherjee, A. B. (2008) Palmitoyl protein thioesterase-1 deficiency impairs synaptic vesicle recycling at nerve terminals, contributing to neuropathology in humans and mice. J Clin Invest 118, 3075-3086

Kokkola, T., Kruse, C., Roy-Pogodzik, E. M., Pekkinen, J., Bauch, C., Honck, H. H., Hennemann, H., and Kreienkamp, H. J. (2011) Somatostatin receptor 5 is palmitoylated by the interacting ZDHHC5 palmitoyltransferase. FEBS Lett 585, 2665-2670

Korycka, J., Lach, A., Heger, E., Boguslawska, D. M., Wolny, M., Toporkiewicz, M., Augoff, K., Korzeniewski, J., and Sikorski, A. F. (2012) Human DHHC proteins: a spotlight on the hidden player of palmitoylation. Eur J Cell Biol 91, 107-117

Lach, A., Grzybek, M., Heger, E., Korycka, J., Wolny, M., Kubiak, J., Kolondra, A., Boguslawska, D. M., Augoff, K., Majkowski, M., Podkalicka, J., Kaczor, J., Stefanko, A., Kuliczkowski, K., and Sikorski, A. F. (2012) Palmitoylation of MPP1 (membrane-palmitoylated protein 1)/p55 is crucial for lateral membrane organization in erythroid cells. J Biol Chem 287, 18974-18984

Lakkaraju, A. K., Abrami, L., Lemmin, T., Blaskovic, S., Kunz, B., Kihara, A., Dal Peraro, M., and van der Goot, F. G. (2012) Palmitoylated calnexin is a key component of the ribosome-translocon complex. EMBO J 31, 1823-1835

Lemonidis, K., Sanchez-Perez, M. C., and Chamberlain, L. H. (2015) Identification of a Novel Sequence Motif Recognized by the Ankyrin Repeat Domain of zDHHC17/13 S-Acyltransferases. J Biol Chem 290, 21939-21950

Levental, I., Grzybek, M., and Simons, K. (2010) Greasing their way: lipid modifications determine protein association with membrane rafts. Biochemistry 49, 6305-6316

Li, S. X., Tang, G. S., Zhou, D. X., Pan, Y. F., Tan, Y. X., Zhang, J., Zhang, B., Ding, Z. W., Liu, L. J., Jiang, T. Y., Hu, H. P., Dong, L. W., and Wang, H. Y. (2014) Prognostic

significance of cytoskeleton-associated membrane protein 4 and its palmitoyl acyltransferase DHHC2 in hepatocellular carcinoma. Cancer 120, 1520-1531

Li, Y., Martin, B. R., Cravatt, B. F., and Hofmann, S. L. (2012) DHHC5 protein palmitoylates flotillin-2 and is rapidly degraded on induction of neuronal differentiation in cultured cells. J Biol Chem 287, 523-530

Liang, X., Nazarian, A., Erdjument-Bromage, H., Bornmann, W., Tempst, P., and Resh, M. D. (2001) Heterogeneous fatty acylation of Src family kinases with polyunsaturated fatty acids regulates raft localization and signal transduction. J Biol Chem 276, 30987-30994

Lin, H., Su, X., and He, B. (2012) Protein lysine acylation and cysteine succination by intermediates of energy metabolism. ACS Chem Biol 7, 947-960

Linder, M. E., and Deschenes, R. J. (2007) Palmitoylation: policing protein stability and traffic. Nat Rev Mol Cell Biol 8, 74-84

Linder, M. E., and Jennings, B. C. (2013) Mechanism and function of DHHC S-acyltransferases. Biochem Soc Trans 41, 29-34

Lobo, S., Greentree, W. K., Linder, M. E., and Deschenes, R. J. (2002) Identification of a Ras palmitoyltransferase in Saccharomyces cerevisiae. J Biol Chem 277, 41268-41273

Lu, D., Sun, H. Q., Wang, H., Barylko, B., Fukata, Y., Fukata, M., Albanesi, J. P., and Yin, H. L. (2012) Phosphatidylinositol 4-kinase IIalpha is palmitoylated by Golgi-localized palmitoyltransferases in cholesterol-dependent manner. J Biol Chem 287, 21856-21865

Lu, J., McKinsey, T. A., Zhang, C. L., and Olson, E. N. (2000) Regulation of skeletal myogenesis by association of the MEF2 transcription factor with class II histone deacetylases. Mol Cell 6, 233-244

Marin, E. P., Derakhshan, B., Lam, T. T., Davalos, A., and Sessa, W. C. (2012) Endothelial cell palmitoylproteomic identifies novel lipid-modified targets and potential substrates for protein acyl transferases. Circ Res 110, 1336-1344

Martin, B. R., and Cravatt, B. F. (2009) Large-scale profiling of protein palmitoylation in mammalian cells. Nat Methods 6, 135-138

Martin, B. R., Wang, C., Adibekian, A., Tully, S. E., and Cravatt, B. F. (2012) Global profiling of dynamic protein palmitoylation. Nat Methods 9, 84-89

Matsuyama, A., Shimazu, T., Sumida, Y., Saito, A., Yoshimatsu, Y., Seigneurin-Berny, D., Osada, H., Komatsu, Y., Nishino, N., Khochbin, S., Horinouchi, S., and Yoshida, M. (2002) In vivo destabilization of dynamic microtubules by HDAC6-mediated deacetylation. EMBO J 21, 6820-6831

Milde, S., and Coleman, M. P. (2014) Identification of palmitoyltransferase and thioesterase enzymes that control the subcellular localization of axon survival factor nicotinamide mononucleotide adenylyltransferase 2 (NMNAT2). J Biol Chem 289, 32858-32870

Mill, P., Lee, A. W., Fukata, Y., Tsutsumi, R., Fukata, M., Keighren, M., Porter, R. M., McKie, L., Smyth, I., and Jackson, I. J. (2009) Palmitoylation regulates epidermal homeostasis and hair follicle differentiation. PLoS Genet 5, e1000748

Mitchell, D. A., Vasudevan, A., Linder, M. E., and Deschenes, R. J. (2006) Protein palmitoylation by a family of DHHC protein S-acyltransferases. J Lipid Res 47, 1118-1127

Mukherjee, A., Mueller, G. M., Kinlough, C. L., Sheng, N., Wang, Z., Mustafa, S. A., Kashlan, O. B., Kleyman, T. R., and Hughey, R. P. (2014) Cysteine palmitoylation of the gamma subunit has a dominant role in modulating activity of the epithelial sodium channel. J Biol Chem 289, 14351-14359

Nadolski, M. J., and Linder, M. E. (2009) Molecular recognition of the palmitoylation substrate Vac8 by its palmitoyltransferase Pfa3. J Biol Chem 284, 17720-17730

O'Brien, P. J., and Zatz, M. (1984) Acylation of bovine rhodopsin by [3H]palmitic acid. J Biol Chem 259, 5054-5057

Ohno, Y., Kashio, A., Ogata, R., Ishitomi, A., Yamazaki, Y., and Kihara, A. (2012) Analysis of substrate specificity of human DHHC protein acyltransferases using a yeast expression system. Mol Biol Cell 23, 4543-4551

Ohno, Y., Kihara, A., Sano, T., and Igarashi, Y. (2006) Intracellular localization and tissue-specific distribution of human and yeast DHHC cysteine-rich domain-containing proteins. Biochim Biophys Acta 1761, 474-483

Oku, S., Takahashi, N., Fukata, Y., and Fukata, M. (2013) In silico screening for palmitoyl substrates reveals a role for DHHC1/3/10 (zDHHC1/3/11)-mediated neurochondrin palmitoylation in its targeting to Rab5-positive endosomes. J Biol Chem 288, 19816-19829

Pedram, A., Razandi, M., Deschenes, R. J., and Levin, E. R. (2012) DHHC-7 and -21 are palmitoylacyltransferases for sex steroid receptors. Mol Biol Cell 23, 188-199

Pedro, M. P., Vilcaes, A. A., Tomatis, V. M., Oliveira, R. G., Gomez, G. A., and Daniotti, J. L. (2013) 2-Bromopalmitate reduces protein deacylation by inhibition of acyl-protein thioesterase enzymatic activities. PLoS One 8, e75232

Percherancier, Y., Planchenault, T., Valenzuela-Fernandez, A., Virelizier, J. L., Arenzana-Seisdedos, F., and Bachelerie, F. (2001) Palmitoylation-dependent control of degradation, life span, and membrane expression of the CCR5 receptor. J Biol Chem 276, 31936-31944

Ren, W., Sun, Y., and Du, K. (2013) DHHC17 palmitoylates ClipR-59 and modulates ClipR-59 association with the plasma membrane. Mol Cell Biol 33, 4255-4265

Resh, M. D. (1996) Regulation of cellular signalling by fatty acid acylation and prenylation of signal transduction proteins. Cell Signal 8, 403-412

Resh, M. D. (2006) Trafficking and signaling by fatty-acylated and prenylated proteins. Nat Chem Biol 2, 584-590

Resh, M. D. (2006) Use of analogs and inhibitors to study the functional significance of protein palmitoylation. Methods 40, 191-197

Resh, M. D. (2012) Targeting protein lipidation in disease. Trends Mol Med 18, 206-214

Rossin, A., Durivault, J., Chakhtoura-Feghali, T., Lounnas, N., Gagnoux-Palacios, L., and Hueber, A. O. (2015) Fas palmitoylation by the palmitoyl acyltransferase DHHC7 regulates Fas stability. Cell Death Differ 22, 643-653

Roth, A. F., Feng, Y., Chen, L., and Davis, N. G. (2002) The yeast DHHC cysteine-rich domain protein Akr1p is a palmitoyl transferase. J Cell Biol 159, 23-28

Salaun, C., Gould, G. W., and Chamberlain, L. H. (2005) Lipid raft association of SNARE proteins regulates exocytosis in PC12 cells. J Biol Chem 280, 19449-19453

Salaun, C., Greaves, J., and Chamberlain, L. H. (2010) The intracellular dynamic of protein palmitoylation. J Cell Biol 191, 1229-1238

Sardjono, C. T., Harbour, S. N., Yip, J. C., Paddock, C., Tridandapani, S., Newman, P. J., and Jackson, D. E. (2006) Palmitoylation at Cys595 is essential for PECAM-1 localisation into membrane microdomains and for efficient PECAM-1-mediated cytoprotection. Thromb Haemost 96, 756-766

Schlesinger, M. J., Magee, A. I., and Schmidt, M. F. (1980) Fatty acid acylation of proteins in cultured cells. J Biol Chem 255, 10021-10024

Segal-Salto, M., Sapir, T., and Reiner, O. (2016) Reversible Cysteine Acylation Regulates the Activity of Human Palmitoyl-Protein Thioesterase 1 (PPT1). PLoS One 11, e0146466

Shahinian, S., and Silvius, J. R. (1995) Doubly-lipid-modified protein sequence motifs exhibit long-lived anchorage to lipid bilayer membranes. Biochemistry 34, 3813-3822

Sharma, C., Rabinovitz, I., and Hemler, M. E. (2012) Palmitoylation by DHHC3 is critical for the function, expression, and stability of integrin alpha6beta4. Cell Mol Life Sci 69, 2233-2244

Sharma, C., Yang, X. H., and Hemler, M. E. (2008) DHHC2 affects palmitoylation, stability, and functions of tetraspanins CD9 and CD151. Mol Biol Cell 19, 3415-3425

Singaraja, R. R., Kang, M. H., Vaid, K., Sanders, S. S., Vilas, G. L., Arstikaitis, P., Coutinho, J., Drisdel, R. C., El-Husseini Ael, D., Green, W. N., Berthiaume, L., and Hayden, M. R. (2009) Palmitoylation of ATP-binding cassette transporter A1 is essential for its trafficking and function. Circ Res 105, 138-147

Smotrys, J. E., and Linder, M. E. (2004) Palmitoylation of intracellular signaling proteins: regulation and function. Annu Rev Biochem 73, 559-587

Solimena, M., Dirkx, R., Jr., Radzynski, M., Mundigl, O., and De Camilli, P. (1994) A signal located within amino acids 1-27 of GAD65 is required for its targeting to the Golgi complex region. J Cell Biol 126, 331-341

Somoza, J. R., Skene, R. J., Katz, B. A., Mol, C., Ho, J. D., Jennings, A. J., Luong, C., Arvai, A., Buggy, J. J., Chi, E., Tang, J., Sang, B. C., Verner, E., Wynands, R., Leahy, E. M., Dougan, D. R., Snell, G., Navre, M., Knuth, M. W., Swanson, R. V., McRee, D. E., and Tari, L. W. (2004) Structural snapshots of human HDAC8 provide insights into the class I histone deacetylases. Structure 12, 1325-1334

Song, I. W., Li, W. R., Chen, L. Y., Shen, L. F., Liu, K. M., Yen, J. J., Chen, Y. J., Chen, Y. J., Kraus, V. B., Wu, J. Y., Lee, M. T., and Chen, Y. T. (2014) Palmitoyl

acyltransferase, Zdhhc13, facilitates bone mass acquisition by regulating postnatal epiphyseal development and endochondral ossification: a mouse model. PLoS One 9, e92194

Stanley, P., Koronakis, V., and Hughes, C. (1998) Acylation of Escherichia coli hemolysin: a unique protein lipidation mechanism underlying toxin function. Microbiol Mol Biol Rev 62, 309-333

Stevenson, F. T., Bursten, S. L., Fanton, C., Locksley, R. M., and Lovett, D. H. (1993) The 31-kDa precursor of interleukin 1 alpha is myristoylated on specific lysines within the 16-kDa N-terminal propiece. Proc Natl Acad Sci U S A 90, 7245-7249

Stevenson, F. T., Bursten, S. L., Locksley, R. M., and Lovett, D. H. (1992) Myristyl acylation of the tumor necrosis factor alpha precursor on specific lysine residues. J Exp Med 176, 1053-1062

Swarthout, J. T., Lobo, S., Farh, L., Croke, M. R., Greentree, W. K., Deschenes, R. J., and Linder, M. E. (2005) DHHC9 and GCP16 constitute a human protein fatty acyltransferase with specificity for H- and N-Ras. J Biol Chem 280, 31141-31148

Tate, E. W., Kalesh, K. A., Lanyon-Hogg, T., Storck, E. M., and Thinon, E. (2015) Global profiling of protein lipidation using chemical proteomic technologies. Curr Opin Chem Biol 24, 48-57

Teng, Y. B., Jing, H., Aramsangtienchai, P., He, B., Khan, S., Hu, J., Lin, H., and Hao, Q. (2015) Efficient demyristoylase activity of SIRT2 revealed by kinetic and structural studies. Sci Rep 5, 8529

Thomas, G. M., Hayashi, T., Chiu, S. L., Chen, C. M., and Huganir, R. L. (2012) Palmitoylation by DHHC5/8 targets GRIP1 to dendritic endosomes to regulate AMPA-R trafficking. Neuron 73, 482-496

Thomas, G. M., Hayashi, T., Huganir, R. L., and Linden, D. J. (2013) DHHC8-dependent PICK1 palmitoylation is required for induction of cerebellar long-term synaptic depression. J Neurosci 33, 15401-15407

Tian, L., Jeffries, O., McClafferty, H., Molyvdas, A., Rowe, I. C., Saleem, F., Chen, L., Greaves, J., Chamberlain, L. H., Knaus, H. G., Ruth, P., and Shipston, M. J. (2008) Palmitoylation gates phosphorylation-dependent regulation of BK potassium channels. Proc Natl Acad Sci U S A 105, 21006-21011

Tian, L., McClafferty, H., Jeffries, O., and Shipston, M. J. (2010) Multiple palmitoyltransferases are required for palmitoylation-dependent regulation of large conductance calcium- and voltage-activated potassium channels. J Biol Chem 285, 23954-23962

Tian, L., McClafferty, H., Knaus, H. G., Ruth, P., and Shipston, M. J. (2012) Distinct acyl protein transferases and thioesterases control surface expression of calcium-activated potassium channels. J Biol Chem 287, 14718-14725

Tomatis, V. M., Trenchi, A., Gomez, G. A., and Daniotti, J. L. (2010) Acyl-protein thioesterase 2 catalyzes the deacylation of peripheral membrane-associated GAP-43. PLoS One 5, e15045

Tsutsumi, R., Fukata, Y., Noritake, J., Iwanaga, T., Perez, F., and Fukata, M. (2009) Identification of G protein alpha subunit-palmitoylating enzyme. Mol Cell Biol 29, 435-447

Valdez-Taubas, J., and Pelham, H. (2005) Swf1-dependent palmitoylation of the SNARE Tlg1 prevents its ubiquitination and degradation. EMBO J 24, 2524-2532

Vannini, A., Volpari, C., Filocamo, G., Casavola, E. C., Brunetti, M., Renzoni, D., Chakravarty, P., Paolini, C., De Francesco, R., Gallinari, P., Steinkuhler, C., and Di Marco, S. (2004) Crystal structure of a eukaryotic zinc-dependent histone deacetylase,

human HDAC8, complexed with a hydroxamic acid inhibitor. Proc Natl Acad Sci U S A 101, 15064-15069

Vannini, A., Volpari, C., Gallinari, P., Jones, P., Mattu, M., Carfi, A., De Francesco, R., Steinkuhler, C., and Di Marco, S. (2007) Substrate binding to histone deacetylases as shown by the crystal structure of the HDAC8-substrate complex. EMBO Rep 8, 879-884

Varner, A. S., Ducker, C. E., Xia, Z., Zhuang, Y., De Vos, M. L., and Smith, C. D. (2003) Characterization of human palmitoyl-acyl transferase activity using peptides that mimic distinct palmitoylation motifs. Biochem J 373, 91-99

Vassilev, A. O., Plesofsky-Vig, N., and Brambl, R. (1995) Cytochrome c oxidase in Neurospora crassa contains myristic acid covalently linked to subunit 1. Proc Natl Acad Sci U S A 92, 8680-8684

Veit, M. (2000) Palmitoylation of the 25-kDa synaptosomal protein (SNAP-25) in vitro occurs in the absence of an enzyme, but is stimulated by binding to syntaxin. Biochem J 345 Pt 1, 145-151

Vesa, J., Hellsten, E., Verkruyse, L. A., Camp, L. A., Rapola, J., Santavuori, P., Hofmann, S. L., and Peltonen, L. (1995) Mutations in the palmitoyl protein thioesterase gene causing infantile neuronal ceroid lipofuscinosis. Nature 376, 584-587

Waltregny, D., Glenisson, W., Tran, S. L., North, B. J., Verdin, E., Colige, A., and Castronovo, V. (2005) Histone deacetylase HDAC8 associates with smooth muscle alpha-actin and is essential for smooth muscle cell contractility. FASEB J 19, 966-968

Wang, J., Xie, Y., Wolff, D. W., Abel, P. W., and Tu, Y. (2010) DHHC protein-dependent palmitoylation protects regulator of G-protein signaling 4 from proteasome degradation. FEBS Lett 584, 4570-4574

Webb, Y., Hermida-Matsumoto, L., and Resh, M. D. (2000) Inhibition of protein palmitoylation, raft localization, and T cell signaling by 2-bromopalmitate and polyunsaturated fatty acids. J Biol Chem 275, 261-270

West, A. C., and Johnstone, R. W. (2014) New and emerging HDAC inhibitors for cancer treatment. J Clin Invest 124, 30-39

Woolfrey, K. M., Sanderson, J. L., and Dell'Acqua, M. L. (2015) The palmitoyl acyltransferase DHHC2 regulates recycling endosome exocytosis and synaptic potentiation through palmitoylation of AKAP79/150. J Neurosci 35, 442-456

Wu, R., Wang, S., Zhou, N., Cao, Z., and Zhang, Y. (2010) A proton-shuttle reaction mechanism for histone deacetylase 8 and the catalytic role of metal ions. J Am Chem Soc 132, 9471-9479

Yamazaki, M., Fukaya, M., Abe, M., Ikeno, K., Kakizaki, T., Watanabe, M., and Sakimura, K. (2001) Differential palmitoylation of two mouse glutamate receptor interacting protein 1 forms with different N-terminal sequences. Neurosci Lett 304, 81-84

Yanai, A., Huang, K., Kang, R., Singaraja, R. R., Arstikaitis, P., Gan, L., Orban, P. C., Mullard, A., Cowan, C. M., Raymond, L. A., Drisdel, R. C., Green, W. N., Ravikumar, B., Rubinsztein, D. C., El-Husseini, A., and Hayden, M. R. (2006) Palmitoylation of huntingtin by HIP14 is essential for its trafficking and function. Nat Neurosci 9, 824-831

Yang, W., Di Vizio, D., Kirchner, M., Steen, H., and Freeman, M. R. (2010) Proteome scale characterization of human S-acylated proteins in lipid raft-enriched and non-raft membranes. Mol Cell Proteomics 9, 54-70

Yang, X. J., and Seto, E. (2008) The Rpd3/Hda1 family of lysine deacetylases: from bacteria and yeast to mice and men. Nat Rev Mol Cell Biol 9, 206-218

Yao, Y. L., and Yang, W. M. (2011) Beyond histone and deacetylase: an overview of cytoplasmic histone deacetylases and their nonhistone substrates. J Biomed Biotechnol 2011, 146493

Yount, J. S., Zhang, M. M., and Hang, H. C. (2011) Visualization and Identification of Fatty Acylated Proteins Using Chemical Reporters. Curr Protoc Chem Biol 3, 65-79

Zeidman, R., Buckland, G., Cebecauer, M., Eissmann, P., Davis, D. M., and Magee, A. I. (2011) DHHC2 is a protein S-acyltransferase for Lck. Mol Membr Biol 28, 473-486

Zhang, J., Planey, S. L., Ceballos, C., Stevens, S. M., Jr., Keay, S. K., and Zacharias, D. A. (2008) Identification of CKAP4/p63 as a major substrate of the palmitoyl acyltransferase DHHC2, a putative tumor suppressor, using a novel proteomics method. Mol Cell Proteomics 7, 1378-1388

Zhou, T., Li, J., Zhao, P., Liu, H., Jia, D., Jia, H., He, L., Cang, Y., Boast, S., Chen, Y. H., Thibault, H., Scherrer-Crosbie, M., Goff, S. P., and Li, B. (2015) Palmitoyl acyltransferase Aph2 in cardiac function and the development of cardiomyopathy. Proc Natl Acad Sci U S A 112, 15666-15671

Zhu, A. Y., Zhou, Y., Khan, S., Deitsch, K. W., Hao, Q., and Lin, H. (2012) Plasmodium falciparum Sir2A preferentially hydrolyzes medium and long chain fatty acyl lysine. ACS Chem Biol 7, 155-159

# CHAPTER 2

# S-PALMITOYLATION OF JUNCTIONAL ADHESION MOLECULE C BY DHHC7 REGULATES CELL MIGRATION

## 2.1 ABSTRACT

Junctional Adhesion Molecule C (JAM-C) is an immunoglobulin superfamily protein expressed in epithelial cells, endothelial cells, and leukocytes. JAM-C has been implicated in leukocyte transendothelial migration, angiogenesis, cell-adhesion, cell polarity, spermatogenesis and metastasis. Here, we show that JAM-C undergoes S-palmitoylation on two juxtamembrane cysteine residues, Cys264 and Cys265. We have identified DHHC7 as a JAM-C palmitoylating enzyme by screening all known palmitoyltransferases (PATs or DHHCs). Ectopic expression of DHHC7, but not a DHHC7 catalytic mutant, enhances JAM-C S-palmitoylation. Moreover, DHHC7 knockdown decreases the S-palmitoylation level of JAM-C. Palmitoylation of JAM-C promotes its localization to cell-cell contact and inhibits transwell migration of A549 lung cancer cells. These results suggest that S-palmitoylation of JAM-C can be potentially targeted to control cancer metastasis.

## 2.2 INTRODUCTION

Junctional adhesion molecules (JAMs) are classified into the Immunoglobulin (IgG) superfamily. The JAM family is composed three JAM proteins: JAM-A, JAM-B and JAM-C. All of these proteins contain two conserved Ig-like domains, including a membrane distal V-type IgG domain, and a membrane proximal $C_2$-type IgG domain (Ebnet et al, 2004). JAMs have been found to be localized at the tight junctions (TJs) of leukocytes and endothelial cells. The JAM family of proteins plays a major role in the regulation of the immune response via leukocyte-endothelial cell transmigration and cell polarity through associations with PDZ-containing proteins at the TJs (Ebnet et al, 2004).

JAM-C, also known as hJAM3 and mJAM-2, is expressed in different types of cells, including endothelial cells, platelets, leukocytes, epithelial cells, fibroblasts, smooth muscle cells and Schwann cells from the peripheral nervous system (Scheiermann et al, 2009). As shown in Figure 2.1, JAM-C is a type I transmembrane protein with a PDZ binding domain motif in the intracellular carboxyl (C)-terminal region. This allows JAM-C to interact with other PDZ motif-containing proteins at the TJs, such as ZO-1 and PAR-3 (Ebnet et al, 2004; Keiper et al, 2005; Bazzoni et al, 2003).

JAM-C has been shown to regulate leukocyte adhesion and transmigration across endothelial cells through a heterophillic interaction with leukocyte integrin MAC-1 (αMβ2) (Weber et al, 2007). Overexpression of JAM-C in endothelial cells facilitates the transendothelial migration of leukocytes, whereas blocking JAM-C using a JAM-C antibody inhibits this migration (Johnson-Léger et al, 2012).

Moreover, JAM-C is involved in spermatogenesis in mice. JAM-C deficient mice have defective spermatid differentiation and infertility. Dissected Jam-C null mice showed the lack of differentiated spermatids. It has been shown that JAM-C is essential for recruiting cell polarity proteins (Par6-Cdc42-PKCλ), which is a critical step prior to spermatid differentiation (Gliki et al, 2004).

Several studies have demonstrated that JAM-C is important for maintaining the integrity of the nervous system and the brain. Knockout of JAM-C in mice leads to neuropathy and development of a severe hydrocephalus, which is an abnormal accumulation of cerebrospinal fluid in the brain (Guo et al, 2014; Wyss et al, 2012). JAM-C mutations in humans have recently been associated to a rare disorder, characterized by hemorrhagic destruction of the brain, calcification, and congenital cataracts (Akawi et al, 2013).

In endothelial cells JAM-C depletion results in a reduction of cell permeability, while overexpression of JAM-C leads to an increase in cell permeability (Li et al, 2009). JAM-C regulates cell permeability of endothelial cells through modulation of beta3 (αvβ3) integrin activity. JAM-C association with beta3 integrin is able to negatively regulate beta3 integrin activity. Overexpression of JAM-C leads to decreased integrin activity and a destabilized tight junction, causing an increase in cell permeability (Li et al, 2009). In contrast, in epithelial cells, JAM-C reinforces the tight junction integrity by reducing the paracellular permeability (Mandicourt et al, 2007).

Recently, JAM-C has been shown to be involved in metastasis and development of certain cancer cells (Hao et al, 2014; Leinster et al, 2013; Arcangeli et al, 2012; Tenan et al, 2010). In melanoma cells, the homophillic JAM-C/JAM-C trans-interaction

between melanoma cells and endothelial cells promotes metastasis (Langer et al, 2011). Additionally, the JAM-C expression level in fibrosarcoma and lung cancer cells is reported to be positively correlated to metastasis. Knocking down JAM-C in highly metastatic lung cancer cells leads to a decrease in cell migration (Hao et al, 2014; Arnold et al, 2011). JAM-C, therefore, could be a therapeutic target for certain cancers.

Cys-palmitoylation (S-palmitoylation), a reversible lipid posttranslational modification, is the addition of a 16-carbon palmitoyl group onto cysteine residues of proteins via a labile thioester bond. S-palmitoylation plays a crucial role in cell signaling, localization and protein-protein interactions (Resh et al, 1999; Smotrys et al, 2004). The palmitoyltransferases (PATs or DHHCs) catalyze S-palmitoylation. To date 23 mammalian DHHCs have been identified (Fukata et al, 2004; Linder et al, 2013). Here we showed for the first time that JAM-C undergoes S-palmitoylation on two membrane-proximal cysteine residues (Cys264 and Cys265) and this modification can be catalyzed by DHHC7. We found that S-palmitoylation of JAM-C promotes its localization to the cell-cell contact region and regulates cell migration.

## 2.3 MATERIALS AND METHODS

### JAM-C cloning and expression

Human JAM-C cDNA was purchased from Transomic (clone ID BC012147). The full length cDNA was PCR-amplified by Platinum® Pfx DNA Polymerase (ThermoFisher) and subcloned into the pCMV-tag 4a vector using the BamHI and EcoRV restriction sites using the following primers:

Sense: 5'**-**AGTCAGGGATCCATGGCGCTG AGGCGGCCA-3'**;**

antisense: 5'-AGTCAGGATATCGATCACAA ACGATGACTTGTGTCT-3'

JAM-C mutants (C264S, C265S and CCSS) were generated by quick change mutagenesis. The JAM-C in pCMV-tag 4a vector was PCR-amplified using Phusion® High-Fidelity DNA polymerase and the following mutagenic primers:

C264S sense: 5'CCCTGATCACGTTGGGCATCAGCTGTGCATACAGACGTGGCTA3',

antisense: 5'GATGCCCAACGTGATCAGGG3';

C265S sense: 5'TGATCACGTTGGGCATCTGC AGTGCATACAGACGTGGCTACTT3',

antisense: 5'GCAGATGCCCAACGTGATCA3'.

CCSS sense:

5'CCCTGATCACGTTGGGCATCAGCAGTGCATACAGACGTGGCTACTT3',

antisense: 5'GATGCCCAACGTGATCAGGG3';

The plasmids of DHHC 1-23 in pEF-BOS-HA vector for screening were generously provided by Prof. Maurine Linder and Prof. Masaki Fukata.

### Cell Culture and Transfection

Human Embryonic Kidney 293T (HEK-293T) cells were cultured in Dulbecco's Modified Eagle Medium (DMEM) supplemented with 10% Fetal Bovine Serum (Invitrogen), and

Jurkat and A549 cells in Roswell Park Memorial Institute (RPMI) 1640 Media (Invitrogen) supplemented with 10% Fetal Bovine Serum (Invitrogen). All cells were incubated in a humidified incubator at 37 °C with 5% $CO_2$. FuGENE® 6 Transfection Reagent (Promega) was used for cell transfection according to the manufacturer's instruction.

**Antibodies**

Anti-FLAG® M2-Peroxidase (HRP) antibody (mouse monoclonal IgG) for western blotting and anti-FLAG® M2 Affinity Gel for immunoprecipitation were purchased from Sigma (catalog #A8592 and #A2220, respectively). Anti-FLAG antibody (mouse monoclonal IgG1) for immunofluorescence was purchased from Cell Signaling (catalog #8146). Secondary Antibody- Alexa Fluor® 488 conjugate (Mouse polyclonal IgG) was purchased from ThermoFisher (catalog #A-11001). Anti-HA-Peroxidase (rat IgG1) was purchased from Roche (catalog #12013819001). The anti-human JAM-C antibody (mouse monoclonal IgG) was purchased from Enzo Life Sciences (catalog #ALX-803-306), and anti-DHHC7 (rabbit IgG) antibody was purchased from AssayBiotech (catalog #R12-3691). All other peroxidase conjugated secondary antibodies were from Santa Cruz Biotechnology.

**Western Blot**

Cells were collected and lysed with 1% NP40 lysis buffer (50 mM Tris-HCl pH 7.4, 150 mM NaCl and 1% v/v NP40 (Igepal) containing Protease Inhibitor Cocktails (Sigma). Protein concentration was determined by Bradford assay (Pierce™ Coomassie Protein Assay Kit). Protein samples were separated by 12% SDS-PAGE and transferred to PVDF membrane (Bio-Rad) for 90 min. The membrane was blocked with 5% bovine

serum albumin (BSA, Santa Cruz) in TBST (25 mM Tris-HCl pH 7.4, 150 mM NaCl, and 0.1% Tween-20) and incubated with the primary antibody for 3 hrs at room temperature, or overnight at 4 $^{o}$C. After washing 5 times with TBST, the membrane was incubated with the secondary antibody for 1 hr at room temperature. The membrane was washed five more times with TBST before it was developed in ECL-Plus western blotting detection reagent (GE Healthcare). The signal was visualized using a Typhoon 9400 Variable Mode Imager (GE Healthcare) with 457 nm excitation and 526 nm detection filters, using a PMT of 600 V (normal sensitivity). The signal was analyzed by Image Quant TL v2005 and Quantity One (Bio-Rad).

**Metabolic labeling of palmitoylation on FLAG-tagged JAM-C**

Cells were transfected with FLAG-tagged JAM-C pCMV4a. After 24 hrs, the cells were incubated with 50 μM Alk14 in media supplemented with 10% FBS for 6 hrs. Cells were collected and washed with 1x phosphate saline buffer (PBS) three times. The cell pellets were lysed with 1% NP40 lysis buffer (50 mM Tris-HCl pH 7.4, 150 mM NaCl, and 1% v/v NP40) containing Protease Inhibitor Cocktails (Sigma). The protein concentration was determined by Bradford assay (Pierce™ Coomassie Protein Assay Kit). The expression of FLAG-JAM-C level was confirmed by western blot. For FLAG-JAM-C immunoprecipitation, 25 μl of Anti-FLAG M2 affinity gel (Sigma) was added into 600 μg of total cell lysate with the final volume of 1 ml in an eppendorf tube. The samples were gently agitated at 4 $^{o}$C for 2 hrs. The samples were then centrifuged at 1,000 xg for 2 min at 4 $^{o}$C to remove the supernatant. The beads were washed three times with 0.1% NP40 lysis buffer. After the last wash, all the buffer was removed. The beads were re-suspended in 15 μl of 0.1% NP40 buffer. To perform the click reaction,

5.6 μl of the reaction master mix was added to each sample (click reaction master mix: 3 μl of 1 mM BODIPY Azide in DMF, 1 μl of 50 mM tris(2-carboxyethyl) phosphine hydrochloride (TCEP.HCl, Calbiochem) in water, 0.6 μl of 10 mM tris [(1-benzyl-1H-1,2,3-triazol-4-yl)methyl] amine (TBTA, Sigma or Anal Tech) in DMF, 1 μl of 50 mM $CuSO_4$ in water). After 1 hr at room temperature, 20 μl of 3x protein loading buffer (187 mM Tris-HCl pH 6.8, 6% SDS, 150 mM DTT, 30% v/v glycerol, 0.006% bromphenol blue) was added to each sample, and the samples were boiled at 95 $^oC$ for 5 min and centrifuged at 17,000x g for 2 min. The supernatants were transferred into new eppendorf tubes and loaded on 12% SDS-PAGE gels. The fluorescent signal was visualized with a Typhoon 9400 Variable Mode Imager (GE Healthcare Life Sciences) using 488 nm excitation and 520 nm detection filters, and a PMT setting of 550 V (normal sensitivity). The signal was analyzed by Image Quant TL v2005, and quantified by Quantity One (Bio-Rad) within a linear range of exposure.

**Generation of DHHC7, 12 and 15 stable knockdown in HEK-293T cell line**

Different DHHC7, 12 and 15 shRNA lentiviral plasmids in pLKO.1-puro vector were purchased from Sigma. To generate the lentiviruses, low passage number of HEK-293T cells in a 10 $cm^3$ plate were transfected with 6 μg of each DHHC7, 12 or 15 shRNA, 4 μg of pCMV-dR8.2, and 2 μg of pM2D.G mixed with 36 μl of FuGENE6 (promega). The cell media containing the lentiviruses were collected after 48 hrs by centrifugation, and filtered through 0.45 μm syringe filter to remove cell debris. The day before infection, $3x10^5$ cells of low passage number HEK-293T cells were split into each well of a 6-well plate and grown overnight in 2 ml of DMEM with 10% FBS. The media were then removed and replaced with a mixture of 1.5 ml of the lentiviruses media collected

above, 0.5 ml of fresh DMEM with 10% FBS, and 6 μg/μl polybrene (Sigma). After 6 hrs, 3 ml of DMEM with 10% FBS was added to each well, and after 48 hrs, 1.5 μg/μl of puromycin dihydrochloride (Santa Cruz) was added into the cells to select for stable DHHC7, 12 and 15 knockdown cells.

**Cell migration assay**

A549 cells were transfected with FLAG-tagged JAM-C WT in pCMV4a, the FLAG-tagged CCSS mutant in pCMV4a, or empty pCMV4a vector (control) for 24 hrs, and then cultured in RPMI serum-free medium for an additional 14 hrs. The cell migration assay was performed in a 24-well transwell plate with 8 mm polycarbonate sterile membrane (Corning Incorporated). A total of $3.5x10^4$ cells, in 200 μl of RPMI serum-free medium, were plated in each upper chamber and then placed in wells containing 600 μl of RPMI medium supplemented with 10% FBS. After 24 hrs, the cells on the upper surface were detached with a cotton swab, and the upper chambers were fixed. The cells in the lower filter were stained with 0.1% crystal violet for 15 minutes and then counted. The quantified results represent three random fields of migrated cells.

**Immunofluorescence Microscopy**

A total of $2x10^5$ A549 cells were split into each glass bottom culture dishes (MatTek) and cultured overnight. The cells were then transfected with either the FLAG-JAM-C WT in pCMV4a vector or the CCSS mutant. After 24 hrs, cells were washed twice with 2 ml of 1x phosphate-buffered saline (PBS, ThermoFisher), fixed with 4% paraformaldehyde in PBS on ice for 15 min, and then kept at room temperature for 5 min. Then cells were subsequently washed three times with 2 ml of 1x PBS and incubated with 0.1% Saponin (TCI-America) with 3% BSA in 1x PBS at room temperature. After 1 hr, the blocking

solution was removed and the anti-FLAG antibody (rabbit monoclonal IgG1, 1:1,000, Cell Signaling) together with the anti ZO-1 antibody (mouse monoclonal IgG1, 1:600, EMD-millipore) in a Saponin-BSA solution was added to the cells at room temperature. After incubated with the primary antibody for one hour, the cells were washed with 1 ml of Saponin-BSA solution five times and then incubated with the secondary antibodies, Alexa Fluor® 488 conjugate (Goat anti-rabbit IgG polyclonal antibody, ThermoFisher) (1:1,000) and Texas Red® conjugate (Goat anti-mouse IgG polyclonal antibody, ThermoFisher) (1:1,1000), in the Saponin-BSA solution at room temperature for 1 hr. The cells were washed with 1 ml of Saponin-BSA solution five times, then mounted with 200 µl of DAPI Fluoromount-G (Southern Biotech) and covered with a cover glass. After 24 hrs, the cells were visualized with a Zeiss LSM 710 confocal microscope with a 63×/1.4 oil immersion objective. Images were viewed and analyzed using ZEN 2012 imaging software (Zeiss). For JAM-C and ZO-1 co-localization analysis, Manders overlap coefficient with automatic thresholds (M1 and M2) were calculated using Coloc2 plugin in the Fiji (background subtraction, rolling ball radius 50 pixels).

**Statistical analysis**

Data were shown as mean ± S.D. (Standard Deviation). Differences were analyzed by two-tailed Student's t- test between two groups. *, $P < 0.05$; **, $P < 0.01$; ***, $P < 0.001$.

## 2.4 RESULTS

### JAM-C is S-palmitoylated on two conserved juxtamembrane cysteine residues, Cys264 and Cys265

In addition to a PDZ-binding domain, the JAM-C intracellular C-terminus contains two transmembrane proximal cysteine residues (Figure 2.1A). These two cysteine residues are conserved across multiple mammalian species, suggesting these residues may have an important role (Figure 2.1B).

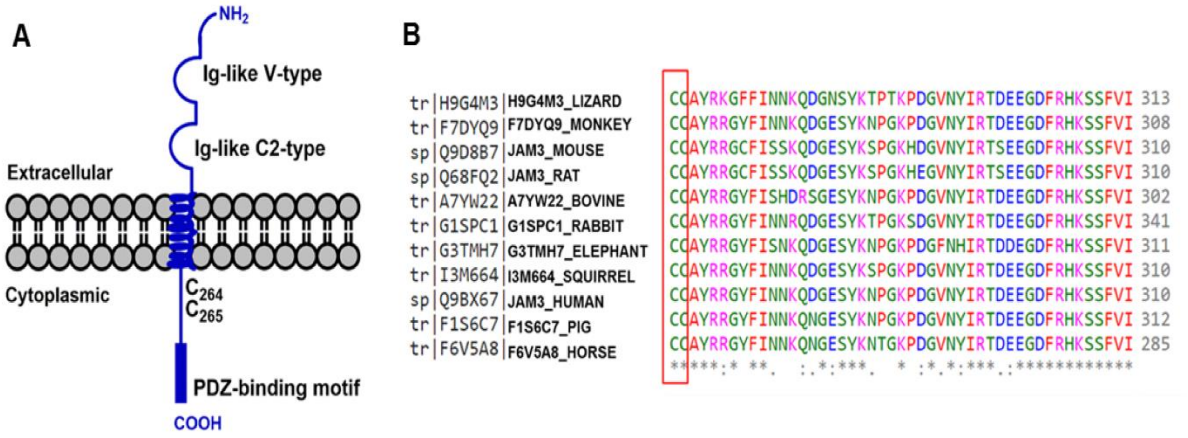


**Figure 2.1 JAM-C is an immunoglobulin superfamily protein containing two conserved cysteine residues (Cys264 and Cys265, human sequence) in different species.** A, schematic structure of JAM-C transmembrane protein with two Ig-like domains in the extracellular region and one PDZ-binding motif in the cytoplasmic region. B, Multiple sequence alignment by Clustal Omega showing the two cytoplasmic cysteine residues that are conserved across multiple species.

We hypothesized these two conserved cysteine residues may be subjected to palmitoylation, a post-translational modification that is frequently found on integral membrane proteins or membrane-associated proteins. To test whether S-palmitoylation occurs on JAM-C, we employed a metabolic labeling strategy using an alkyne-tagged palmitic acid analogue (Alk14) (Yount et al, 2011; Wilson et al, 2011). Human T lymphocyte Jurkat cells and human umbilical vein endothelial cells (HUVEC) were cultured in the presence of Alk14, and endogenous JAM-C was immunoprecipitated and conjugated to BODIPY-azide (B-$N_3$) via click chemistry (Figure 2.2A). JAM-C was fluorescent-labeled suggesting that it contains fatty acylation (Figure 2.2B). Similar results were obtained from ectopically expressed FLAG-tagged JAM-C in Human Embryonic Kidney 293T (HEK-293T) cells (Figure 2.2C). To further confirm that this modification occurs on cysteine residues, we mutated these residues to serine. We observed a significant decrease in the fluorescent signal in the single cysteine mutants, C264S and C265S. However, the C264S mutation had a more profound effect on the fluorescent signal. Furthermore, we observed no fluorescent signal for the double cysteine mutant (CC264-265SS). These results indicated that JAM-C undergoes S-palmitoylation on both Cys264 and Cys265, with Cys264 as the major palmitoylation site (Figure 2.2D-E). We found that the Alk14 labeling signal on JAM-C was largely resistant to hydroxylamine treatment, which was similar to the lysine fatty acylation that was previously reported to occur on TNF-α (Jiang et al, 2013). To rule out that JAM3 has lysine fatty acylation, we mutated all the cytosolic lysine residues to arginine (K276R, K283R, and K287R or 3KR; K276R, K283R, K287R and K305R or 4KR) and detected the fatty acylation signal. We observed no significant change in the fluorescent

signal with the 3KR and 4KR mutants compared to WT JAM-C (Figure 2.2F). Together, these results suggest that the fatty acylation occurs on cysteine residues of JAM-C.

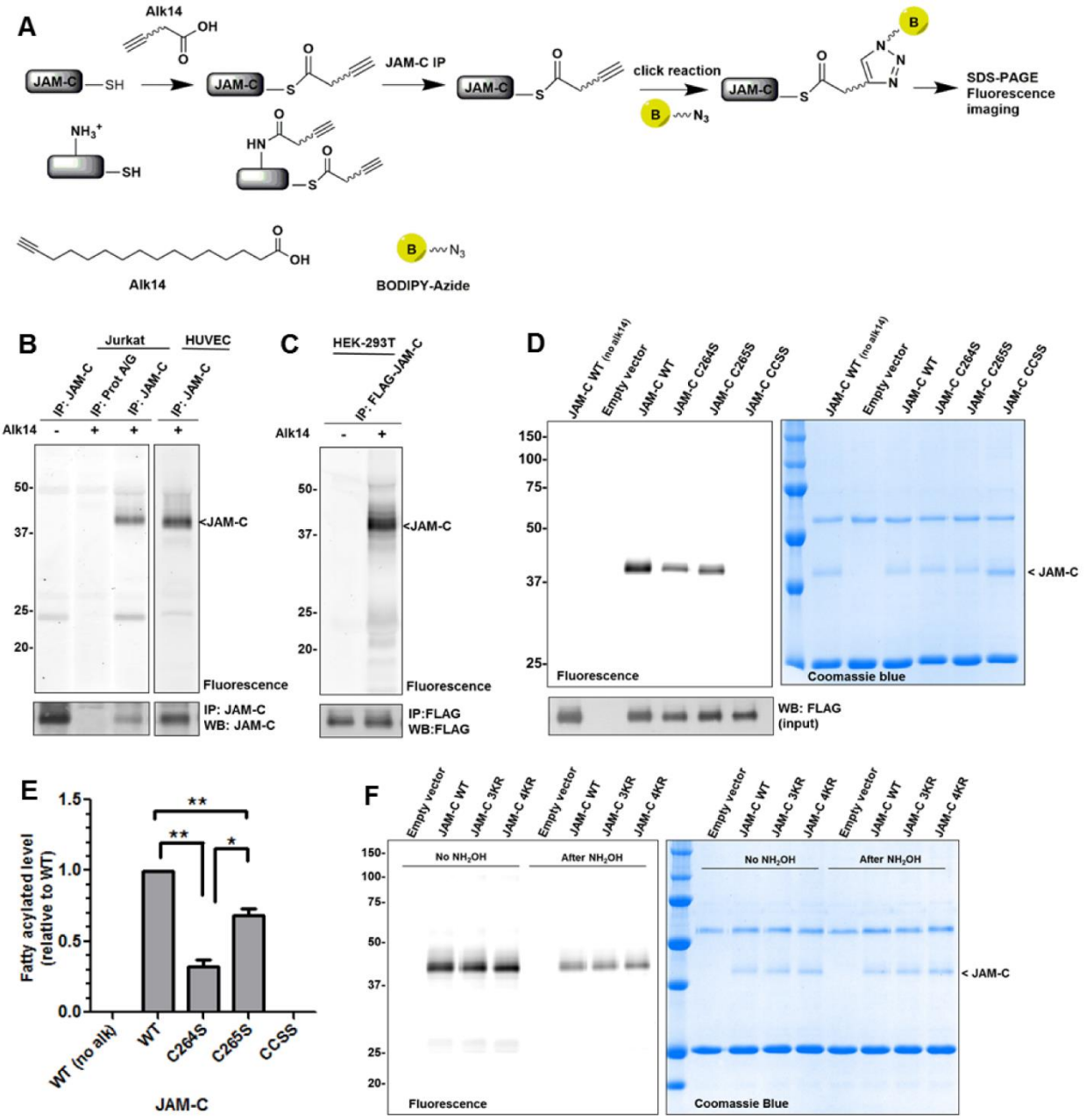


**Figure 2.2 JAM-C contains S-palmitoylation on Cys264 and Cys265.** A, Method for the detection of S-palmitoylation in JAM-C with Alk14. Cells were cultured with the

palmitic acid analogue (Alk14) to allow metabolic labeling to occur. JAM-C was immunoprecipitated from total lysate. BODIPY-azide was then conjugated to the alkyne group using click chemistry and the fluorescent signal was imaged after SDS-PAGE. B, Endogenous JAM-C in both Jurkat and HUVEC cells was fatty acylated by Alk14. C, Overexpressed FLAG-tagged JAM-C in HEK-293T cells also contained fatty acylation. D, The C264S and C265S mutations of JAM-C decreased the Alk14 labeling signal. Compared to the wild type JAM-C, palmitoylation in the single cysteine mutants (C264S and C265S) in HEK-293T cells was reduced whereas it was abolished in the double cysteine mutant (CCSS). The palmitoylation signal was quantified and normalized by the protein level on the Coomassie blue gel using Quantity One software (Bio-Rad). E, Quantified fatty acylation level of the JAM-C mutants relative to WT (mean ± S.D., n =2). *, $P < 0.05$; **, $P < 0.01$; ***, $P < 0.001$. F, The cytosolic lysine to arginine mutants, 3KR (K276R, K283R and K287R) and 4KR (K276R, K283R, K287R, and K305R) of JAM-C did not significantly reduce the Alk14 labeling signal. Representative results from two independent experiments are shown.

**JAM-C is palmitoylated by DHHC7**

We next wanted to identify the palmitoyltransferase that controls JAM-C S-palmitoylation. In mammals, there are 23 DHHC enzymes known to act as palmitoyltransferases. We co-overexpressed HA-tagged DHHC1-23 with FLAG-tagged JAM-C in HEK-293T cells and examined the fatty acylation level using the Alk14 metabolic labeling approach (Figure 2.3A). After the first round of DHHC-screening and signal quantification (Figure 2.3B), we observed that several DHHCs (DHHC7, 10, 15)

could potentially increase the JAM-C palmitoylation signal. For further confirmation, we co-expressed these DHHCs again with Flag-tagged JAM-C in HEK-293T cells and found that DHHC7 overexpression can most significantly enhance S-palmitoylation on JAM-C (Figure 2.3C-D).

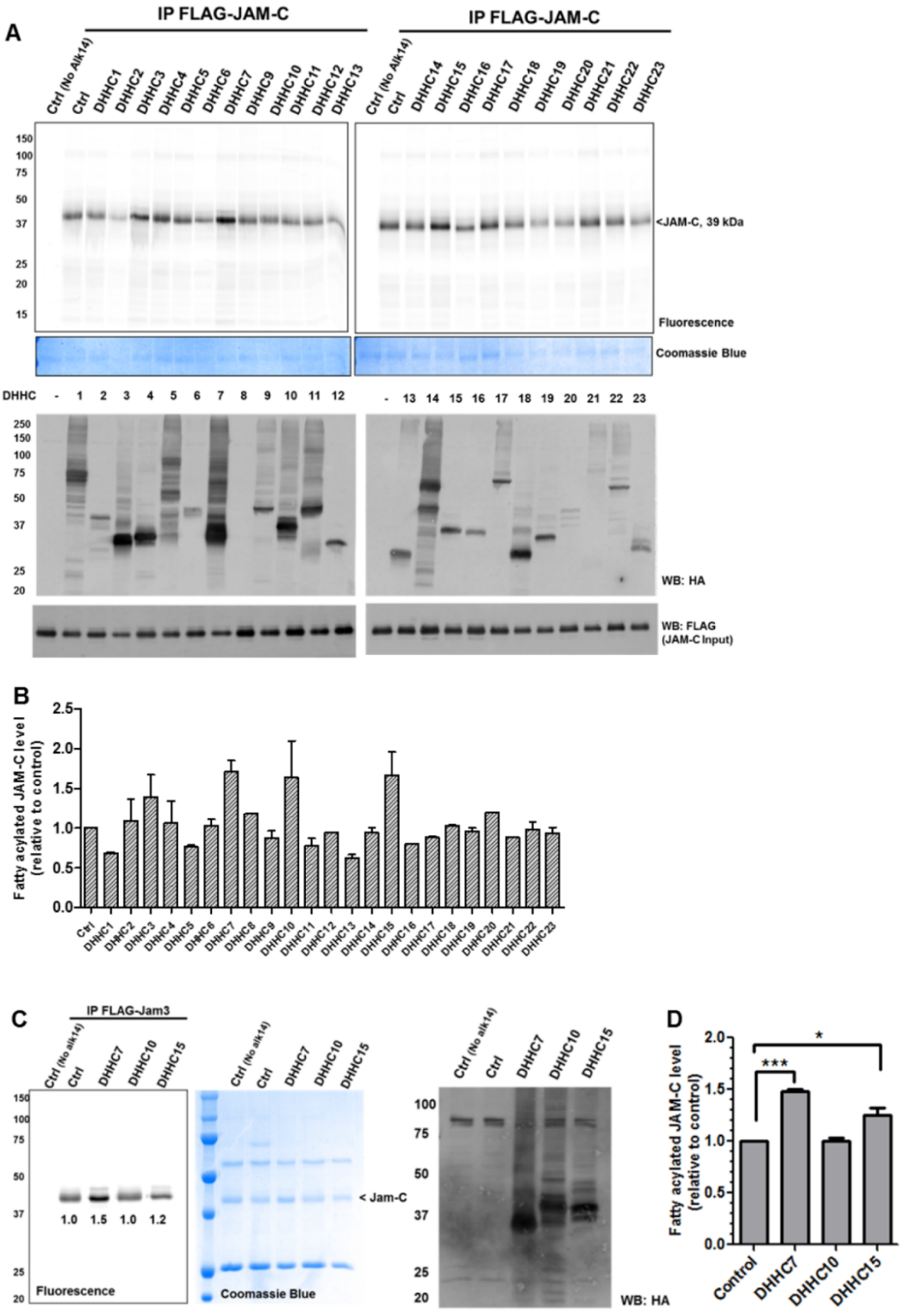


**Figure 2.3 DHHC7 overexpression enhanced the palmitoylation of JAM-C.** A, The

palmitoylation levels of JAM-C co-overexpressed with different DHHC1-23 in HEK-293T cells. B, Quantification of the results shown in A. The palmitoylation signal was quantified and normalized with the protein levels on Coomassie blue gel using Quantity One software (Bio-Rad). The signal in control cells without DHHC overexpression was set to 1.00 and serves as the reference point for all other samples. C, DHHC7 overexpression most significantly increased JAM-C palmitoylation. A representative result from two independent experiments is shown. D, The quantified fatty acylation level of JAM-C co-overexpressed with DHHC 7, 10 or 15 relative to control (mean ± S.D., n=2). *, $P < 0.05$; **, $P < 0.01$; ***, $P < 0.001$.

To further confirm that DHHC7 can directly catalyze the palmitoylation of JAM-C, we examined the S-palmitoylation of JAM-C with co-expression of wild type DHHC7 or a catalytic dead mutant, DHHS7, in which the conserved catalytic cysteine residue is mutated to serine. As expected, only overexpression of DHHC7, but not DHHS7, augmented the JAM-C fatty acylation level in HEK293T cells (Figure 2.4A). Similar results were also obtained in U87 cells (Figure 2.4B). These results suggest that catalytic activity of DHHC7 is required for the S-palmitoylation of JAM-C.

Additionally, we investigated whether DHHC7 could interact with JAM-C. HA-tagged DHHC7 was co-overexpressed with FLAG-tagged JAM-C in HEK293T cells. After HA pull down, we carried out western blot to detect FLAG-tagged JAM-C. Indeed, HA-tagged DHHC7 was able to pull down Flag-tagged JAM-C, suggesting that that JAM-C physically interacts with DHHC7 (Figure 2.4C).

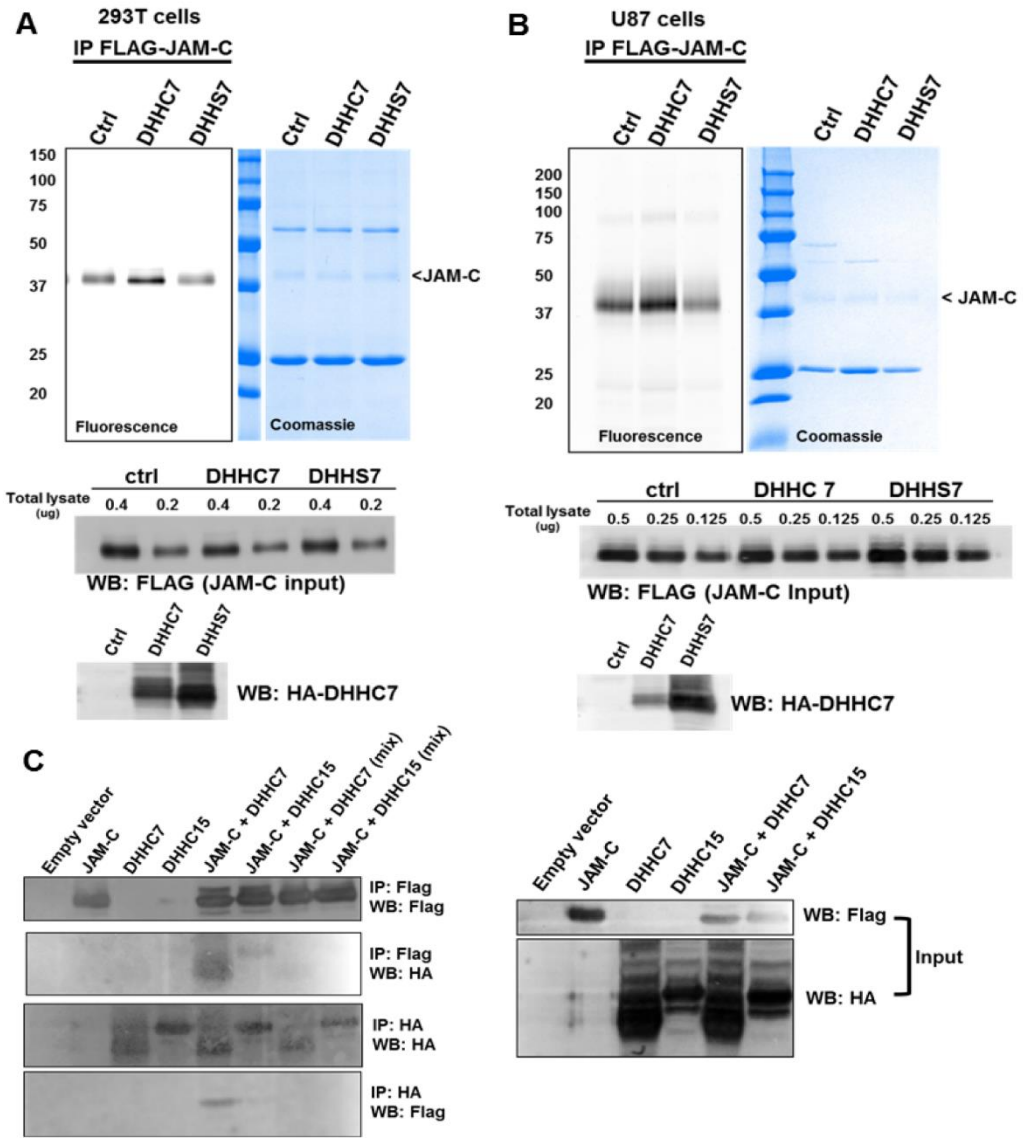


**Figure 2.4 DHHC7 interacts with JAM-C and its catalytic activity is required for JAM-C S-palmitoylation.** *A,* Overexpression of DHHC7, but not DHHS7, increased JAM-C S-palmitoylation in HEK-293T cells. DHHC7 or DHHS7 were co-overexpressed with FLAG-tagged JAM-C. FLAG-tagged JAM-C was pulled down for palmitoylation detection. *B,* The same experiment as in *A* was performed in U87 cells. *C,* DHHC7

interacts with JAM-C. HA-tagged DHHC7 was co-overexpressed with FLAG-tagged JAM-C in HEK-293T cells. HA-DHHC7 was pulled down and FLAG-tagged JAM-C was detected by western blot. A representative result from two independent experiments is shown.

**Knockdown of DHHC7 decreases JAM-C S-palmitoylation level**

Ectopic expression of the DHHCs might affect the selectivity of the enzyme and possibly lead to an increase in S-palmitoylation of non-specific targets (Dietrich et al, 2004). To verify that JAM-C is a palmitoylation target of endogenous DHHC7, we generated stable DHHC7 knockdown HEK293T cells and examined the JAM-C palmitoylation level (Figure 2.5A). Knockdown of DHHC7 but not DHHC12 and 15 led to a decrease in the JAM-C palmitoylation level, compared to the control with scrambled shRNA (Figure 2.5A-C), demonstrating that JAM-C is a palmitoylation target of endogenous DHHC7. Based on BioGPS gene database (http://biogps.org/), DHHC7 gene expression level in lung tissue is relatively high when compared to other tissues. Thus, we also chose to look at JAM-C palmitoylation in A549 lung cancer cells. Stable DHHC7 knockdown A549 cells were generated, and the JAM-C palmitoylation level was detected. In A549 cells, DHHC7 knockdown also led to a decrease in JAM-C palmitoylation (Figure 2.5D-E).

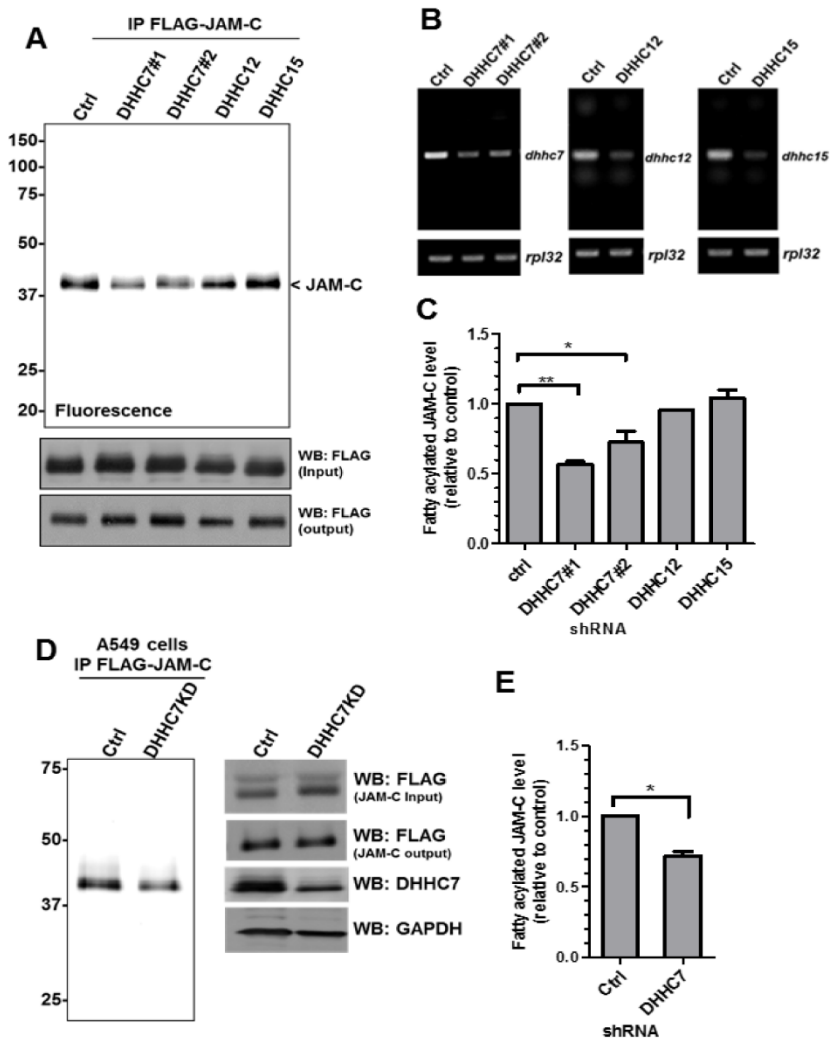


**Figure 2.5 JAM-C palmitoylation level was decreased by DHHC7 knockdown.** *A,* HEK-293T cells were infected with lentiviruses containing scramble shRNA (control) or DHHC7, DHHC12 and DHHC15 shRNAs. Puromycin resistant cells were selected for stable DHHC7, DHHC12 and DHHC15 knockdown cells and used for FLAG-tagged JAM-C overexpression. The FLAG-tagged JAM-C in the DHHC knockdown cells was then immunoprecipitated and detected for the palmitoylation level by fluorescent labeling. The palmitoylation level from each group was quantified and normalized with the corresponding protein level from the output western blot using Quantity One

software (Bio-Rad). The signal from FLAG-tagged JAM-C in the control knockdown cells was set to 1.00 and served as the reference point for the other samples. *B,* Semi-quantitative RT-PCR showed mRNA levels of *dhhc7, dhhc12 and dhhc15* in DHHC7, DHHC12 and DHHC15 stably knocked down HEK-293T cells, respectively. *C,* Quantified fatty acylated level of FLAG-tagged JAM-C overexpressed in DHHC7, DHHC12 and 15 knockdown HEK-293T cells relative to control (mean ± S.D., n=2). *D,* DHHC7 knockdown in A549 cells also decreased the palmitoylation of JAM-C. The experiments were carried out similar to that described in A. *E,* Quantified fatty acylated level of JAM-C in A549 cells, mean ± SD (n = 2). *, $P < 0.05$; **, $P < 0.01$; ***, $P < 0.001$.

**S-palmitoylation promotes JAM-C localization to the cell tight junction region**

To further understand the physiological function of JAM-C S-palmitoylation, we investigated whether this modification is required for specific localization of JAM-C. FLAG-tagged JAM-C WT and the palmitoylation deficient CCSS mutant were ectopically expressed in A549 lung cancer cells. The cells were stained with an anti-FLAG antibody to visualize JAM-C. JAM-C WT was more concentrated at the tight junction (white arrow), while the CCSS mutant was distributed more evenly across the whole cell membrane and the cytosol (Figure 2.6). The co-localization between JAM-C and ZO-1 was quantified using the coloc2 plugin in the Fiji software and was presented as the mean of Manders coefficient (M1 and M2) ± SEM. For JAM-C WT, M1: 0.66 ± 0.015; M2: 0.58 ± 0.021; n =15. For JAM-C CCSS mutant, M1: 0.45 ± 0.027; M2 0.40 ± 0.02; n =15 (Figure 2.6). Thus, it appears that S-palmitoylation of JAM-C facilitates its localization to the cell tight jucntion region.

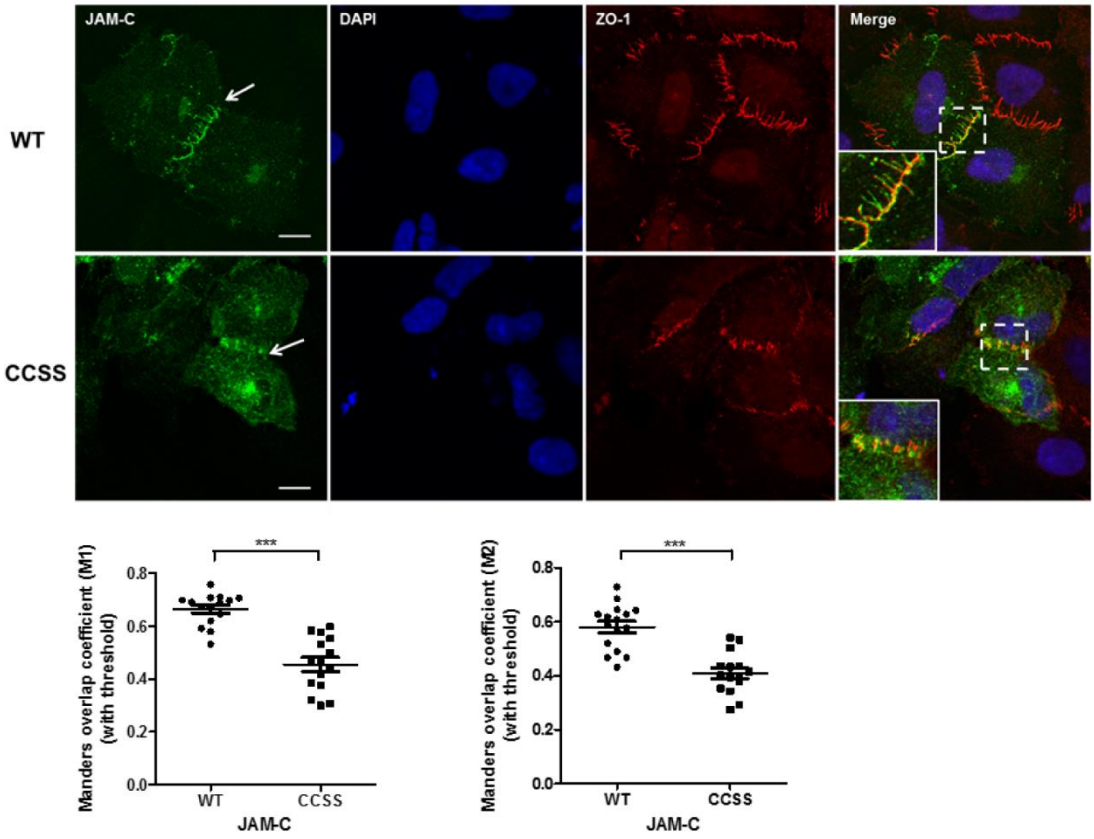


**Figure 2.6 S-palmitoylation promotes JAM-C localization to the cell tight junction.** FLAG-tagged JAM-C WT and the CCSS mutant were ectopically expressed in A549 cells. The cells were immunofluorescently stained with anti-FLAG antibody after fixation. JAM-C WT was more concentrated in the cell tight junction region (a white arrow), while the CCSS mutant was distributed more evenly across the cell membrane and the cytosol. JAM-C and ZO-1 (a tight junction marker) were demonstrated in green and red, respectively. The cells were visualized at the room temperature with a Zeiss LSM 710 confocal microscope with a 63×/1.4 oil immersion objective. Images were viewed and analyzed using ZEN 2012 imaging software (Zeiss). Scale bar, 10 μm. The co-localization between JAM-C and ZO-1 was analyzed by the coloc2 plugin in the Fiji

software and was presented as the mean of Mander's coefficient (M1 and M2) ± SEM, n = 15 with three independent experiments. *** p ≤0.0001, unpaired Student's *t*-test.

**JAM-C S-palmitoylation affects cell migration**

Since JAM-C palmitoylation affects its localization to the cell-cell contact regions, we wondered if it would also affect cell-cell adhesion. We therefore decided to check if JAM-C S-palmitoylation could affect cell migration, which is influenced by cell-cell adhesion. A549 cells were transfected with FLAG-tagged JAM-C WT or the CCSS mutant for 24 hrs. We used a transwell migration assay, which was performed in a 24-well transwell plate with 8 mm polycarbonate sterile membranes. Overexpression of JAM-C WT dramatically decreased cell migration compared to control cells that was transfected with an empty vector. In contrast, overexpression of the non-palmitoylable CCSS mutant only slightly decreased the cell migration compared to control cells that was transfected with an empty vector (Figure 2.7A-B). The difference in cell migration was not due to the variation of cell proliferation as there was no significant difference in cell proliferation when JAM-C WT and the CCSS mutant were overexpressed (data not shown). Thus, S-palmitoylation of JAM-C affects cell migration.

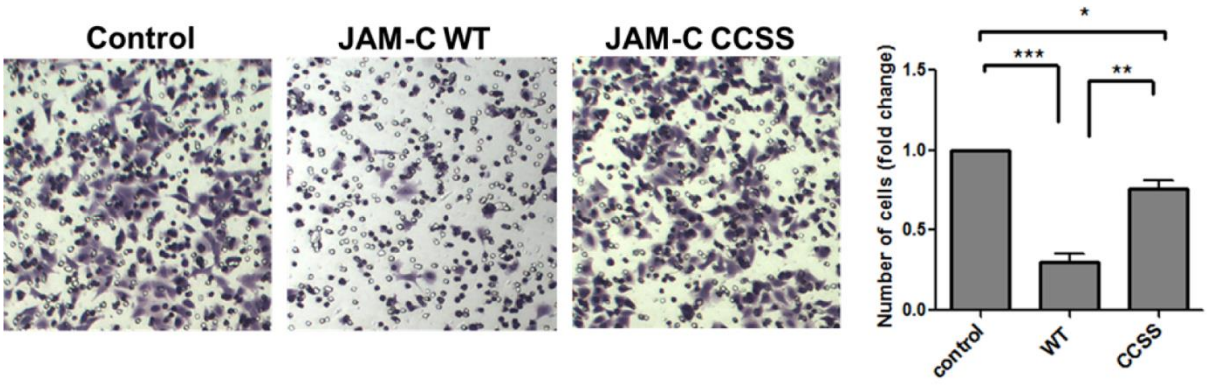


**Figure 2.7 JAM-C S-palmitoylation affects cell migration.** A549 cells were transfected with FLAG-tagged JAM-C WT or the CCSS mutant for 24 hr and then cultured in RPMI serum-free medium for 14 hr. The cell migration assay was then performed in a 24-well transwell plate with 8 mm polycarbonate sterile membranes. A total of 3.5 x 104 cells in 200 µl of RPMI serum-free medium were plated into each upper chamber and placed in wells containing 600 µl of RPMI medium supplemented with 10% FBS. After 24 hr, cells on the upper surface were detached with a cotton swab. The chambers were fixed and cells in the lower filter were stained with 0.1% crystal violet for 15 minutes and counted. The quantified results were calculated by counting three random fields of migrated cells. The control cells were transfected with an empty pCMV4a vector. A, representative images of migrated cells from three independent experiments are shown. B, The number of migrated cells per field was quantified and normalized by the value of the control. Bars, mean ± SD (n = 3). *, $P < 0.05$; **, $P < 0.01$; ***, $P < 0.001$.

## 2.5 DISCUSSION

Protein lipidation has become a more widely identified class of protein post-translational modifications, and has been found to be involved in numerous biological pathways (Resh et al, 1999; Resh et al, 2012). Here, using a bio-orthogonal palmitic acid probe (Yount et al, 2011; Wilson et al, 2011), we demonstrated that both endogenous and ectopically expressed JAM-C contain S-palmitoylation. S-palmitoylation occurs on Cys264 and Cys265 of JAM-C. We, surprisingly, found that the S-palmitoylation on these residues was resistant to high concentrations of hydroxylamine. Nevertheless, we observed no obvious change in the fatty acylation signal after mutating all the cytosolic lysine residues to arginine. These findings indicated that Jam-C is palmitoylated on cysteine residues, but not on lysine residues.

The palmitoyl acyltransferase (PAT) family members share a conserved Asp-His-His-Cys (DHHC)-cysteine rich domain (CRD) as a catalytic domain of the enzyme (Roth et al, 2002; Lobo et al, 2002). DHHCs have broad substrate specificity, and how substrate specificity is determined remains unclear. By screening the 23 DHHCs, we have found that overexpression of DHHC7 can substantially increase the JAM-C palmitoylation level. Notably, other DHHCs may also be able to enhance JAM-C palmitoylation, but not to the same extent as DHHC7. It is possible that some DHHCs have redundant functions and act on the same targets. Moreover, we showed that knockdown of DHHC7 decreased the S-palmitoyl level of JAM-C, supporting that JAM-C is a direct palmitoylation target of endogenous DHHC7.

JAM-C has previously been shown to be phosphorylated at Ser281, and JAM-C localization at the cell-cell contact region is negatively regulated by Ser281

phosphorylation (Mandicourt et al, 2007; Ebnet et al, 2003). The JAM-C S281A mutant led to the mis-localization and diffusion from the cell-cell contact region. In our case, we observed that JAM-C WT was concentrated at the cell-cell contact region, while the CCSS mutant was distributed more evenly on the cell membrane, which is similar to the effect of S281A. JAM-C has been reported to have homophilic interactions with JAM-C and heterophilic interactions with other PDZ-containing domain proteins such as ZO-1 and PAR3 at the cell tight junction. A possible explanation for the effect of palmitoylation on JAM-C localization is that S-palmitoylation facilitates the interaction of JAM-C with its interacting partners leading to the enrichment of JAM-C WT at the cell-cell contact regions.

We demonstrated for the first time that JAM-C palmitoylation can affect cell migration. Overexpression of WT JAM-C decreased migration of A549 cells, but overexpression of the non-palmitoylatable JAM-C mutant did not affect the migration much. S-palmitoylation of CD44, an adhesion protein, has previously been found to decrease the migration of breast cancer cells, and the invasiveness of cancer is negatively correlated with palmitoylation status of CD44 (Babina et al, 2014). This is similar to our result that WT JAM-C decreases the cell migration of A549 cells but the non-palmitoylatable mutant did not. The effect of JAM-C palmitoylation on cell migration is likely connected to its effect on the cell-cell contact localization of JAM-C and cell tight junction integrity. However, exactly how JAM-C palmitoylation regulates cell migration remains elusive. Previously, JAM-C phosphorylation on Ser281 was reported to be involved in cell migratory phenotype via β3-integrin modulation (Mandicourt et al, 2007). The S281A JAM-C mutant can activate β3-integrin thereby enhancing the cell migration

when compared to that of the wild type JAM-C (Mandicourt et al, 2007). JAM-C S-palmitoylation may also affect β3-integrin activation. Since S-palmitoylation is labile and reversible, the change in palmitoylation level might be a way to dynamically control homophillic or heterophillic interactions of JAM-C and thus regulate cell migration.

Currently, only a few substrate proteins for DHHC7 are known, including Fas (Rossin et al, 2015), sex steroid receptors (Pedram et al, 2012), phosphatidylinositol 4-kinase Iiα (Lu et al, 2012), Gα (Tsutsumi et al, 2009) and stress-regulated exon (STREX) (Tian et al, 2010). Our finding thus significantly expands the substrate scope of DHHC7. Interestingly, a decrease in DHHC7 levels has been related to tumorigenesis (Gaspar et al, 2008), suggesting that DHHC7 may play a role in preventing tumorigenesis. Our finding that JAM-C palmitoylation affects cancer cell migration and that DHHC7 directly controls the palmitoylation level of JAM-C suggests that pharmacologically controlling DHHC7 could potentially be a useful strategy to control cancer cell migration, and possibly cancer metastasis. However, to fully take advantage of this, a more detailed understanding of the function of DHHC7 is needed.

## 2.6 REFERENCES

Akawi, N. A., Canpolat, F. E., White, S. M., Quilis-Esquerra, J., Morales Sanchez, M., Gamundi, M. J., Mochida, G. H., Walsh, C. A., Ali, B. R., and Al-Gazali, L. (2013) Delineation of the clinical, molecular and cellular aspects of novel JAM3 mutations underlying the autosomal recessive hemorrhagic destruction of the brain, subependymal calcification, and congenital cataracts. Hum. Mutat. 34, 498-505

Arcangeli, M. L., Frontera, V., Bardin, F., Thomassin, J., Chetaille, B., Adams, S., Adams, R. H., and Aurrand-Lions, M. (2012) The Junctional Adhesion Molecule-B regulates JAM-C-dependent melanoma cell metastasis. FEBS Lett. 586, 4046-4051

Babina, I. S., McSherry, E. A., Donatello, S., Hill, A. D., and Hopkins, A. M. (2014) A novel mechanism of regulating breast cancer cell migration via palmitoylation-dependent alterations in the lipid raft affiliation of CD44. Breast Cancer Res 16, R19

Bazzoni, G. (2003) The JAM family of junctional adhesion molecules. Curr. Opin. Cell Biol. 15, 525-530

Dietrich, L. E., and Ungermann, C. (2004) On the mechanism of protein palmitoylation. EMBO Rep 5, 1053-1057

Ebnet, K., Aurrand-Lions, M., Kuhn, A., Kiefer, F., Butz, S., Zander, K., Meyer zu Brickwedde, M. K., Suzuki, A., Imhof, B. A., and Vestweber, D. (2003) The junctional adhesion molecule (JAM) family members JAM-2 and JAM-3 associate with the cell polarity protein PAR-3: a possible role for JAMs in endothelial cell polarity. J. Cell Sci. 116, 3879-3891

Ebnet, K., Suzuki, A., Ohno, S., and Vestweber, D. (2004) Junctional adhesion molecules (JAMs): more molecules with dual functions? J. Cell Sci. 117, 19-29

Fukata, M., Fukata, Y., Adesnik, H., Nicoll, R. A., and Bredt, D. S. (2004) Identification of PSD-95 palmitoylating enzymes. Neuron 44, 987-996

Fuse, C., Ishida, Y., Hikita, T., Asai, T., and Oku, N. (2007) Junctional adhesion molecule-C promotes metastatic potential of HT1080 human fibrosarcoma. J. Biol. Chem. 282, 8276-8283

Gaspar, C., Cardoso, J., Franken, P., Molenaar, L., Morreau, H., Moslein, G., Sampson, J., Boer, J. M., de Menezes, R. X., and Fodde, R. (2008) Cross-species comparison of human and mouse intestinal polyps reveals conserved mechanisms in adenomatous polyposis coli (APC)-driven tumorigenesis. Am J Pathol 172, 1363-1380

Gliki, G., Ebnet, K., Aurrand-Lions, M., Imhof, B. A., and Adams, R. H. (2004) Spermatid differentiation requires the assembly of a cell polarity complex downstream of junctional adhesion molecule-C. Nature 431, 320-324

Guo, J., Wang, L., Zhang, Y., Wu, J., Arpag, S., Hu, B., Imhof, B. A., Tian, X., Carter, B. D., Suter, U., and Li, J. (2014) Abnormal junctions and permeability of myelin in PMP22-deficient nerves. Ann. Neurol. 75, 255-265

Hao, S., Yang, Y., Liu, Y., Yang, S., Wang, G., Xiao, J., and Liu, H. (2014) JAM-C promotes lymphangiogenesis and nodal metastasis in non-small cell lung cancer. Tumour Biol 35, 5675-5687

Jiang, H., Khan, S., Wang, Y., Charron, G., He, B., Sebastian, C., Du, J., Kim, R., Ge, E., Mostoslavsky, R., Hang, H. C., Hao, Q., and Lin, H. (2013) SIRT6 regulates TNF-alpha secretion through hydrolysis of long-chain fatty acyl lysine. Nature 496, 110-113

Johnson-Leger, C. A., Aurrand-Lions, M., Beltraminelli, N., Fasel, N., and Imhof, B. A. (2002) Junctional adhesion molecule-2 (JAM-2) promotes lymphocyte transendothelial migration. Blood 100, 2479-2486

Keiper, T., Santoso, S., Nawroth, P. P., Orlova, V., and Chavakis, T. (2005) The role of junctional adhesion molecules in cell-cell interactions. Histol Histopathol 20, 197-203

Langer, H. F., Orlova, V. V., Xie, C., Kaul, S., Schneider, D., Lonsdorf, A. S., Fahrleitner, M., Choi, E. Y., Dutoit, V., Pellegrini, M., Grossklaus, S., Nawroth, P. P., Baretton, G., Santoso, S., Hwang, S. T., Arnold, B., and Chavakis, T. (2011) A novel function of junctional adhesion molecule-C in mediating melanoma cell metastasis. Cancer Res. 71, 4096-4105

Leinster, D. A., Colom, B., Whiteford, J. R., Ennis, D. P., Lockley, M., McNeish, I. A., Aurrand-Lions, M., Chavakis, T., Imhof, B. A., Balkwill, F. R., and Nourshargh, S. (2013) Endothelial cell junctional adhesion molecule C plays a key role in the development of tumors in a murine model of ovarian cancer. FASEB J. 27, 4244-4253

Linder, M. E., and Jennings, B. C. (2013) Mechanism and function of DHHC S-acyltransferases. Biochem. Soc. Trans. 41, 29-34

Lobo, S., Greentree, W. K., Linder, M. E., and Deschenes, R. J. (2002) Identification of a Ras palmitoyltransferase in Saccharomyces cerevisiae. J. Biol. Chem. 277, 41268-41273

Lu, D., Sun, H. Q., Wang, H., Barylko, B., Fukata, Y., Fukata, M., Albanesi, J. P., and Yin, H. L. (2012) Phosphatidylinositol 4-kinase IIalpha is palmitoylated by Golgi-localized palmitoyltransferases in cholesterol-dependent manner. J. Biol. Chem. 287, 21856-21865

Mandicourt, G., Iden, S., Ebnet, K., Aurrand-Lions, M., and Imhof, B. A. (2007) JAM-C regulates tight junctions and integrin-mediated cell adhesion and migration. J. Biol. Chem. 282, 1830-1837

Pedram, A., Razandi, M., Deschenes, R. J., and Levin, E. R. (2012) DHHC-7 and -21 are palmitoylacyltransferases for sex steroid receptors. Mol Biol Cell 23, 188-199

Resh, M. D. (1999) Fatty acylation of proteins: new insights into membrane targeting of myristoylated and palmitoylated proteins. Biochim. Biophys. Acta 1451, 1-16

Resh, M. D. (2012) Targeting protein lipidation in disease. Trends Mol. Med. 18, 206-214

Rossin, A., Durivault, J., Chakhtoura-Feghali, T., Lounnas, N., Gagnoux-Palacios, L., and Hueber, A. O. (2015) Fas palmitoylation by the palmitoyl acyltransferase DHHC7 regulates Fas stability. Cell Death Differ. 22, 643-653

Roth, A. F., Feng, Y., Chen, L., and Davis, N. G. (2002) The yeast DHHC cysteine-rich domain protein Akr1p is a palmitoyl transferase. J. Cell Biol. 159, 23-28

Scheiermann, C., Colom, B., Meda, P., Patel, N. S., Voisin, M. B., Marrelli, A., Woodfin, A., Pitzalis, C., Thiemermann, C., Aurrand-Lions, M., Imhof, B. A., and Nourshargh, S. (2009) Junctional adhesion molecule-C mediates leukocyte infiltration in response to ischemia reperfusion injury. Arterioscler Thromb Vasc Biol 29, 1509-1515

Smotrys, J. E., and Linder, M. E. (2004) Palmitoylation of intracellular signaling proteins: regulation and function. Annu. Rev. Biochem. 73, 559-587

Tenan, M., Aurrand-Lions, M., Widmer, V., Alimenti, A., Burkhardt, K., Lazeyras, F., Belkouch, M. C., Hammel, P., Walker, P. R., Duchosal, M. A., Imhof, B. A., and Dietrich, P. Y. (2010) Cooperative expression of junctional adhesion molecule-C and -B supports growth and invasion of glioma. Glia 58, 524-537

Tian, L., McClafferty, H., Jeffries, O., and Shipston, M. J. (2010) Multiple palmitoyltransferases are required for palmitoylation-dependent regulation of large

conductance calcium- and voltage-activated potassium channels. J. Biol. Chem. 285, 23954-23962

Tsutsumi, R., Fukata, Y., Noritake, J., Iwanaga, T., Perez, F., and Fukata, M. (2009) Identification of G protein alpha subunit-palmitoylating enzyme. Mol. Cell. Biol. 29, 435-447

Weber, C., Fraemohs, L., and Dejana, E. (2007) The role of junctional adhesion molecules in vascular inflammation. Nat. Rev. Immunol. 7, 467-477

Wilson, J. P., Raghavan, A. S., Yang, Y. Y., Charron, G., and Hang, H. C. (2011) Proteomic analysis of fatty-acylated proteins in mammalian cells with chemical reporters reveals S-acylation of histone H3 variants. Mol. Cell. Proteomics 10, M110 001198

Wyss, L., Schafer, J., Liebner, S., Mittelbronn, M., Deutsch, U., Enzmann, G., Adams, R. H., Aurrand-Lions, M., Plate, K. H., Imhof, B. A., and Engelhardt, B. (2012) Junctional adhesion molecule (JAM)-C deficient C57BL/6 mice develop a severe hydrocephalus. PLoS One 7, e45619

Yount, J. S., Zhang, M. M., and Hang, H. C. (2011) Visualization and Identification of Fatty Acylated Proteins Using Chemical Reporters. Curr Protoc Chem Biol 3, 65-79

# CHAPTER 3

# LYSINE DEFATTY-ACYLATION OF HDAC8

## 3.1 ABSTRACT

The zinc-dependent histone deacetylases (HDACs) are a family of enzymes that regulate several biological pathways through the deacetylation of lysine residues on histone and non-histone proteins. Aberrant expression of HDACs has been implicated in several diseases. A class I family member of HDACs, HDAC8, has been shown to have low deacetylation activity compared to other HDACs *in vitro.* Recent studies showed that several nicotinamide adenine dinucleotide ($NAD^+$)-dependent protein lysine deacetylases, or sirtuins, with low deacetylase activities can actually hydrolyze other acyl lysine modifications more efficiently. Inspired by this, we tested the activity of HDAC8 using a variety of different acyl lysine peptides. Screening a panel of peptides with different acyl lysine modifications, we found that HDAC8 can catalyze the removal of acyl groups with 2-16 carbons from lysine 9 of the histone H3 peptide (H3K9). Interestingly, the catalytic efficiencies ($k_{cat}/K_m$) of HDAC8 on octanoyl, dodecanoyl, and myristoyl lysine are several folds better than that on acetyl lysine. The increased catalytic efficiencies of HDAC8 on larger fatty acyl groups are due to the much lower $K_m$ values. T-cell leukemia Jurkat cells treated with a HDAC8 specific inhibitor, PCI-34051, exhibited an increase in global fatty acylation compared to control treatment. Thus, the defatty-acylation activity of HDAC8 is likely physiologically relevant and further investigation to identify HDAC8 defatty-acylation targets is warranted.

## 3.2 INTRODUCTION

Epigenetic modification of histones plays a crucial role in the regulation of gene expression. Histone acetylation and deacetylation on lysine residues is mediated by histone acetyltransferases (HATs) and histone deacetylases (HDACs), respectively (Yang et al, 2007). HDACs have been classified into four classes: class I, homologous to yeast Rpd3, consists of HDAC1, 2, 3 and 8; class II, homologous to yeast Hda1, is divided into two subclasses: IIa (HDAC4, 5, 7, 9) and IIb (HDAC6, 10) that contain one and two catalytic domains, respectively; class III HDACs are $NAD^+$-dependent deacetylases, known as sirtuins; and class IV is comprised solely of HDAC11 which contains a deacetylase domain homologous to class I and class II (Delcuve et al, 2012).

HDAC8 was first cloned from the human kidney, and identified as a new member of the Class I family of HDACs by Winkler and colleagues in 2000 (Hu et al, 2000). The gene is encoded for 377 amino acids (~44 kDa), it has a shorter C-terminal region relative to other class I members. HDAC8 protein is expressed ubiquitously in different tissues, including lung, heart, pancreas and kidney tissues. HDAC8 also has ubiquitous expression in various different tumor cell lines (Buggy et al, 2000).

### 3.2.1 HDAC8 localization

HDAC8 was initially identified as a nucleus-localized enzyme, similar to HDAC1 and HDAC2, but later several studies suggested that it is also present in the cytosol. Through immunocytochemistry, cell fractionation and immunofluorescence,

Waltregny et al revealed that HDAC8 is distributed in the cytosol of different cell lines, including myoepithelial cells, visceral and vascular smooth muscle cells and murine NIH-3T3 fibroblasts (Waltregny et al 2004). Other groups also showed that endogenous HDAC8 from human myometrial cells was localized in both the nucleus and cytosol (Karolczak-Bayatti et al, 2011). Therefore, HDAC8 is located both in the nucleus and cytosol; however, its intracellular localization might be cell-type dependent.

### 3.2.2 Physiological functions of HDAC8

HDAC8 plays an essential role in development, in particular skull morphogenesis; and HDAC8 deletion in mice causes death shortly after birth (Haberland et al, 2009). HDAC8 knockout mice showed a defect with cranial neural crest patterning, leading to skull instability, brain trauma, and subsequently perinatal lethality. From the transcriptional profiling of the cranial neural crest it was found that *Otx2* and *Lhx1*, and other homeobox transcription factors are up-regulated in the HDAC8 knockout mice. Interestingly, transgenic overexpression of Otx2 and Lhx1 showed skull defective phenotypes similar to what was observed in the HDAC8 deletion mice. This suggests that HDAC8 represses the expression of *Otx2* and *Lhx1* in the cranial neural crest, and that the unregulated expression of these homeobox transcription factors leads to the aberrant skull morphogenesis. It is, however, still not clear whether HDAC8 directly, or indirectly regulate the expression of *Otx2* and *Lhx1.*

HDAC8 has been shown to be indispensable for cancer cell survival. HDAC8 knockdown inhibits the growth of various cancer lines, such as A549 (lung cancer), HeLa (breast cancer), and HCT1162 (colorectal cancer) (Vannini et al, 2004). Moreover, high HDAC8 expression level is positively correlated to the poor prognosis and metastasis of neuroblastoma cells, and knockdown of HDAC8 leads to cell cycle arrest and a decrease in cell proliferation (Oehme et al, 2009). Similarly, the up-regulation of HDAC8 mRNA levels was observed in breast cancer, and high HDAC8 expression is associated with a poor prognosis of early-stage of breast cancer while HDAC8 depletion or inhibition can decrease the cancer cell migration (Hsieh et al, 2016). Therefore, HDAC8 is considered as a promising therapeutic target for different cancers.

Furthermore, HDAC8 is essential for entry of Influenza A virus into host cells. Knockdown of HDAC8 leads to a drastic change in the microtubule organization system, including the centrosome splitting due to the disruption of microtubule organizing center (MTOC) and decreasing late endosome and lysosomes motility. Influenza A virus generally enters host cells by endocytosis. The virus capsids penetrate into the cytosol from the late endosomes or endolysosomes and finally target to the host genome. Therefore, reduction in the motility of late endosomes/lysosomes can decrease the virus infection efficiency. This study suggests that HDAC8 promotes the microtubule organization system by increasing the association between microtubules and MTOC even though it remains unclear if HDAC8 directly acts on any protein components of microtubules or MTOC (Yamauchi et al, 2011).

As mentioned above, HDAC8 has been implicated in diverse biological functions. The direct substrates of HDAC8 that promote these phenotypes, however, have remained elusive.

### 3.2.3 HDAC8 deacetylation targets

To date, only two proteins have been validated as HDAC8 deacetylation targets. These proteins are estrogen-related receptor alpha (ERRα) (Wilson et al, 2010) and structural maintenance of chromosomes protein 3 (SMC3) (Deardorff et al, 2012).

#### Estrogen-Related Receptor α (ERRα)

The estrogen-related receptor alpha (ERRα) is an orphan nuclear hormone receptor that serves as a metabolic regulator. ERRα knockout mice are resistant to a high-fat diet-induced obesity (Luo et al, 2003). The DNA binding domain of ERRα is acetylated on four lysine residues (K129, K138, K160, and K162) by the p300 coactivator associated factor (PCAF). Co-expression between ERRα and PCAF significantly decreases the ability of ERRα to activate the transcription of target genes. Based on HDAC and sirtuin screenings, it was found that both HDAC8 and Sirt1 can enhance the transcriptional activity of ERRα. Also, these two enzymes interact directly with ERRα, and can deacetylate ERRα *in vitro*. Moreover, knockdown of either enzyme leads to an elevated acetylation of ERRα. These lines of evidence demonstrate that ERRα is a target of HDAC8 and the dynamics of

acetylation and deacetylation can regulate the ERRα transcriptional activity (Wilson et al, 2010).

**Structural maintenance of chromosomes protein 3 (SMC3)**

SMC3 is one component of a cohesin protein complex containing SMC1A, SMC3, and RAD21. SMC3 undergoes acetylation by ESCO1 and ESCO2. Recently, Deardorff and colleagues demonstrated that HDAC8 can deacetylase SMC3, and that SMC3 deacetylation is required for cohesin recycling in the cell cycle (Deardorff et al, 2012). Knockdown or inhibition of HDAC8 leads to an increase in acetylated SMC3 in both soluble and chromatin fractions. However, an elevation of acetylated SMC3 in HDAC8 KD cells in soluble fraction implies that acetylated SMC3 is dissociated from chromatin. Also, the defective sister chromatid cohesion was observed in HDAC8-depleted cells. It is proposed that hyperacetylated SMC3, resulting from the loss of HDAC8 activity, leads to an inefficient reload of the cohesin complex on the chromatin, thereby leading to a defect of sister chromatic cohesion in the cell cycle.

The defect in SMC3 deacetylation in HDAC8 deficient cells has been linked to Cornelia de Lange Syndrome (CdLS) which is a congenital anomaly disorder caused by several gene mutations of cohesion complex components (SMC1A, SMC3, and RAD21) and the cohesin loading protein (NIPBL). Several HDAC8 nonsense and missense mutations have been identified in CdLS patients. These HDAC8 mutations (H180R and G320R) were expressed in *E. coli* and tested for deacetylation activity and showed a drastic decrease in activity relative to the wild

type. Moreover, the transcriptional profiling of these HDAC8 mutations is correlated with that of NIPBL mutations in CdLs patients. These results therefore suggest that the loss of HDAC8 activity is associated with CdLS and leads to the decrease in bound cohesin complex (Deardorff et al, 2012).

### 3.2.4 Regulation of HDAC8 by phosphorylation

HDAC8 is phosphorylated on Ser39 by cyclic AMP-dependent protein kinase A (PKA). This modification has been shown to negatively regulate the deacetylation activity of HDAC8. Mutation of Ser39 to Ala residue on HDAC8 or treating with a PKA inhibitor, H89, decreases the HDAC8 phosphorylation level. Interestingly, the prevention of phosphorylation enhances the HDAC8 deacetylase activity. On the other hand, the Ser39 to Glu mutation on HDAC8 or treating cells with forskolin, which is an activator for adenyl cyclase that converts ATP to cAMP, decreases HDAC8 deacetylation activity. In line with these results, when HDAC8 is hyper-phosphorylated, the acetylation level of histone H3, and H4 is increased, and vice versa. This suggests that the phosphorylation status of HDAC8 might either directly or indirectly regulate the global acetylation of histones (Lee et al, 2004).

### 3.2.5 HDAC8 Inhibitors and activator

Most of the current HDAC inhibitors have been developed with a common pharmacophore. Firstly, as a metal or zinc-binding group can interact with a zinc ion at the active site of enzymes, the current inhibitors aim to disrupt the metal binding that is necessary for the enzymatic activity of HDACs. So far, hydroxamic acid is the

most potent metal binding group, and it has been extensively studied (Chen et al, 2014). Secondly, a hydrophobic linker group of inhibitor is designed to mimic an N-acetyl-lysine side chain. Thirdly, a surface recognition domain or capping structure selectively interacts with protein surface (Bowers et al, 2008). The interaction with the protein surface and the properties of the metal binding group of the inhibitors mostly contribute to the potency of the HDAC inhibitor (Chen et al, 2014).

Several HDAC8 specific inhibitors have been developed, with different potencies. PCI-34051, an HDAC8-specific inhibitor, was first developed in 2008 and showed selectivity for HDAC8 over HDAC1, 2, 3, 6, and 10 (Balasubramanian et al, 2008). This inhibitor induces apoptosis in T-cell leukemias e.g. Jurkat, HuT78 and Molt-4 cells, but not in other solid tumor or hematopoietic tumor lines. However, T-cell signaling is not required for the PCI-34051-induced cell death as both T-cell receptor and ZAP-70 kinase knockouts do not affect the apoptotic phenotype. Instead, the inhibitor activates phospholipase-C γ1 (PLC- γ1), leading to increased calcium uptake by mitochondria and the release of cytochrome C into the cytosol. These effects finally result in caspase-activated apoptosis. Nevertheless, it remains unclear how HDAC8 inhibition leads to the PLC-γ1 activation. Presumably, certain adaptor proteins in the PLC-γ1 activation pathway may be HDAC8 deacetylation targets even though an off-target effect is plausible (Balasubramanian et al, 2008).

Other HDAC8-specific inhibitors have since been developed and have different potencies and cytotoxic properties. For example, C149 was demonstrated to have a lower $IC_{50}$ than PCI-34051, and it can inhibit the growth of both T-cell lymphomas and neuroblastoma cells (Suzuki et al, 2012). Another HDAC8 inhibitor

is Jδ, which is not selective to HDAC8 as it can also inhibit HDAC1. Jδ has been shown to activate the gene expression of Otx2 and Lhx1 which are known to be negatively regulated by HDAC8 (Haberland et al, 2009 and Saha et al, 2013). A dual HDAC6/HDAC8 inhibitor, BRD73954, has also been reported (Olson et al 2013).

Through a fluorogenic assay, it was found that a *N*-acetylthiourea derivative, N-(phenylcarbamothioyl)benzamide (TM-2-51), can selectively activate the *in vitro* deacetylase activity of HDAC8. This activator can increase the catalytic efficiency of HDAC8 by decreasing its deacetylation $K_{m,}$ and enhancing the $K_{cat}$ (Singh et al, 2011). TM-2-51 has been shown to improve the compromised HDAC8 catalytic activities of certain mutants found in Cornelia de Lange Syndrome (CdLS), suggesting it might be a promising therapeutic approach for CdLS (Decroos et al, 2014).

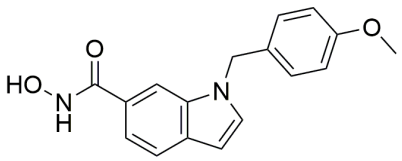

PCI-34051

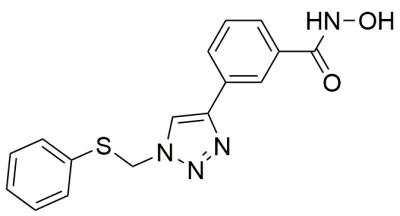

C149

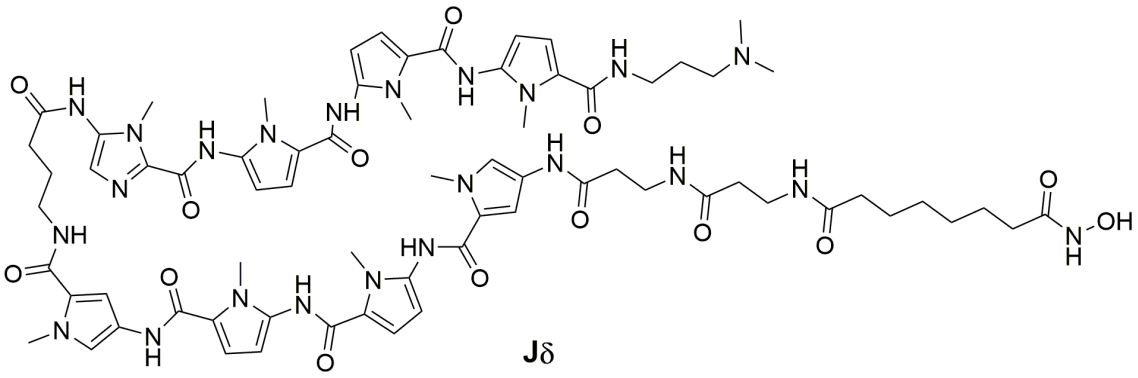

Jδ

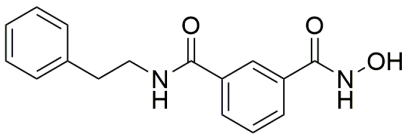

BRD73954

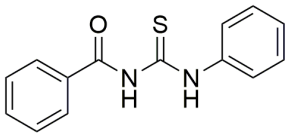

N-(phenylcarbamothioyl)benzamide
TM-2-51

**Figure 3.1 Structures of HDAC8 inhibitors and HDAC8 activator**

### 3.2.6 Methods to study HDAC8 deacylation activity

Previous studies of the *in vitro* HDAC catalytic activity have commonly relied on two techniques, a fluorogenic assay and a HPLC-based method. Some studies have been done using the [$^3$H] radioactive labeling on acetyl peptides (Buggy et al, 2000) and mass spectrometry based assay (Gurard-Levin et al, 2008).

The fluorogenic assay, or Fluor-de-lys assay, employs a synthesized histone H4 or p53 tetramer peptide containing an acetyl lysine and a methylcoumarin moiety at the C terminus. Upon deacetylation, the peptide can be cleaved by trypsin, and then release the fluorescent methylcoumarin molecule that can be detected at 460 nm (Wegener et al, 2002). This assay has been useful for a high-throughput screening aimed at identifying HDAC inhibitors, and the kit for the assay is commercially available. Nevertheless, the methylcoumarin is bulky, and might interfere with the enzyme binding. Moreover, it has been reported that the methylcoumarin fluorophore can react with some HDACs and increase the activity, leading to an inaccuracy of the tested reaction (Wolfson et al, 2012; Gurard-Levin et al, 2009). Also, due to a confined set of peptide sequences, this technique might not be suitable for showing the selectivity of enzymes.

For the HPLC-based method, each enzymatic reaction consists of a peptide substrate which is incubated with the enzymes. The reaction is analyzed by reverse phase HPLC column, and the product formation is verified by LC-MS. The product peak is identified by comparing the retention time to a standard product peak, the same peptide backbone with no modification. The peak area is measured and a conversion percentage is calculated to roughly estimate the enzyme activity. Since

both the fluorogenic and HPLC-based assays rely on the substrate peptides from established HDAC targets, these assays might not holistically reflect the activity of a specific HDAC. Furthermore, these assays do not account for physiological conditions where the HDAC would be in contact with the full length protein substrate, and not just a specific peptide sequence.

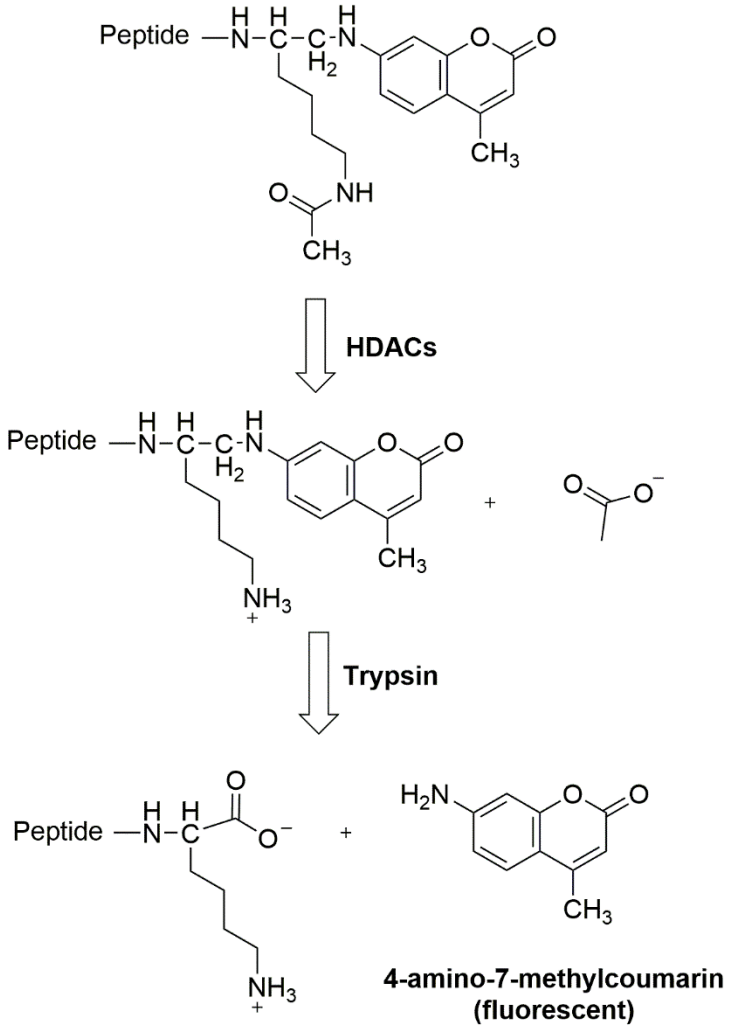


**Figure 3.2** The fluorogenic assay for HDACs (Wegener et al, 2002). The peptide sequences are from N-terminal tail of histone H4 (ac-K-G-G-A-Kac-methylcoumarin) and p53 (ac-R-H-Kac-Kac-methylcoumarin) (Wolfson et al, 2012).

### 3.2.7 *In vitro* deacetylase activity of HDAC8

Schultz and colleagues have reported a detailed kinetics study of various HDACs including HDAC1, 2, 3, 6, 8 and 10. They employed a fluorogenic assay which used an acetyl lysine histone H4 peptide as the substrate (Schultz et al, 2004). Most HDACs had a similar Km value of approximately 30 uM, except for HDAC8 whose Km (>200 μM) was significantly higher. This higher Km value lead to a lower kcat/Km value for HDAC8 deacetylation activity (~60±7 $M^{-1}.S^{-1}$) when compared to other HDACs. This result suggests that HDAC8 might have other activities beyond deacetylation.

It is known that the deacetylation activity of the HDAC family is zinc dependent. Fierke and co-workers, however, demonstrated that other divalent metal ions, including $Co^{2+}$, $Ni^{2+}$ and $Fe^{2+}$ can also activate HDAC8 deacetylation *in vitro*. Using the fluorogenic assay, they showed that the addition of $Fe^{2+}$, in a 1:1 stoichiometric ratio between the metal and HDAC8, increases the HDAC8 catalytic efficiency ($k_{cat}/K_M$) approximately three times when compared to the catalytic efficiency found when $Zn^{2+}$ is present. Their findings suggest that HDAC8 might be modulated by metal ions other than $Zn^{2+}$ (Gantt et al, 2006).

Recently, a substrate specificity profiling of different HDACs (HDAC2, HDAC3, HDAC8, and Sirt1) was done using an array containing a 361-member hexapeptide with an acetylated lysine at the C-terminus (Gurard-Levin et al, 2010). The different peptide sequences [Ac-G-R-KAc-**X**-**Z**-C-NH2 where X and Z are any amino acids except cysteine] were immobilized to the array via maleimide-terminated monolayer and after incubating the array with the different enzymes the acetylation status of the different peptides was determined by Mass Spectrometry. HDAC8 showed the high substrate specificity toward the peptide sequence R-Kac-F. Moreover, if a Gly or Gln residue is at the Z position of Ac-G-R-KAc-**X**-**Z**-C-NH2, this will lead to the most and the least active activity, respectively (Gurard-Levin et al, 2010).

### 3.2.8 Rationale behind the research

One of the key limiting factors towards understanding the function of HDAC8 is the weak deacetylase activity of HDAC8 *in vitro*. Previous kinetics studies of different HDACs (HDAC1, 2, 3, 6, 8 and 10) show that all of the HDACs have $K_m$ values between 20-40 μM, except for HDAC8 which has a significantly higher $K_m$ (>200 μM) (Schultz et al, 2004). Overall, HDAC8 has lowest $k_{cat}/K_m$ value on acetyl lysine peptides (~60±7 $M^{-1}S^{-1}$) when compared to other HDACs tested (Schultz et al, 2004). Recently, several class III HDACs, or sirtuins, that possess weak acetylation activity *in vitro*, have been shown to efficiently remove other acyl groups from lysine residues. For example, SIRT5 exhibits efficient lysine desuccinylation and demalonylation activity (Du et al, 2011) and SIRT1, 2, 3 and SIRT6 are capable

of hydrolyzing long chain fatty acyl groups from lysine residues (Jiang et al, 2013; Feldman et al, 2013; Teng et al, 2015). Therefore, we hypothesized that HDAC8 may have other enzymatic activities beyond deacetylation.

Here, we have synthesized a library of peptides with different acyl lysine modifications and examined the ability of HDAC8 to remove the acyl groups from the peptides. We have found that HDAC8 can catalyze the removal of long chain fatty-acyl groups from different peptide backbone sequences. The defatty-acylation activity of HDAC8 is several folds higher than its deacetylation activity. We have also obtained data suggesting that the defatty-acylase activity of HDAC8 is likely physiologically relevant.

## 3.3 MATERIALS AND METHODS

**Reagents** -Recombinant human HDAC8 from *Sf9* cells was purchased from BPS Bioscience (cat#50008). HDAC inhibitors (PCI-34051, SAHA, Panobinostat, and Mecetinostat) were purchased from Selleckchem.com (cat#S2012, S1047, S1030, S1122, respectively). Solvents for peptide synthesis were purchased from Fisher unless otherwise indicated. Wang resin, Fmoc-protected amino acids, and derivatives were purchased from Chem-Impex.

**Antibody** -Anti-acetyl Lysine antibody (Rabbit polyclonal IgG) was purchased from Abcam (cat# 80178). The secondary antibody, rabbit anti-goat IgG-HRP, was purchased from SantaCruz (cat# 2768).

**Cell Culture** -HeLa, Human Embryonic Kidney 293T (HEK293T) and MDA-MB-231 cells were cultured in Dulbecco's Modified Eagle Medium (DMEM) supplemented

with 10% Fetal Bovine Serum (FBS) (Invitrogen). Jurkat cells were cultured in Roswell Park Memorial Institute (RPMI) 1640 Media (Invitrogen) supplemented with 10% FBS. Cells were incubated in a humidified incubator at 37 °C with 5% $CO_2$.

**Cloning, expression and purification of HDAC8** -Human HDAC8 cDNA was purchased from Open Biosystems (clone ID: 5761745). The full length cDNA was PCR-amplified by Platinum® Pfx DNA Polymerase (ThermoFisher) and subcloned into the pET28a vector using the EcoRI and XhoI restriction sites with the following primers:

Sense: 5'-agtcagGAATTCATGGAGGAGCCGGAGGAACC-3'

Antisense: 5'-agtcagCTCGAGCTAGACCACATGCTTCAGATT-3'

The plasmid was transformed into *E. coli* BL21 Rosetta™ 2 competent cells (Novagen, Cat# 71402) for protein expression. The cells pellets were collected and washed with deionized water once before being dispersed in Buffer 1 (20 mM Tris-HCl pH 8.0, 500 mM NaCl, 10 mM $MgCl_2$, 5 mM Imidazole, 5% glycerol, 10 µg/mL phenylmethylsulfonyl fluoride (PMSF)). The cells were lysed by passing through an EmulsiFlex$^{TM}$-C3 cell disruptor (AVESTIN) three to four times, and the cell lysate was centrifuged to remove cell debris at 20,000 rpm at 4 $^{o}$C for 45 min (Beckman Coulter). The supernatant containing HDAC8 was then loaded onto Ni-NTA agarose beads (QIAGEN, Cat#30210) and the beads were gently agitated at 4 $^{o}$C for 2 hrs. The unbound supernatant was removed by gravity flow, and the beads were washed three times with Buffer 2 (20 mM Tris-HCl pH 8.0, 500 mM NaCl, 30 mM Imidazole). The protein was then eluted from the beads into eppendorf tubes with Buffer 3 (20 mM Tris-HCl pH 8.0, 500 mM NaCl, 10 mM KCl, and 50-300 mM

Imidazole). Each collected fraction was run on SDS-PAGE to check for the presence of HDAC8 (molecular weight around 46 kDa). The fractions containing HDAC8 were combined and concentrated to 2-3 mL with an Amicon Ultra-4 10 kDa concentrator, and subsequently loaded onto a gel filtration column (Sephadex-75, GE healthcare), which was pre-equilibrated with 40 mM Tris-HCl pH 8.0, 110 mM NaCl, and 2.2 mM KCl. Each fraction, with UV absorption at 280 nm, was resolved by SDS-PAGE to detect HDAC8. The fractions containing HDAC8 with greater than 80% purity were pooled and concentrated using an Amicon Ultra-0.5 mL 10 kDa concentrator (EMD Millipore) and subsequently aliquoted into small volumes and stored at -80 $^{o}$C.

***In vitro* HDAC8 activity and kinetics assay** -The *in vitro* activity of HDAC8 was detected using an HPLC assay. Each enzymatic reaction consists of 25 μM of different acyl peptides in the reaction buffer (25 mM Tris-HCl pH 8, 137 mM NaCl, 2.7 mM KCl, 1 mM $MgCl_2$) with a final volume of 60 μl. To begin a reaction, 1-5 μM of HDAC8 (depending on the activity) was added into the reaction and incubated at 37 $^{o}$C for 1 hr. The reactions were quenched with 60 μl of quench buffer (100 mM hydrochloric acid, 160 mM acetic acid in 50% acetonitrile) and centrifuged at 17,000x g for 15 min at room temperature to remove HDAC8. The reaction was analyzed by reverse phase HPLC with a Kinetex 5U XB C18 column (100A, 150 mm × 4.60 mm, Phenomenex) monitoring at the wavelength 280 nm. The mobile phase A was water with 0.1% (v/v) trifluoroacetic acid (TFA), the mobile phase B was acetonitrile with 0.1% (v/v) TFA. The gradient used was 10 to 100% mobile

phase B over 30 min with the flow rate of 0.5 mL/min. The product formation was verified by LC-MS (LCQ Fleet, Thermo Scientific).

The kinetics parameters of different acyl peptides were determined using the above reaction conditions and by varying the concentrations of each substrate as follows, 0-1,200 μM for acetyl H3K9; 0-400 μM for butyryl H3K9; 0-400 μM for octanoyl H3K9; 0-100 μM for dodecanoyl H3K9; 0-100 μM for myristoyl H3K9; 0-65 μM for palmitoyl H3K9. Each reaction was incubated with 1 μM HDAC8 at 37 $^{o}$C for 1 hr. Each reaction was performed in duplicate to ensure reproducibility. After separation by HPLC, the product and remaining substrate peaks were quantified and converted to initial rates. The plots between substrate concentrations and the initial rates were fitted using GraphPad Prism® (± S.D., Standard Deviation).

**Acyl peptide synthesis** -The different acyl peptide backbones were synthesized using standard solid phase peptide synthesis (Zhu et al, 2012). Two tryptophan residues were added to the C-terminal of each peptide to enable facile detection of the peptide at 280 nm. A total of 300 mg of Wang resin (100-200 mesh, 1% DVB, 10 mmole/g) (Chem-Impex) was swollen in 5 mL of dichloromethane (DCM) in a peptide synthesis vessel at room temperature with shaking for 6 hrs and washed three times with 5 mL of N,N-dimethylformamide (DMF).

The first amino acid solution containing 0.32 mmoles of Fmoc-protected amino acid dissolved in 5 mL of DMF, 0.32 mmoles of N,N,N′,N′-Tetramethyl-O-(1H-benzotriazol-1-yl)uronium hexafluorophosphate (HBTU), 0.13 mmoles of 4-(dimethylamino) pyridine (DMAP) and 0.64 mmoles of N,N-Diisopropylethylamine (DIEA), was added to the resin, and reaction mixture was shaken overnight at room

temperature. The resin was subsequently washed five times with 5 mL of DMF, and then incubated with a mixture of 2 mL of acetic anhydride, 1 mL of pyridine, and 3 mL of DMF at room temperature for 30 min, to cap any remaining reactive functional groups on the resin. To remove the Fmoc protecting group, 5 mL of 20% (v/v) piperidine in DMF was added to the resin, and the vessel was gently agitated at room temperature for 10 min, repeated twice. The resin was then washed two times with 5mL of DMF, followed by two washes with 5mL of DCM, and then washed three additional times with 5mL of DMF.

The coupling of the rest of the amino acids was performed by mixing the resin with the solution of 0.24 mmoles of Fmoc-protected amino acids dissolved in DMF, 0.24 mmoles of HBTU, 0.21 mmoles of 1-Hydroxybenzotriazole hydrate (HOBT) and 0.48 mmoles of DIEA, and incubated at room temperature with gently agitating for 2 hrs. In between the addition of each additional amino acid, the Fmoc protecting group was removed, and the resin was extensively washed as described above. The modified lysine residue was introduced by the incorporation of an Alloc protected lysine building block. To add the acyl groups to the lysine residues, after synthesis of the peptide backbone, the Alloc group was selectively removed by adding 100 mg of resin to 100 mg of Tetrakis(triphenylphosphine)palladium(0) (Sigma) in a solution of 0.1 mL of 2.5% morpholine (Sigma), 0.2 mL of acetic acid, and 4 mL of DCM. The solution was stirred for 3 hrs at room temperature under nitrogen. To remove the palladium, the resin was washed three times with 5 mL of 0.5% (v/v) DIEA in DCM, followed by three washes with 5 mL of 0.02 M sodium diethyldithiocarbamate in DMF. For the lysine modification step, the mixture solution

of 0.24 mmoles of acetic anhydride, butyric acid, octanoic acid, dodecanoic acid, myristic acid, palmitic acid, biotin, or lipoic acid; 0.24 mmoles of HBTU; 0.21 mmoles of HOBT; and 0.48 mmoles of DIEA in DMF, was added to the resin and the reaction was allowed to proceed for 3 hrs at room temperature. For the malonyl and succinyl peptides, the modified lysine amino acids were incorporated using Fmoc-Lys(tBu-malonyl)-OH and Fmoc-Lys(tBu-succinyl)-OH, respectively (Du et al, 2011).

The resin was washed three times with DMF and the peptides were cleaved from the resin using a solution of 8.2 mL of TFA, 0.5 mL of water, 0.5 g of phenol, 0.5 mL of ethanedithiol and 0.5 mL of thioanisole. The resin was gently agitated in the solution at room temperature for 2 hrs. The crude peptide was precipitated by ether, and subsequently purified by preparative HPLC on a Targa C18 reverse phase column (10 μm, 250x20 mm, Higgins Analytical, Inc.). The synthesized peptides were verified using LC-MS (LCQ Fleet, Thermo Scientific).

**Metabolic labeling of mammalian cells treated with PCI-34051** -The metabolic labeling method was modified from Yount *et al* 2011. A total of $1x10^6$ Jurkat cells in each flask were grown overnight, and then incubated with 25 or 50 μM PCI-34051 or DMSO (control) for 15 hrs. The cells were then treated with 50 μM Alk12 (or Alk14) in the presence of the inhibitor for an additional 6 hrs. Cells were collected and washed with 1x phosphate saline buffer (PBS) three times. The cell pellets were lysed with 4% sodium dodecyl sulfate (SDS) buffer (50 mM triethanolamine pH 7.4, 150 mM NaCl, 4% (w/v) SDS) containing protease inhibitor cocktails (Sigma). A nuclease (Pierce™ Universal Nuclease for Cell Lysis) was added into the total

lysate. The protein concentration was determined by the bicinchoninic acid (BCA) assay using the Pierce™ BCA Protein Assay Kit (ThermoFisher). A total of 50 µg of proteins from each sample was aliquoted, and adjusted to a final volume of 45 µl with 4% SDS buffer.

To perform the click reaction, 5.6 µl of the click chemistry reaction master mix was added to each sample (click reaction master mix per sample: 3 µl of 1 mM BODIPY Azide in DMF, 1 µl of 50 mM tris(2-carboxyethyl) phosphine hydrochloride (TCEP-HCl, Calbiochem) in water, 0.6 µl of 10 mM tris [(1-benzyl-1H-1,2,3-triazol-4-yl)methyl] amine (TBTA, Anal Tech) in DMF, 1 µl of 50 mM $CuSO_4$ in water). After 1 hr at room temperature, 200 µl methanol, 75 µl chloroform and 150 µl water were added to each sample. After vortexing, the samples were centrifuged at 17,000 xg for 20 min at 4 $^oC$. The supernatant was gently removed by pipetting, and to each pellet was added 1 mL of methanol. The samples were again vortexed and spun down at 17,000 xg for 10 min at 4˚C. The methanol was removed, and the protein pellets were washed again with 1 mL methanol. After the second methanol wash, the protein pellets were air dried at room temperature for 10-15 min, and then resolubilized in 50 µl of 4% SDS buffer (50 mM triethanolamine pH 7.4, 150 mM NaCl, 4% (w/v) SDS). To each sample, 10 µl of 6x loading buffer (374 mM Tris-HCl pH 6.8, 12% SDS, 600 mM DTT, 60% v/v glycerol, 0.06% bromophenol blue) was added, and the samples were boiled at 95 $^oC$ for 5 min. To remove cysteine palmitoylation, 9 µl of each sample was mixed with 1 µl of 5 M Hydroxylamine pH 8.0, and heated at 95 $^oC$ for 7 min. The samples were then resolved on 12% SDS-PAGE gel. The gel was destained in

50% (v/v) acetic acid, 40% (v/v) methanol and 10% (v/v) water for at least 2 hrs at room temperature (or overnight at 4 $^{o}$C), and destained in water for another 30 min. The fluorescent signal was visualized with a Typhoon 9400 Variable Mode Imager (GE Healthcare Life Sciences) using 488 nm excitation and 520 nm detection filters, and a PMT setting of 550 V. The signal was analyzed by Image Quant TL v2005.

**Western Blot for protein lysine acetylation** -Cells were collected and lysed with 4% SDS buffer containing Protease Inhibitor Cocktails and nuclease. Protein concentration was determined by BCA assay. Protein samples were separated by 12% SDS-PAGE and transferred to PVDF membrane (Bio-Rad) for 120 min. The membrane was blocked with 5% bovine serum albumin (BSA, Santa Cruz) and incubated with the primary antibody at 4 $^{o}$C overnight. The membrane was incubated with the secondary antibody for another 1 hr at room temperature. The membrane was developed using ECL-Plus western blotting detection reagent (GE Healthcare). The signal was visualized using a Typhoon 9400 Variable Mode Imager (GE Healthcare) with 457 nm excitation and 526 nm detection filters, using a PMT of 600 V. The signal was analyzed by Image Quant TL v2005.

## 3.4 RESULTS

**HDAC8 can remove long chain fatty acyl groups *in vitro*.** We overexpressed and purified recombinant HDAC8 from *E. coli* BL21 cells for studying the enzymatic activity of HDAC8. For peptide substrates (Table 1), we first focused on the H3K9 peptide sequence and varied the acyl groups. Using an HPLC-based assay, we found HDAC8 could remove both acetyl and several larger acyl groups (butyryl, octanoyl, dodecanoyl, myristoyl, and palmitoyl) from the lysine residue of H3K9 peptides (Table 3.1 and Figure 3.3). However, HDAC8 could not remove the negatively charged succinyl or malonyl groups from H3K9 peptides. The bulkier biotionyl and lipoyl groups were also not good HDAC8 substrates (Table 3.1).

We then compared the deacetylation and demyristoylation activities on a few different peptide sequences. We were able to detect both deacetylation and demyristoylation activity on the H3K9 and H2BK19 peptides (Figure 3.4A-B). However, only deacetylation activity was observed on H3K18 peptides (Figure 3.4C), and neither activity was detected on H4K16 and TNFα K20 peptides (Figure 3.4D). Therefore, HDAC8 enzymatic activity is dependent on the peptide sequence.

Recently, lysine crotonylation and 2-hydroxyisobutyrylation have also been reported to occur on histone proteins (Tan et al, 2011; Dai et al, 2014). Thus, we also tested HDAC8 on a few histone peptides bearing crotonyl (H2AK119, and H3K56) and 2-hydroxyisobutyryl groups (H2BK5, H3K122, H4K8, and H4K77) (Table 3.1). Except H3K56 crotonylation, all other sites have been reported to have the crotonyl or 2-hydroxyisobutyryl modifications. HDAC8 could remove acetyl groups, but not crotonyl groups from both the H2AK119 and H3K56 peptides.

Similarly, HDAC8 could not remove 2-hydroxyisobutyryl groups from any of the peptides tested.

**Table 3.1 The acyl peptide library for HDAC8 activity screening.**

| Proteins | Peptide sequences[a] | Acyl group | Substrate of HDAC8? Yes (Y) / No (N) |
|---|---|---|---|
| Histone H3K9 | KQTARKSTGGWW | acetyl | Y |
| | | butyryl | Y |
| | | octanoyl | Y |
| | | dodecanoyl | Y |
| | | myristoyl | Y |
| | | palmitoyl | Y |
| | | succinyl | N |
| | | malonyl | N |
| | | biotinyl | N |
| | | lipoyl | N |
| Histone H4K16 | KGGAKRHRKWW | acetyl | N |
| | | myristoyl | N |
| Histone H2BK12 | APAPKKGSKKWW | acetyl | Y |
| | | myristoyl | Y |
| Histone H3K18 | GGKAPRKQLATKAWW | acetyl | Y |
| | | myristoyl | N |

| Proteins | Peptide sequences[a] | Acyl group | Substrate of HDAC8? Yes (Y) / No (N) |
|---|---|---|---|
| TNFα | EALPKKTGGPQWW | acetyl | N |
| | | myristoyl | N |
| Histone H2AK119 | VLLPKKTESHWW | acetyl | Y |
| | | crotonyl | N |
| Histone H3K56 | YQKSTELLWW | acetyl | Y |
| | | crotonyl | N |
| Histone H2BK5 | PEPSKSAPAPKWW | 2-hydroxyisobutyryl | N |
| Histone H3K122 | TIMPKDIQLAWW | 2-hydroxyisobutyryl | N |
| Histone H4K8 | RGKGGKGLGKGWW | 2-hydroxyisobutyryl | N |
| Histone H4K77 | TEHAKRKTVWW | 2-hydroxyisobutyryl | N |
| Gelsolin | GLGLSYLSSWW | myristoyl | N |
| PAK2 | GAAKSLDKQKWW | | N |
| Gα protein | GGDASGEWW | | N |

[a] *The modified residue is underlined*

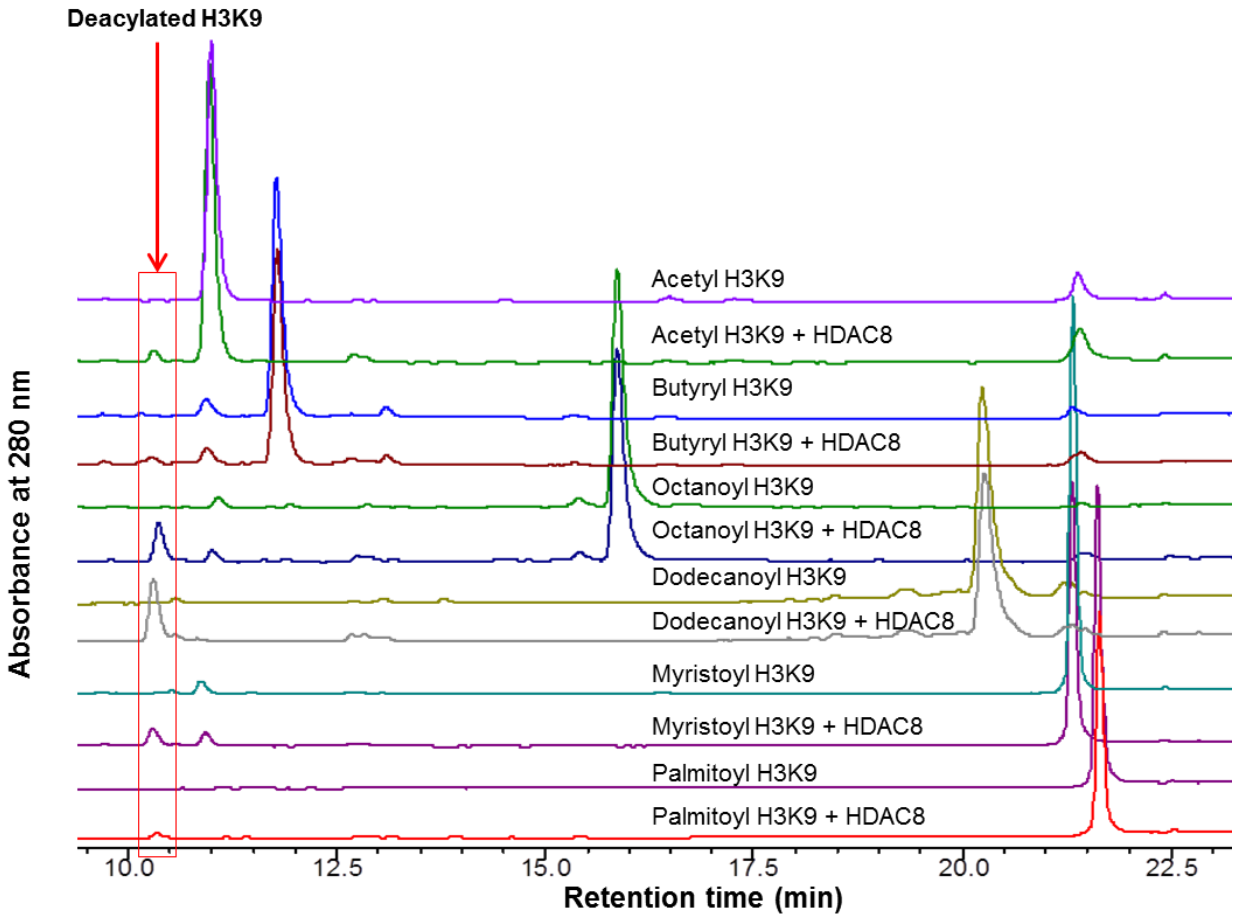


**Figure 3.3 HPLC traces of HDAC8 activity assay with different acyl peptides as substrates.** HDAC8 can remove the acetyl group, and other long chain acyl groups with different efficiencies. Each reaction was performed with 25 μM substrate peptide, 1 μM HDAC8, 25 mM Tris-HCl pH 8.0, 137 mM NaCl, 2.7 mM KCl, 1 mM $MgCl_2$ and incubated at 37 $^{o}$C for 60 min.

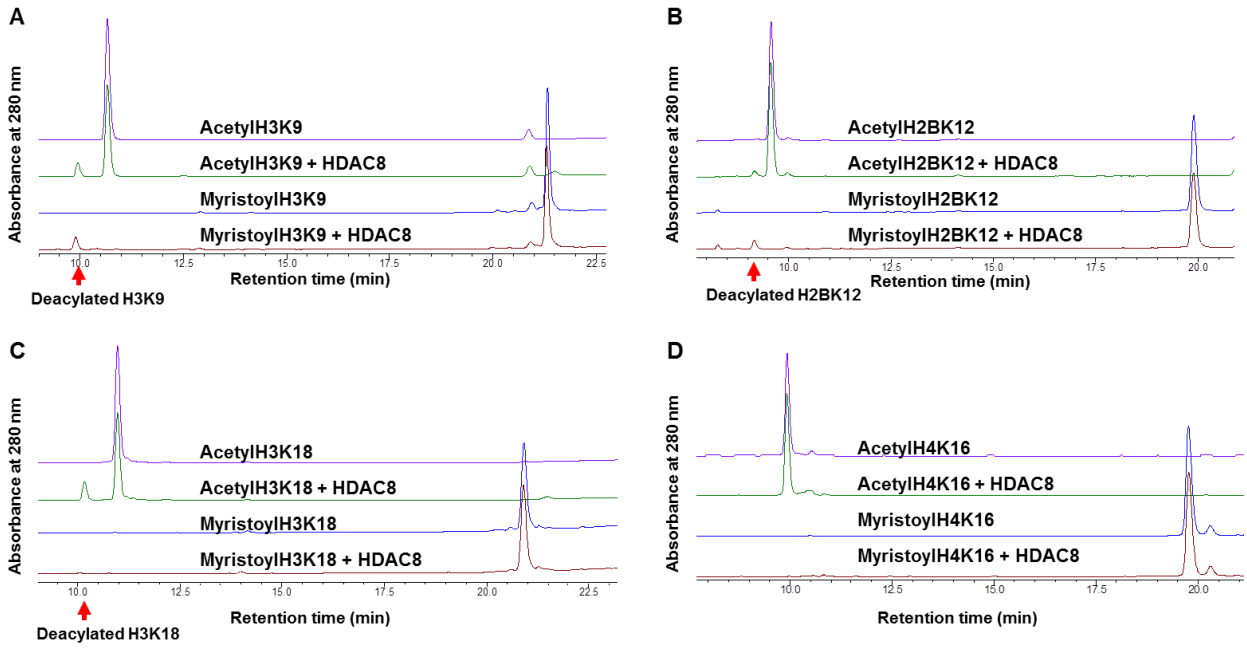


**Figure 3.4 HPLC traces showing HDAC8 selectivity on different histone peptides.** *A-B*, HDAC8 can catalyze deacetylation and demyristoylation on both H3K9 and H2BK12 peptides. *C,* only deacetylation activity was detected on H3K18 peptide. *D,* No deacylation activity was detected on the H4K16 peptide. Each reaction was performed with 25 μM substrate peptide, 1 μM HDAC8, 25 mM Tris-HCl pH 8.0, 137 mM NaCl, 2.7 mM KCl, 1 mM $MgCl_2$ and incubated at 37 $^{o}$C for 60 min.

Protein N-terminal glycine myristoylation is a well-known PTM that is important for cell signaling. Given that HDAC8 can catalyze lysine demyristoylation, we also synthesized several peptides bearing N-terminal glycine myristoylation, and tested whether HDAC8 could catalyze glycine demyristoylation. These peptides are from three proteins that are known to be modified by glycine myristoylation: gelsolin (Sakurai et al, 2006), p21-activated kinase 2 (PAK2) (Vilas et al, 2006), and $G_\alpha$ protein, transducin (Sankaram et al, 1994). However, none of the N-terminal glycine myristoylated peptides were HDAC8 substrates.

To further investigate the defatty-acylation activity of HDAC8, we carried out kinetics studies using H3K9 peptides with different acyl groups as the substrates. The kinetics parameters and the Michaelis-Menten plots of each acyl peptide substrate are shown in Table 3.2 and Figure 3.5, respectively. The HDAC8 catalytic efficiencies ($k_{cat}/K_m$ values) on the longer fatty acyl groups, octanoyl-, dodecanoyl-, and myristoyl-H3K9, are two to three times higher than that on the acetyl peptide. For deacetylation, we could not obtain the $K_m$ values as the initial reaction rate was linear with the acetyl peptide concentrations we used. In contrast, the $K_m$ value for the myristoyl H3K9 peptide was approximately 16 μM.

The catalytic efficiencies of HDAC8 on acetyl and myristoyl H3K9 peptides were still low compared to other HDACs. Our *E. coli* expression system for HDAC8 might have caused the low activity of HDAC8 due to a lack of certain post-translational modifications (PTMs) (Baneyx et al, 2004). Therefore, we also used HDAC8 expressed from *Sf9* insect cells for kinetics studies for both the acetyl- and myristoyl-H3K9 peptides. Indeed, we obtained higher $k_{cat}/K_m$ values for both

deacetylation and demyristoylation from HDAC8 expressed from *Sf9* insect cells. Although the HDAC8 purified from insect cells gave much higher activity, the demyristoylation catalytic efficiency remained >2 times higher than that of deacetylation.

**Table 3.2 Kinetics parameters (± S.D.) of recombinant HDAC8 on different H3K9 acyl peptides.**

| Substrate | $k_{cat}$ ($S^{-1}$) | $K_m$ (uM) | $k_{cat}/K_m$ ($S^{-1} \cdot M^{-1}$) |
|---|---|---|---|
| Acetyl H3K9 | ND[a] | >600 | 58.0 ± 1.1 |
| | ND[a,b] | >300[b] | 480.8[b] |
| Butyryl H3K9 | ND[a] | >200 | 12.6 ± 0.3 |
| Octanoyl H3K9 | 0.0202 ± 0.0005 | 145.8 ± 10.3 | 139 ± 13 |
| Dodecanoyl H3K9 | 0.0123 ± 0.0013 | 69.5 ± 10.1 | 177 ± 7 |
| Myristoyl H3K9 | 0.0019 ± 0.0003 | 15.8 ± 5.1 | 120 ± 11 |
| | 0.0755[b] | 60.5[b] | 1,246[b] |
| Palmitoyl H3K9 | 0.00050 ± 0.00007 | 18.3 ± 7.4 | 28.8 ± 7 |

[a] ND: Not determined since initial rate ($V_0$) versus [Substrate] was linear. The $k_{cat}/K_m$ value was obtained from the slope of the linear plot.

[b] Recombinant HDAC8 from *Sf9* insect cells

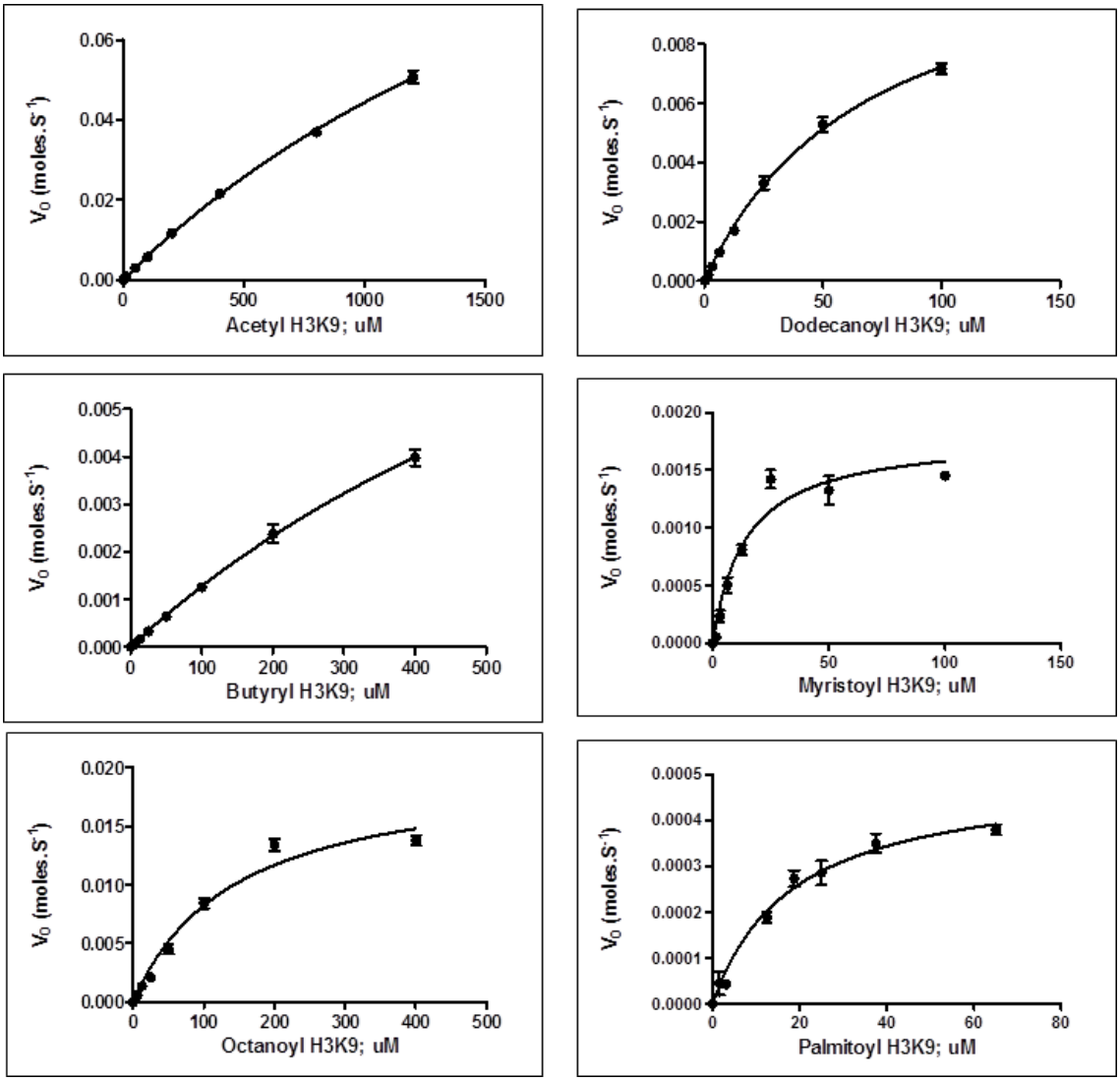


**Figure 3.5 Michaelis-Menten plot for HDAC8 defatty acylation on different acyl H3K9 peptides**

**HDAC inhibitors, PCI-34051 and SAHA, can inhibit both the demyristoylation and deacetylation activities of HDAC8**

Several HDAC inhibitors have been developed which can inhibit the deacetylation activity of HDACs (West and Johnstone, 2014). We wanted to test whether they would inhibit the deacetylation and demyristoylation activities differently. We tested both a HDAC8 specific inhibitor, PCI-34051 (Balasubramanian et al, 2008), and a pan-HDAC inhibitor, SAHA. As shown in Figure 3.6, both the demyristoylation and deacetylation activities of HDAC8 were inhibited by the two inhibitors in a dose response manner. PCI-34051 was able to inhibit both catalytic activities with ten times lower $IC_{50}$ values compared to SAHA (Table 3.3). Therefore, PCI-34051 can efficiently inhibit both of demyristoylation and deacetylation activities of HDAC8.

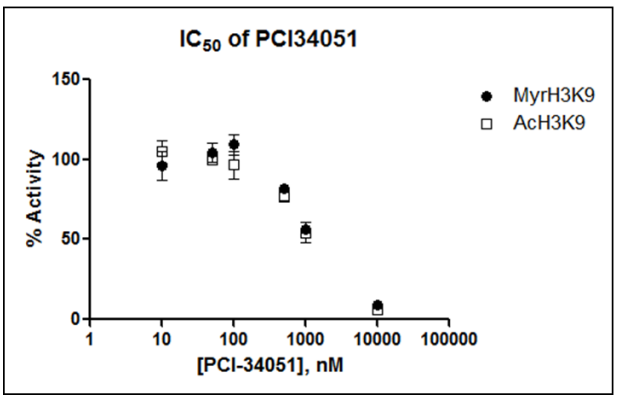


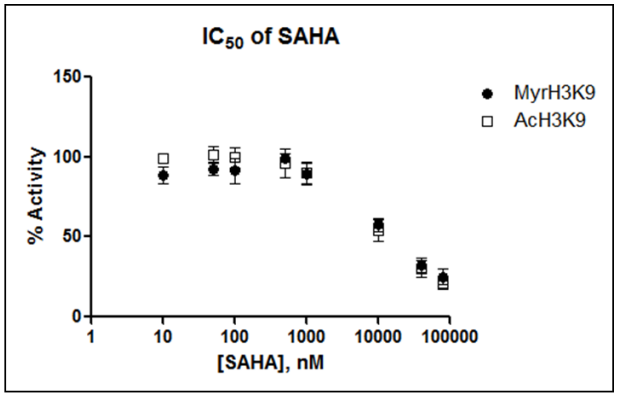


**Figure 3.6** Inhibition curves of PCI-34051 and SAHA on the demyristoylation and deacetylation activities of HDAC8. Each reaction in this assay was performed with 1 μM of HDAC8 in the reaction buffer (25 mM Tris-HCl pH 8.0, 137 mM NaCl, 2.7 mM KCl, 1 mM $MgCl_2$), which was pre-incubated with different concentrations of the inhibitors at room temperature for 15 min. Subsequently, 25 μM of the substrate peptide was added and the reaction was incubated at 37 $^oC$ for 60 min before HPLC analysis to determine the amount of product formed. The data (± S.D.) were fitted by using GraphPad Prism® to give the $IC_{50}$ values shown in Table 3.

**Table 3.3** $IC_{50}$ (± S.D.) of PCI-34051 and SAHA for HDAC8's deacetylation and demyristoylation activities on H3K9 peptides.

| HDAC inhibitors | $IC_{50}$ ± SD (μM) | |
|---|---|---|
| | Demyristoylation | Deacetylation |
| **PCI-34051** | 0.98 ± 0.04 | 1.15 ± 0.14 |
| **SAHA** | 9.92 ± 0.50 | 9.56 ± 0.58 |

**Effect of the HDAC8 specific inhibitor (PCI-34051) on global fatty acylation level in mammalian cells**

Since PCI-34051 can efficiently inhibit HDAC8 demyristoylation *in vitro,* we hypothesized that if the HDAC8 defatty-acylation activity is physiologically relevant, treating cells with PCI-34051 should increase protein lysine fatty-acylation. To test this, we employed a metabolic labeling method using a bioorthogonal probe for protein myristoylation, an alkyne-tagged myristic acid analogue (Alk12) (Yount et al, 2011). After treating different mammalian cell lines with PCI-34051, we cultured them in the presence of Alk12 which was metabolically incorporated into fatty-acylated proteins. The alkyne-labeled proteins were conjugated to a fluorescent tag (BODIPY-azide) via click chemistry. The proteins were then precipitated and incubated in 0.5 M hydroxylamine solution pH 8.0 at 95 $^{o}$C for 7 min to remove fatty acyl modifications on cysteine residues (Jiang et al, 2013). The fluorescently labeled proteins were then visualized after SDS-PAGE separation (Figure 3.7A). We found that HeLa, HEK-293T, and MDA-MB 231 cells treated with PCI-34051 showed slightly increased fatty acylation compared to the control that was treated with DMSO (Figure 3.8). In contrast, the treatment of T lymphocyte Jurkat cells with PCI-34051 significantly increased the fatty acylation level (Figure 3.7C). The increase in protein lysine fatty acylation was time-dependent (Figure 3.7C) and PCI-3451 concentration-dependent (Figure 3.9).

To further prove that the elevated fatty acylation level was specific to PCI-34051, we treated Jurkat cells with 25 μM of different HDAC inhibitors, including SAHA, Panobinostat (LBH589), and Mecetinostat (MGCD0103) (Figure 3.7B).

SAHA and Panobinostat are pan-HDAC inhibitors (Richon et al, 1998; Scuto et al, 2008) while Mocetinostat can inhibit HDAC1, 2, 3 and 11 but not HDAC4, 5, 6, 7, and 8 (Fournel et al, 2008). As we expected, only PCI-34051-treated Jurkat cells exhibited enhanced global protein lysine fatty acylation (Figure 3.7D). We also detected the global lysine acetylation level by Western blot, and found that SAHA and Panobinostat predominantly increased the acetylation of protein bands around 55 kDa, while PCI-34051 and Mecetinostat did not noticeably increase protein lysine acetylation (Figure 3.7E). Notably, the global fatty acylation labeling signal from the cells treated with SAHA and Panobinostat was much lower than the control. The lower fatty acylation labeling signal could be due to the cytotoxicity of these inhibitors. To decrease the toxicity, we also treated the cells with lower concentrations of these inhibitors, but still did not observe an increase in the fatty acylation signal (Figure 3.9). This suggests that the HDAC8-specific inhibitor PCI-34051 is unique in the ability to increase protein fatty acylation.

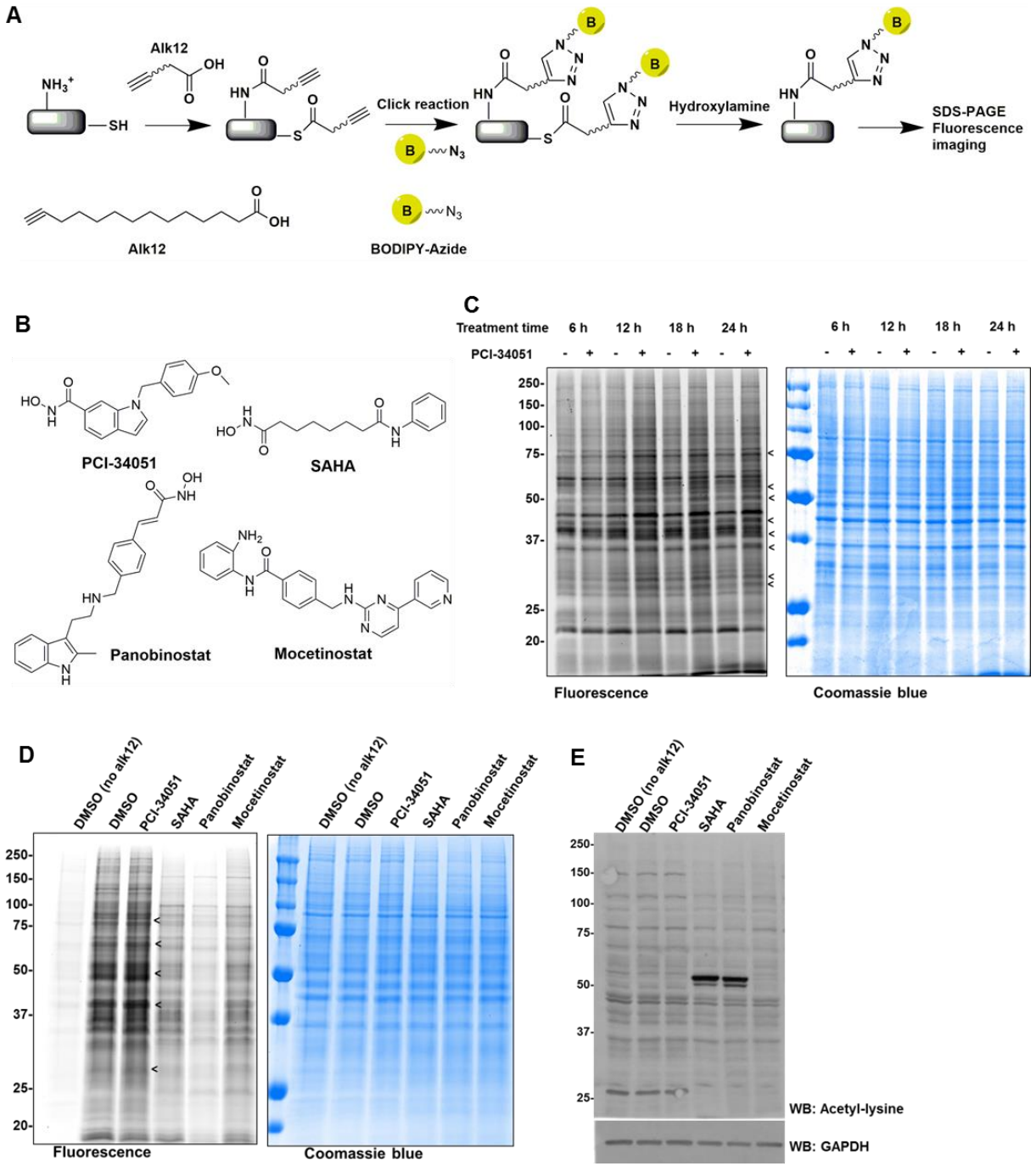


**Figure 3.7 Global fatty acylation Jurkat cells treated with PCI-34051.** *A,* Method for the detection of global protein lysine fatty acylation in Jurkat cells. Cells were cultured with the myristic acid analogue (Alk12) to allow metabolic labeling to occur.

BODIPY-azide (B-$N_3$) was then conjugated to the alkyne group using click chemistry. The modifications on cysteine residues were removed by treating with 0.5 M hydroxylamine, pH 8.0, and the fluorescent signal was imaged after SDS-PAGE. *B,* Chemical structures of different HDAC inhibitors. *C,* Global fatty acylation of Jurkat cells treated with 50 μM PCI-34051 with different treatment times. The cells treated with PCI-34051 showed an increase in global protein fatty acylation over time compared to the control. The arrows point to several protein bands with elevated fatty acylation signals. *D,* The increase in global fatty acylation was specific to PCI-34051. Jurkat cells treated with 25 μM of different HDAC inhibitors for 15 hrs. Only PCI-34051 treated cells showed higher fatty acylation when compared to the control and other HDAC inhibitor treated cells. *E,* Western blot showing the global acetylation pattern of Jurkat cells treated with different HDAC inhibitors. SAHA and Parabinostat increased protein lysine acetylation while other inhibitors did not.

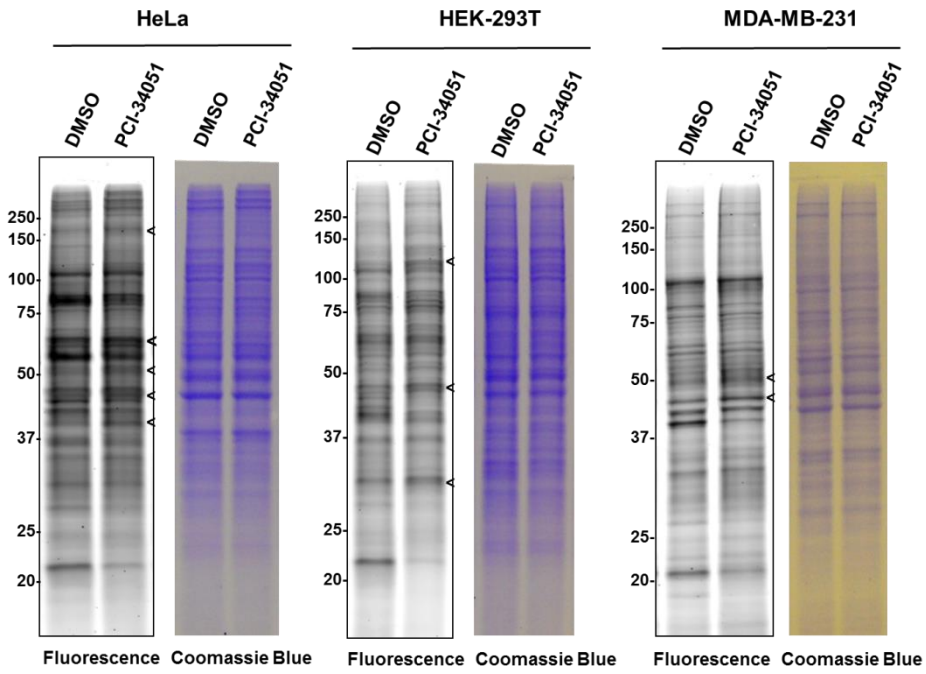


**Figure 3.8** Global protein fatty acylation of different mammalian cell lines, including HeLa, HEK-239T, and MDA-MB-231 cell lines. The cells were treated with 50 μM PCI-34051 for 15 hrs and further incubated with Alk12 for 6 hrs. The arrows indicate the bands with increased fatty acylation.

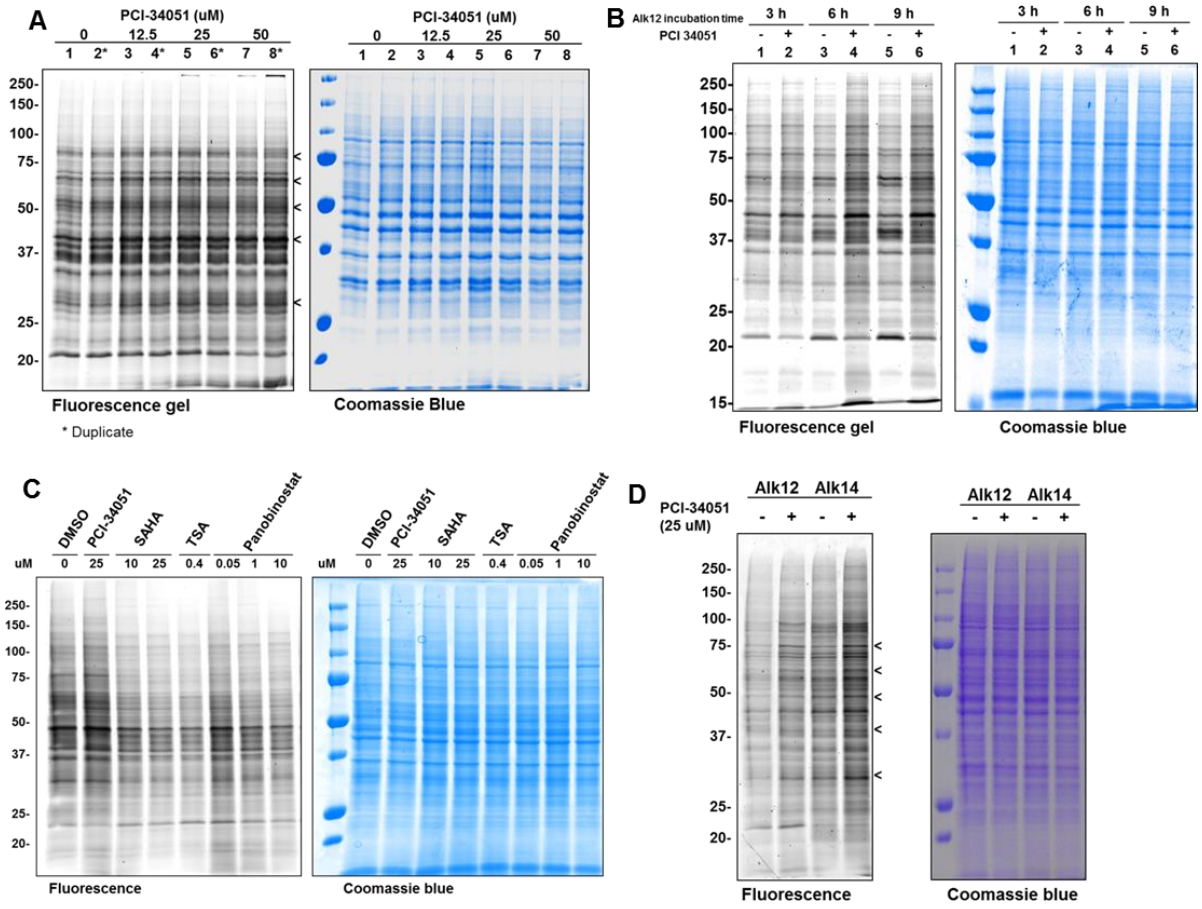


**Figure 3.9** Global protein fatty acylation of Jurkat cells treated with PCI-34051 in different conditions. *A,* Global protein fatty acylation of Jurkat cells treated with different concentrations of PCI-34051. *B,* Global protein fatty acylation of Jurkat cells treated with 50 μM of PCI-34051 for 15 hrs and then incubated with Alk12 for different time periods. *C,* Global protein lysine fatty acylation of Jurkat cells treated with different HDAC inhibitors at different concentrations. *D,* Comparison of the global protein fatty acylation of Jurkat cells treated with PCI-34051 in the presence between Alk12 and Alk14, which are myristic acid and palmitic acid probes, respectively.

## 3.5 DISCUSSION

We showed here that HDAC8 can efficiently catalyze defatty-acylation, including deoctanoylation, dedodecanoylation, and demyristoylation. While some of the sirtuins, the $NAD^+$-dependent HDACs, have been recognized as protein defatty-acylases (Du et al, 2011; Feldman et al, 2013; Teng et al, 2015), this is the first report of a zinc-dependent HDAC possessing this enzymatic activity. The myristoyl peptide has a much lower $K_m$ values compared to the acetyl peptide leading to a higher catalytic efficiency of demyristoylation over deacetylation.

Crystal structures of human HDAC8, in complex with different inhibitors, have been reported; they revealed a single α/β-domain with a core eight-stranded parallel β-sheet and 11 α-helices (Somoza et al, 2004; Vannini et al, 2004; Vannini et al, 2007). Interestingly, the complexes between HDAC8 and the inhibitors displayed structural variation on the surface of HDAC8 around the binding pocket. This region has been suggested to be conformational flexible, and this property might allow HDAC8 to accommodate different substrates (Somoza et al, 2004). This therefore may allow the binding of long chain fatty acyl peptides at the active site, enabling the defatty-acylation activity.

Protein fatty acylation has been known to play an essential role in cell signaling, membrane trafficking, protein-membrane interactions, and cellular localization (Resh et al, 2006). The majority of these fatty-acylated proteins have been reported to have N-glycine myristoylation or S-palmitoylation, while only a few proteins are reported to have lysine fatty acylation (Stevenson et al, 1992; Jiang et al 2013). Several $NAD^+$-dependent deacetylases, SIRT1, SIRT2, SIRT3 and SIRT6,

have been previously reported to possess lysine defatty-acylation activities. In this study, we also showed that zinc-dependent deacetylase, HDAC8, is another lysine defatty-acylase.

PCI-34051, a potent and selective HDAC8 inhibitor, can inhibit not only the deacetylation, but also the demyristoylation activity of HDAC8. PCI-34051 treatment in mammalian cells can enhance the global fatty acylation in a dose response manner, while other HDAC inhibitors did not. These results suggest that HDAC8 lysine defatty-acylation is likely physiologically relevant. The identification of an additional enzyme with lysine defatty-acylation activity suggests that lysine fatty acylation might be a more abundant modification than previously recognized, and it may play important roles in biology.

Thus far, only two direct HDAC8 targets have been substantially validated. We identified the first zinc dependent HDAC to possess defatty-acylase activity. The discovery of the defatty-acylase activity suggests that when searching for other HDAC8 targets we also need to consider the defatty-acylase activity of HDAC8. Our work will thus further facilitate the identification of additional substrate proteins for HDAC8 and help elucidate the physiological role of this enzyme.

## 3.6 REFERENCES

Balasubramanian, S., Ramos, J., Luo, W., Sirisawad, M., Verner, E., and Buggy, J. J. (2008) A novel histone deacetylase 8 (HDAC8)-specific inhibitor PCI-34051 induces apoptosis in T-cell lymphomas. Leukemia 22, 1026-1034

Baneyx, F., and Mujacic, M. (2004) Recombinant protein folding and misfolding in Escherichia coli. Nature biotechnology 22, 1399-1408

Bowers, A. A., Greshock, T. J., West, N., Estiu, G., Schreiber, S. L., Wiest, O., Williams, R. M., and Bradner, J. E. (2009) Synthesis and conformation-activity relationships of the peptide isosteres of FK228 and largazole. J Am Chem Soc 131, 2900-2905

Buggy, J. J., Sideris, M. L., Mak, P., Lorimer, D. D., McIntosh, B., and Clark, J. M. (2000) Cloning and characterization of a novel human histone deacetylase, HDAC8. Biochem J 350 Pt 1, 199-205

Dai, L., Peng, C., Montellier, E., Lu, Z., Chen, Y., Ishii, H., Debernardi, A., Buchou, T., Rousseaux, S., Jin, F., Sabari, B. R., Deng, Z., Allis, C. D., Ren, B., Khochbin, S., and Zhao, Y. (2014) Lysine 2-hydroxyisobutyrylation is a widely distributed active histone mark. Nature chemical biology 10, 365-370

Deardorff, M. A., Bando, M., Nakato, R., Watrin, E., Itoh, T., Minamino, M., Saitoh, K., Komata, M., Katou, Y., Clark, D., Cole, K. E., De Baere, E., Decroos, C., Di Donato, N., Ernst, S., Francey, L. J., Gyftodimou, Y., Hirashima, K., Hullings, M., Ishikawa, Y., Jaulin, C., Kaur, M., Kiyono, T., Lombardi, P. M., Magnaghi-Jaulin, L., Mortier, G. R., Nozaki, N., Petersen, M. B., Seimiya, H., Siu, V. M., Suzuki, Y., Takagaki, K., Wilde, J. J., Willems, P. J., Prigent, C., Gillessen-Kaesbach, G., Christianson, D. W., Kaiser, F. J., Jackson, L. G., Hirota, T., Krantz, I. D., and Shirahige, K. (2012) HDAC8 mutations in Cornelia de Lange syndrome affect the cohesin acetylation cycle. Nature 489, 313-317

Decroos, C., Bowman, C. M., Moser, J. A., Christianson, K. E., Deardorff, M. A., and Christianson, D. W. (2014) Compromised structure and function of HDAC8 mutants identified in Cornelia de Lange Syndrome spectrum disorders. ACS chemical biology 9, 2157-2164

Delcuve, G. P., Khan, D. H., and Davie, J. R. (2012) Roles of histone deacetylases in epigenetic regulation: emerging paradigms from studies with inhibitors. Clinical epigenetics 4, 5

Du, J., Zhou, Y., Su, X., Yu, J. J., Khan, S., Jiang, H., Kim, J., Woo, J., Kim, J. H., Choi, B. H., He, B., Chen, W., Zhang, S., Cerione, R. A., Auwerx, J., Hao, Q., and Lin, H. (2011) Sirt5 is a NAD-dependent protein lysine demalonylase and desuccinylase. Science 334, 806-809

Feldman, J. L., Baeza, J., and Denu, J. M. (2013) Activation of the protein deacetylase SIRT6 by long-chain fatty acids and widespread deacylation by mammalian sirtuins. The Journal of biological chemistry 288, 31350-31356

Fournel, M., Bonfils, C., Hou, Y., Yan, P. T., Trachy-Bourget, M. C., Kalita, A., Liu, J., Lu, A. H., Zhou, N. Z., Robert, M. F., Gillespie, J., Wang, J. J., Ste-Croix, H., Rahil, J., Lefebvre, S., Moradei, O., Delorme, D., Macleod, A. R., Besterman, J. M., and Li, Z. (2008) MGCD0103, a novel isotype-selective histone deacetylase inhibitor, has broad spectrum antitumor activity in vitro and in vivo. Molecular cancer therapeutics 7, 759-768

Gantt, S. L., Gattis, S. G., and Fierke, C. A. (2006) Catalytic activity and inhibition of human histone deacetylase 8 is dependent on the identity of the active site metal ion. Biochemistry 45, 6170-6178

Gurard-Levin, Z. A., Kilian, K. A., Kim, J., Bahr, K., and Mrksich, M. (2010) Peptide arrays identify isoform-selective substrates for profiling endogenous lysine deacetylase activity. ACS chemical biology 5, 863-873

Gurard-Levin, Z. A., Kim, J., and Mrksich, M. (2009) Combining mass spectrometry and peptide arrays to profile the specificities of histone deacetylases. Chembiochem 10, 2159-2161

Gurard-Levin, Z. A., and Mrksich, M. (2008) The activity of HDAC8 depends on local and distal sequences of its peptide substrates. Biochemistry 47, 6242-6250

Haberland, M., Mokalled, M. H., Montgomery, R. L., and Olson, E. N. (2009) Epigenetic control of skull morphogenesis by histone deacetylase 8. Genes & development 23, 1625-1630

Hsieh, C. L., Ma, H. P., Su, C. M., Chang, Y. J., Hung, W. Y., Ho, Y. S., Huang, W. J., and Line, R. K. (2016) Alterations in histone deacetylase 8 lead to cell migration and poor prognosis in breast cancer. Life Sci

Hu, E., Chen, Z., Fredrickson, T., Zhu, Y., Kirkpatrick, R., Zhang, G. F., Johanson, K., Sung, C. M., Liu, R., and Winkler, J. (2000) Cloning and characterization of a novel human class I histone deacetylase that functions as a transcription repressor. The Journal of biological chemistry 275, 15254-15264

Jiang, H., Khan, S., Wang, Y., Charron, G., He, B., Sebastian, C., Du, J., Kim, R., Ge, E., Mostoslavsky, R., Hang, H. C., Hao, Q., and Lin, H. (2013) SIRT6 regulates TNF-alpha secretion through hydrolysis of long-chain fatty acyl lysine. Nature 496, 110-113

Karolczak-Bayatti, M., Sweeney, M., Cheng, J., Edey, L., Robson, S. C., Ulrich, S. M., Treumann, A., Taggart, M. J., and Europe-Finner, G. N. (2011) Acetylation of heat shock protein 20 (Hsp20) regulates human myometrial activity. The Journal of biological chemistry 286, 34346-34355

Lee, H., Rezai-Zadeh, N., and Seto, E. (2004) Negative regulation of histone deacetylase 8 activity by cyclic AMP-dependent protein kinase A. Mol Cell Biol 24, 765-773

Luo, J., Sladek, R., Carrier, J., Bader, J. A., Richard, D., and Giguere, V. (2003) Reduced fat mass in mice lacking orphan nuclear receptor estrogen-related receptor alpha. Mol Cell Biol 23, 7947-7956

Martin, D. D., Beauchamp, E., and Berthiaume, L. G. (2011) Post-translational myristoylation: Fat matters in cellular life and death. Biochimie 93, 18-31

Oehme, I., Deubzer, H. E., Wegener, D., Pickert, D., Linke, J. P., Hero, B., Kopp-Schneider, A., Westermann, F., Ulrich, S. M., von Deimling, A., Fischer, M., and Witt, O. (2009) Histone deacetylase 8 in neuroblastoma tumorigenesis. Clinical cancer research : an official journal of the American Association for Cancer Research 15, 91-99

Olson, D. E., Wagner, F. F., Kaya, T., Gale, J. P., Aidoud, N., Davoine, E. L., Lazzaro, F., Weiwer, M., Zhang, Y. L., and Holson, E. B. (2013) Discovery of the first histone deacetylase 6/8 dual inhibitors. J Med Chem 56, 4816-4820

Resh, M. D. (2006) Trafficking and signaling by fatty-acylated and prenylated proteins. Nature chemical biology 2, 584-590

Richon, V. M., Emiliani, S., Verdin, E., Webb, Y., Breslow, R., Rifkind, R. A., and Marks, P. A. (1998) A class of hybrid polar inducers of transformed cell differentiation inhibits histone deacetylases. Proceedings of the National Academy of Sciences of the United States of America 95, 3003-3007

Saha, A., Pandian, G. N., Sato, S., Taniguchi, J., Hashiya, K., Bando, T., and Sugiyama, H. (2013) Synthesis and biological evaluation of a targeted DNA-binding transcriptional activator with HDAC8 inhibitory activity. Bioorg Med Chem 21, 4201-4209

Sakurai, N., and Utsumi, T. (2006) Posttranslational N-myristoylation is required for the anti-apoptotic activity of human tGelsolin, the C-terminal caspase cleavage product of human gelsolin. The Journal of biological chemistry 281, 14288-14295

Sankaram, M. B. (1994) Membrane interaction of small N-myristoylated peptides: implications for membrane anchoring and protein-protein association. Biophysical journal 67, 105-112

Schultz, B. E., Misialek, S., Wu, J., Tang, J., Conn, M. T., Tahilramani, R., and Wong, L. (2004) Kinetics and comparative reactivity of human class I and class IIb histone deacetylases. Biochemistry 43, 11083-11091

Scuto, A., Kirschbaum, M., Kowolik, C., Kretzner, L., Juhasz, A., Atadja, P., Pullarkat, V., Bhatia, R., Forman, S., Yen, Y., and Jove, R. (2008) The novel histone deacetylase inhibitor, LBH589, induces expression of DNA damage response genes and apoptosis in Ph- acute lymphoblastic leukemia cells. Blood 111, 5093-5100

Singh, R. K., Mandal, T., Balsubramanian, N., Viaene, T., Leedahl, T., Sule, N., Cook, G., and Srivastava, D. K. (2011) Histone deacetylase activators: N-acetylthioureas serve as highly potent and isozyme selective activators for human histone deacetylase-8 on a fluorescent substrate. Bioorg Med Chem Lett 21, 5920-5923

Somoza, J. R., Skene, R. J., Katz, B. A., Mol, C., Ho, J. D., Jennings, A. J., Luong, C., Arvai, A., Buggy, J. J., Chi, E., Tang, J., Sang, B. C., Verner, E., Wynands, R., Leahy, E. M., Dougan, D. R., Snell, G., Navre, M., Knuth, M. W., Swanson, R. V., McRee, D. E., and Tari, L. W. (2004) Structural snapshots of human HDAC8 provide insights into the class I histone deacetylases. Structure 12, 1325-1334

Stevenson, F. T., Bursten, S. L., Locksley, R. M., and Lovett, D. H. (1992) Myristyl acylation of the tumor necrosis factor alpha precursor on specific lysine residues. The Journal of experimental medicine 176, 1053-1062

Suzuki, T., Ota, Y., Ri, M., Bando, M., Gotoh, A., Itoh, Y., Tsumoto, H., Tatum, P. R., Mizukami, T., Nakagawa, H., Iida, S., Ueda, R., Shirahige, K., and Miyata, N. (2012) Rapid discovery of highly potent and selective inhibitors of histone

deacetylase 8 using click chemistry to generate candidate libraries. J Med Chem 55, 9562-9575

Tan, M., Luo, H., Lee, S., Jin, F., Yang, J. S., Montellier, E., Buchou, T., Cheng, Z., Rousseaux, S., Rajagopal, N., Lu, Z., Ye, Z., Zhu, Q., Wysocka, J., Ye, Y., Khochbin, S., Ren, B., and Zhao, Y. (2011) Identification of 67 histone marks and histone lysine crotonylation as a new type of histone modification. Cell 146, 1016-1028

Teng, Y. B., Jing, H., Aramsangtienchai, P., He, B., Khan, S., Hu, J., Lin, H., and Hao, Q. (2015) Efficient demyristoylase activity of SIRT2 revealed by kinetic and structural studies. Scientific reports 5, 8529

Vannini, A., Volpari, C., Filocamo, G., Casavola, E. C., Brunetti, M., Renzoni, D., Chakravarty, P., Paolini, C., De Francesco, R., Gallinari, P., Steinkuhler, C., and Di Marco, S. (2004) Crystal structure of a eukaryotic zinc-dependent histone deacetylase, human HDAC8, complexed with a hydroxamic acid inhibitor. Proceedings of the National Academy of Sciences of the United States of America 101, 15064-15069

Vannini, A., Volpari, C., Gallinari, P., Jones, P., Mattu, M., Carfi, A., De Francesco, R., Steinkuhler, C., and Di Marco, S. (2007) Substrate binding to histone deacetylases as shown by the crystal structure of the HDAC8-substrate complex. EMBO reports 8, 879-884

Vilas, G. L., Corvi, M. M., Plummer, G. J., Seime, A. M., Lambkin, G. R., and Berthiaume, L. G. (2006) Posttranslational myristoylation of caspase-activated p21-activated protein kinase 2 (PAK2) potentiates late apoptotic events. Proceedings of the National Academy of Sciences of the United States of America 103, 6542-6547

Waltregny, D., De Leval, L., Glenisson, W., Ly Tran, S., North, B. J., Bellahcene, A., Weidle, U., Verdin, E., and Castronovo, V. (2004) Expression of histone

deacetylase 8, a class I histone deacetylase, is restricted to cells showing smooth muscle differentiation in normal human tissues. Am J Pathol 165, 553-564

Waltregny, D., Glenisson, W., Tran, S. L., North, B. J., Verdin, E., Colige, A., and Castronovo, V. (2005) Histone deacetylase HDAC8 associates with smooth muscle alpha-actin and is essential for smooth muscle cell contractility. FASEB journal : official publication of the Federation of American Societies for Experimental Biology 19, 966-968

Wegener, D., Wirsching, F., Riester, D., and Schwienhorst, A. (2003) A fluorogenic histone deacetylase assay well suited for high-throughput activity screening. Chemistry & biology 10, 61-68

West, A. C., and Johnstone, R. W. (2014) New and emerging HDAC inhibitors for cancer treatment. The Journal of clinical investigation 124, 30-39

Wilson, B. J., Tremblay, A. M., Deblois, G., Sylvain-Drolet, G., and Giguere, V. (2010) An acetylation switch modulates the transcriptional activity of estrogen-related receptor alpha. Molecular endocrinology 24, 1349-1358

Wolfson, N. A., Pitcairn, C. A., and Fierke, C. A. (2013) HDAC8 substrates: Histones and beyond. Biopolymers 99, 112-126

Yamauchi, Y., Boukari, H., Banerjee, I., Sbalzarini, I. F., Horvath, P., and Helenius, A. (2011) Histone deacetylase 8 is required for centrosome cohesion and influenza A virus entry. PLoS pathogens 7, e1002316

Yang, X. J., and Seto, E. (2007) HATs and HDACs: from structure, function and regulation to novel strategies for therapy and prevention. Oncogene 26, 5310-5318

Yount, J. S., Zhang, M. M., and Hang, H. C. (2011) Visualization and Identification of Fatty Acylated Proteins Using Chemical Reporters. Current protocols in chemical biology 3, 65-79

Zhu, A. Y., Zhou, Y., Khan, S., Deitsch, K. W., Hao, Q., and Lin, H. (2012) Plasmodium falciparum Sir2A preferentially hydrolyzes medium and long chain fatty acyl lysine. ACS chemical biology 7, 155-159

# CHAPTER 4

# SUMMARY AND FUTURE DIRECTIONS

## 4.1 S-ACYLATION OF JAM-C

### 4.1.1 The role of S-acylation on JAM-C localization and cell migration

We have demonstrated that S-palmitoylation of JAM-C facilitates its cell-cell contact localization. However, how this modification regulates JAM-C localization is not clear. It is possible that S-palmitoylation of JAM-C is important for interacting with other tight junction proteins. JAM-C undergoes heterophilic interactions with JAM-B and other PDZ-containing proteins such as ZO-1 and PAR-3 at the cell tight junctions (Arrate et al, 2001; Ebnet et al, 2003). PAR-3 forms a complex with aPKC and PAR-6, which is essential for cell tight junction formation and cell polarity. Knockdown of PAR3 in epithelial cells leads to the disruption of tight junctions (Chen and Macara, 2005). The S-palmitoylation thus may help orient JAM-C in a direction that allows it to interact with these proteins, leading to the enrichment of JAM-C in the cell-cell contact regions. Further investigation is required to prove this hypothesis.

S-palmitoylation of JAM-C is also involved in cell migration. Revealed through a transwell migration assay, the CCSS JAM-C showed an increase in cell migration relative to the WT JAM-C. How S-palmitoylation regulates the cell migration of JAM-C remains unknown. Cell migration requires several coordinated molecular components to drive cell movement. Previously, S281A JAM-C has been shown to activate αvβ3 integrin activity, and enhance the cell migration (Mandicour

et al, 2007). JAM-C has been reported to associate with several integrins, including α4β1, αMβ2, αXβ2 and αvβ3, and these interactions have been implicated in different biological functions (Cunningham et al, 2002; Santoso, S. et al. 2002; Li et al, 2009). Integrins are type I transmembrane receptors that facilitate the interaction between the extracellular matrix (ECM) and the actin cytoskeleton during cell migration (Huttenlocher and Horwitz, 2011). It is therefore possible that S-palmitoylation of JAM-C affects the cell-migration through integrin modulation. However, further experiments are needed to address this issue.

We found that DHHC7 regulates the S-palmitoylation on JAM-C and the non-palmitoylable JAM-C mutant exhibits a significant increase in cell migration. It has been known that uncontrolled cell motility can lead to metastasis. Our finding thus suggests that DHHC7 might play a role in regulating cancer metastasis.

### 4.1.2 Interplay between S-acylation and phosphorylation

Numerous cellular proteins undergo a variety of modifications. In addition to S-palmitoylation, Junctional adhesion (JAM-C) has been previously shown to be phosphorylated at Ser281. The JAM-C phosphorylation is important for tight junction (TJ) localization as the S281A JAM-C mutant leads to the mislocalization of JAM-C with more distribution on the cell border, while the JAM-C wild type is generally more enriched at the apical region of the lateral membrane or the tight junction (Mandicourt et al, 2007). The interplay between S-acylation and phosphorylation of JAM-C is thus possible as reported for several proteins. For example, the phosphorylation of phosphodiesterase 10A (PDE10A) has been shown to interfere

the S-palmitoylation of PDE10A and prevent its membrane association (Charych et al, 2010). In contrast, s-palmitoylation has been shown to negatively regulate phosphorylation of GluR1, a subunit of AMPA receptor. The non-palmitoylatable GluR1 mutant was demonstrated to enhance the phosphorylation on both the Ser816 and Ser818 residues of GLuR1. Enhancing the phosphorylation further mediated the interaction of GluR1 with other protein complexes, which subsequently allowed for plasma membrane insertion (Lin et al., 2009).

A palmitoylation deficiency in β2 adrenergic G-protein coupled receptor results in an enhanced phosphorylation level, and subsequent loss of G-protein coupling (Salaun et al, 2010). Dependence between the phosphorylation and S-palmitoylation was also seen with the protein STREX, a spliced variant of “large conductance calcium- and voltage-gated potassium channels” or “BK channel”. The phosphorylation of STREX at the C-terminus, mediated by PKA, leads to a conformational change inhibiting its channel activity. The S-palmitoylation on STREX is required for membrane association. The phosphomimetic mutant of STREX can dissociate STREX from the plasma membrane and subsequently inhibit its channel activity. However, the PKA-mediated inhibitory effect is abolished in the non-palmitoylable cysteine to serine mutant. This suggests that phosphorylated-mediated inhibition of STRX is dependent on its S-palmitoylation status (Tian et al, 2008).

Salaun et al presented different possibilities to explain the interplay between S-palmitoylation and phosphorylation. For transmembrane proteins, the negative charge of phosphorylation might prevent the S-palmitoylation by inhibiting the

membrane interaction with DHHCs. Alternatively, the phosphorylation may increase the depalmitoylation rate of the modified proteins by changing the protein structure and making the proteins more accessible to thioesterases in the cytosol. On the other hand, the S-palmitoylation of the protein can orient the phosphorylation site protein closed to the membrane thus preventing the binding of protein kinase, which decreases the phosphorylation. For some peripheral proteins, it is possible that the phosphorylation can interfere or block the membrane interaction of the S-palmitoylated proteins (Salaun et al, 2010).

Nevertheless, it has recently been shown that both phosphorylation and S-palmitoylation of the neuronal growth-associated protein (GAP43), a peripheral membrane protein, are required for its plasma membrane association (Gauthier-Kemper et al, 2014). The negative charge of phosphorylation can modulate the protein conformation via protein-protein or protein-membrane interactions. The non-phosphorylable GAP43 mutant showed a decrease in membrane association, but the S-palmitoylation level of GAP43 was not affected. Interestingly, the phosphomimetic mutation enhanced both the S-palmitoylation and membrane association of GAP43. GAP43 phosphorylation presumably mediates its membrane association, thereby increasing the chance for palmitoylation by DHHCs (Gauthier-Kemper et al, 2014). This shows that the dynamics between phosphorylation and S-palmitoylation are more complicated than previously expected.

Notably, from our studies, the non-palmitoylable CCSS JAM-C mutant is likely to have similar phenotypes to the non-phosphorylable S281A JAM-C mutant, reported by Mandicourt and co-workers (Mandicourt et al, 2007). Both the CCSS

and S281A mutants are more evenly localized on the cell membrane, rather than enriched in the cell-cell contact region as observed in the wild type. The cell migration of both the CCSS JAM-C mutant, reported by us, and the S281A JAM-C mutant, reported by Mandicourt et al, is increased relative to wild type JAM-C. It remains unclear whether these two modifications are related to each other. It is possible that JAM-C phosphorylation can regulate S-palmitoylation and/or vice-versa. Further investigation is required to address these questions.

## 4.2 N-LYSINE DEFATTY-ACYLASE ACTIVITY OF HDAC8

### 4.2.1 Identification of HDAC8 target

We showed that HDAC8 can efficiently catalyze defatty-acylation *in vitro*, including deoctanoylation, dedodecanoylation and demyristoylation. Both the deacetylation and demyristoylation activities of HDAC8 are sequence specific, and HDAC8 exhibited different selectivity on various histones peptides. This is consistent with a previous study showing that some amino acid residues on specific positions of peptides can affect the activity of HDAC8 (Gurard-Levin et al, 2010).

In an attempt to probe the physiological relevance of HDAC8's defatty-acylation activity, we compared the global fatty acylation between the cells treated with HDAC8 specific inhibitor (PCI-34051) and the control (DMSO). Interestingly, we indeed observed a significant increase in the lipid profiling from the cells treated with HDAC8 inhibitor, suggesting that HDAC8's defatty-acylase activity might be relevant to its physiological function.

Nevertheless, it is highly possible that the global fatty acylation signal we observed is mostly from N-glycine fatty acylation, rather than N-lysine fatty acylation. The abundance of N-glycine myristoylated proteins in mammals has been predicted to be approximately ~ 1.5-3% (Martin et al, 2010), while that of lysine-fatty acylation is still unknown. Our data showed that HDAC8 does not remove the myristoyl group from the N-glycine myristoylated peptides. However, the elevated fatty acylation of the cells treated with HDAC8 inhibitor might result from indirect effects of the inhibitor. For example, the HDAC8 inhibitor might activate the transcription of N-myristoyl transferases, thereby increasing the fatty acylation level. To rule out these possibilities, we knocked down HDAC8 and performed the global labeling. We saw an increase in fatty acylation, albeit it was less obvious than the result obtained from the inhibitor treatment. These results suggest that it is likely that HDAC8 defatty-acylase activity is likely physiologically relevant. The next step was to determine HDAC8 defatty-acylation targets.

We used SILAC (stable isotope labeling by amino acids in cell culture), a quantitative proteomics technique, together with the metabolic labeling to try to identify HDAC8 targets. HDAC8 knockdown and control cells were grown in heavy and light amino acid containing media, respectively. From the total lysates, lysine-fatty acylated proteins were enriched by conjugation to biotin azide via click chemistry and purified using streptavidin beads. The lists of candidate proteins with a high heavy to light ratio were selected to validate as HDAC8 targets. Unfortunately, we have yet to identify a direct HDAC8 defatty-acylation target. The major drawback of this technique is high false positive rate. For example, certain

proteins we validated did not contain fatty acylation, this might be due to nonspecific interactions with streptavidin beads. Moreover, some of the proteins only had S-acylation, but not lysine fatty acylation. Interestingly, this might be due to hydroxylamine resistant cysteine palmitoylation. Also, the high heavy-to-light ratios of certain proteins result from the higher protein expression level, not because of the higher fatty acylation level in knockdown cells. Moreover, our method may not allow us to detect proteins that are targets but present in low abundance. To solve these problems, several controls should be included. For example, the SILAC of protein expression in both HDAC8 knockdown and control cells should be performed to rule out the changes in protein levels. Also, reverse SILAC by growing knockdown and control cells in the light and heavy amino acid containing media, respectively, should be carried out to confirm the candidate proteins. Moreover, a SILAC experiment aimed at identifying the HDAC8 interactome might be useful to help narrow down potential targets.

## 4.3 REFERENCES

Arrate, M. P., Rodriguez, J. M., Tran, T. M., Brock, T. A., and Cunningham, S. A. (2001) Cloning of human junctional adhesion molecule 3 (JAM3) and its identification as the JAM2 counter-receptor. J Biol Chem 276, 45826-45832

Charych, E. I., Jiang, L. X., Lo, F., Sullivan, K., and Brandon, N. J. (2010) Interplay of palmitoylation and phosphorylation in the trafficking and localization of phosphodiesterase 10A: implications for the treatment of schizophrenia. J Neurosci 30, 9027-9037

Chen, X., and Macara, I. G. (2005) Par-3 controls tight junction assembly through the Rac exchange factor Tiam1. Nat Cell Biol 7, 262-269

Cunningham, S. A., Rodriguez, J. M., Arrate, M. P., Tran, T. M., and Brock, T. A. (2002) JAM2 interacts with alpha4beta1. Facilitation by JAM3. J Biol Chem 277, 27589-27592

Ebnet, K., Aurrand-Lions, M., Kuhn, A., Kiefer, F., Butz, S., Zander, K., Meyer zu Brickwedde, M. K., Suzuki, A., Imhof, B. A., and Vestweber, D. (2003) The junctional adhesion molecule (JAM) family members JAM-2 and JAM-3 associate with the cell polarity protein PAR-3: a possible role for JAMs in endothelial cell polarity. J Cell Sci 116, 3879-3891

Gauthier-Kemper, A., Igaev, M., Sundermann, F., Janning, D., Bruhmann, J., Moschner, K., Reyher, H. J., Junge, W., Glebov, K., Walter, J., Bakota, L., and Brandt, R. (2014) Interplay between phosphorylation and palmitoylation mediates plasma membrane targeting and sorting of GAP43. Mol Biol Cell 25, 3284-3299

Gurard-Levin, Z. A., Kilian, K. A., Kim, J., Bahr, K., and Mrksich, M. (2010) Peptide arrays identify isoform-selective substrates for profiling endogenous lysine deacetylase activity. ACS Chem Biol 5, 863-873

Huttenlocher, A., and Horwitz, A. R. (2011) Integrins in cell migration. Cold Spring Harb Perspect Biol 3, a005074

Lamagna, C., Meda, P., Mandicourt, G., Brown, J., Gilbert, R. J., Jones, E. Y., Kiefer, F., Ruga, P., Imhof, B. A., and Aurrand-Lions, M. (2005) Dual interaction of JAM-C with JAM-B and alpha(M)beta2 integrin: function in junctional complexes and leukocyte adhesion. Mol Biol Cell 16, 4992-5003

Lin, D. T., Makino, Y., Sharma, K., Hayashi, T., Neve, R., Takamiya, K., and Huganir, R. L. (2009) Regulation of AMPA receptor extrasynaptic insertion by 4.1N, phosphorylation and palmitoylation. Nat Neurosci 12, 879-887

Mandicourt, G., Iden, S., Ebnet, K., Aurrand-Lions, M., and Imhof, B. A. (2007) JAM-C regulates tight junctions and integrin-mediated cell adhesion and migration. J Biol Chem 282, 1830-1837

Martin, D. D., Beauchamp, E., and Berthiaume, L. G. (2011) Post-translational myristoylation: Fat matters in cellular life and death. Biochimie 93, 18-31

Salaun, C., Greaves, J., and Chamberlain, L. H. (2010) The intracellular dynamic of protein palmitoylation. J Cell Biol 191, 1229-1238

Santoso, S., Sachs, U. J., Kroll, H., Linder, M., Ruf, A., Preissner, K. T., and Chavakis, T. (2002) The junctional adhesion molecule 3 (JAM-3) on human platelets is a counterreceptor for the leukocyte integrin Mac-1. J Exp Med 196, 679-691

Tian, L., Jeffries, O., McClafferty, H., Molyvdas, A., Rowe, I. C., Saleem, F., Chen, L., Greaves, J., Chamberlain, L. H., Knaus, H. G., Ruth, P., and Shipston, M. J. (2008) Palmitoylation gates phosphorylation-dependent regulation of BK potassium channels. Proc Natl Acad Sci U S A 105, 21006-21011